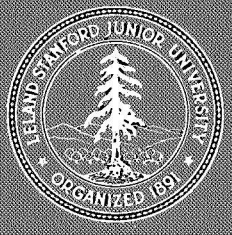

STANFORD UNIVERSITY
ENGINEERING IN MEDICINE AND BIOLOGY

THEORETICAL STUDIES ON HIGH FREQUENCY WAVE PROPAGATION IN BLOOD VESSELS

PH. D. DISSERTATION

BY

J. A. BAILIE

BIOMECHANICS LABORATORY

DEPARTMENT OF AERONAUTICS AND ASTRONAUTICS

JUNE
1969

This work was carried out at the Ames Research Center of NASA
under a collaborative research arrangement with Stanford University
(NASA Grant NGR 05-020-223)

SUDAAR
NO. 378

Department of Aeronautics and Astronautics
Stanford University
Stanford, California

THEORETICAL STUDIES ON HIGH FREQUENCY WAVE PROPAGATION IN BLOOD VESSELS

Ph.D. Dissertation

by

J. A. Bailie

SUDAAR NO. 378
June 1969

This work was carried out at the Ames Research Center of NASA under a collaborative research arrangement with Stanford University (NASA Grant NGR 05-020-223).

ACKNOWLEDGMENT

While this dissertation bears the name of only one author, it is in reality, a cooperative effort. To Professor Max Anliker, without whom this work would not have been done; go my heartfelt thanks for tolerating a part time student, his benevolent attitude toward my work and his guidance throughout my studentship. Unfortunately space does not permit naming individually the many faculty members who, by their teaching in the classroom and during tutorial sessions, made the years at Stanford such an inspiring experience.

All serious digital computer programming done on behalf of this study is the work of others. My colleagues C. J. Bonner (Chapter I), I. C. Hanson (Chapter II), and J. E. McFeely (Chapters III and IV) gave many hours of their spare time to provide the programs from which the numerical data were extracted.

To Lockheed Missiles and Space Company goes my gratitude for sponsoring me through the course work that led up to this dissertation.

Many hours were spent as an "Unpaid Guest Worker" at the Ames Research Center of the N.A.S.A., in the Environmental Biology Division, headed by Eric Odgen, M.D. This opportunity to take the first faltering steps in the fascinating field of Cardiovascular Physiology, is deeply appreciated.

The sacrifices of my parents, over many difficult years, to provide my early education, deserve a lot more than is in my power to give.

My wife Georgina's cheerfulness, patience and attractive companionship meant so very much.

Gail Lemmond's excellence as a technical typist and Julie Mungall's skill as a technical illustrator are obvious to anyone reading this work.

SUMMARY

Four problems related to high frequency wave propagation in blood vessels have been investigated. They are sufficiently different to justify a self contained treatment for each one.

A simple plate theory model is utilized to demonstrate that Korotkoff sounds generated during the systolic phase of the auscultatory measurement of the blood pressure can be interpreted as a phenomenon of dynamic instability of the partially collapsed brachial artery. A previous study of Korotkoff sounds at diastole indicated that the segment of the brachial artery affected by the pneumatic cuff is dynamically unstable whenever the intraluminal pressure falls sufficiently below the cuff pressure. Under conditions of instability the brachial segment acts like a mechanical amplifier capable of magnifying certain perturbations inherent in the arterial pressure pulse beyond the audibility threshold. A similar instability phenomenon is also hypothesized as the cause of the sounds heard at systole when the intraluminal pressure exceeds sufficiently the cuff pressure. The theory presented agrees in many respects with evidence obtained from experimental studies on physical models. For large curvatures of the wall and certain types of fluid perturbations, the predicted stability boundaries cannot be explained on physical grounds at the present time and must be reexamined in a separate investigation.

The equations of the theory of elasticity for a transversely isotropic cylinder are applied to study the influence of wall thickness and material properties on the phase velocities in a fluid filled cylinder. The analysis is restricted to axially symmetric waves and unprestressed cylinder walls. It shows that for distension and axial waves, the predicted phase velocities agree closely with those from thin shell theory. The phase velocities of distension waves exhibit a dependence of thickness to mean radius ratio that is in close agreement with the Moens Korteweg equation. The influence of transversely isotropic walls on axial phase velocities is small, but is considerable for distension waves. Experimentally observed phase velocities in the carotid arteries of anesthetized dogs suggest that the circumferential modulus can exceed the axial by as much as 200%.

To detect whether small deviations from a circular cross section can account for a definite trend in the phase velocities, the analysis of wave propagation in a cylinder of elliptic cross section is undertaken. The assumptions made are not valid for large eccentricities and the one waveform from which data is obtained is that which converges to the axially symmetric case when the ellipse tends to a circle. The numerical results show an extremely small influence of eccentricity, at least for values less than 0.5.

A number of thin shell theories proposed for the analysis of prestressed thin cylinders are reviewed in regard to their use for the prediction of the wave transmission properties of blood vessels. The importance of accounting for the stress resultants due to the transmural pressure and their rotations induced by the shell deformation is illustrated by showing that their neglect results in physically meaningless results for torsion waves. An approximate theory allowing for large strains only in the prestressed state is given. The resulting displacement equilibrium equations are nonself adjoint, but this is shown to have a negligible effect for the physiological problems of immediate interest.

TABLE OF CONTENTS

CHAPTER PAGE

LIST OF FIGURES

INTRODUCTION

The study of wave propogation in the major blood vessels of mammals is, for the theoretician, a subject of considerable complexity. The significant difference between the problems of biomechanics and those of metallic and other inert structures is in the material properties. The difficulties of measuring the behavior of even local segments of the cardiovascular system in a living mammal without markedly influencing the outcome by anesthetics, response to traumas, or interfering with incredibly complex metabolic and control mechanisms, are immense. Two of the advantages a specialist in classic applied mechanics has over a researcher in biomechanics are the abilities to measure material properties and define an initial or stress-strain free state that is in the neighborhood of those being investigated. For example, in metal shell structures at room temperature, material properties of small samples that apply directly to the analysis can be found at all but the highest strain rates, with considerable accuracy. Excising segments of a blood vessel and using these material properties can lead to large errors. A change in the mean pressure in segments of the aortic arch, carotid sinus etc., trigger baroreceptors that result in changes of cardiac output. Subtle chemical changes result in vasoconstriction or vasodilation, leading to huge changes in elastic stiffness of parts of the system, particularly the arterioles; resulting in changes of the prestressed state, throughout much of the system. No such difficulties befall most of the investigations of classical

applied mechanics. The second difficulty facing the analyst of cardiovascular problems is the defining the prestressed state and the influence of surrounding tissues, muscle, bone etc. The mean strains in many arteries are of the order 0.3, at least an order of magnitude larger than considered in virtually all engineering shell structures. Also the surrounding tissue beds, for example, interact with the vessel wall in a manner that is difficult to assess accurately.

Since so much remains to be discovered about blood vessel wall behavior it was considered that any serious attempt to account for their conjectured behavior was doomed to failure for two reasons. Firstly because of our lack of basic knowledge and secondly because the resulting mathematical complication of the analyses would virtually preclude the extraction of numerical data. Therefore a basic assumption of all four chapters was that the wall material would be treated as a physically elastic solid and the blood could be adequately represented for our particular needs as an inviscid, incompressible, Newtonian fluid.

The four chapters are addressed to subjects that are sufficiently different to warrant each being completely self contained with its own notation, references and figures. Chapter 1 is a dynamic stability investigation of an elastic walled fluid container that can be considered as a simple model of the behavior of the brachial artery with a cuff around the arm at pressures near systolic. The intent was to see what available evidence could be obtained to support or invalidate the hypothesis that the Kortkoff sounds at systole, that are heard by a physician taking blood pressure, are a manifestation of fluid-structural instability induced by the cuff pressure.

The theory of rotationally symmetric waves in a circular cylinder are studied in Chapter II using the theory of elasticity to study the relationship of these results to those of thin (Kirchoff-Love) shell theory and the influence of wall thickness and transversely isotropic wall properties.

In many situations tissues exert a force on the blood vessels that tend to distort the cross section from its circular configuration. Chapter III addresses the problem of the influence of a slightly elliptic cross section on the phase velocities.

The final chapter is a review of various thin shell theories that were developed for the study of metallic shells and their application to the study of waves in prestressed circular cylinders. Some of the assumptions on which they are based are discussed and their influence on the phase velocities of the three types of waves of primary physiological interest are illustrated.

CHAPTER I

KOROTKOFF SOUNDS AT SYSTOLE, A PHENOMENON OF DYNAMIC INSTABILITY

1.1. Introduction.

Anliker and Raman [1] have hypothesized the cause of the Korotkoff sounds at diastolic pressure as a dynamic instability of fluid induced oscillations in a circular tube. At systolic pressure the assumption of the artery as a circular tube is, of course, untenable since it is virtually occluded. At pressures in the neighborhood of systolic, the artery cross section is markedly flattened, (see Fig. 1a) having a very small radius of curvature at two diametrically opposite points and is relatively flat over most of its profile between these corners. In the regions of large changes of curvature the artery is much stiffer than elsewhere and this fact leads us to the model we shall use in an attempt to show that Korotkoff sounds at systolic pressure are also a manifestation of dynamic instability. This analysis is a continuation and extension of that by Raman [2], [3] in which the experimental and initial theoretical work is described.

The system we intend to analyse is shown in Figure 1b. We assume that the two regions of large curvature can be replaced by rigid walls and that the remainder of the artery can be modelled as two plates which can undergo large displacements normal to their surfaces. Initially these plates are subjected to axial tension, to represent the axial stretch of the arterial wall and steady state plus perturbation transmural pressures. The analysis follows the well known techniques for such situations. We assume the stresses, deflections, pressures etc. consist of two components, one quasi-static which accounts for the axial stretch and transmural

pressure and the second which analyses the perturbations about the quasi-static configuration. The justification for the quasi-static prestress state is that the pulse frequency is about 1 cps while the human ear can only perceive perturbations with frequencies greater than 20 cps.

1.2. Quasi-Static Stress in the Artery at Pressures Near Systolic.

Due to the extremely complex constitutive laws needed to accurately define the behavior of animal tissues over any but a small range of loadings, a general theoretical analysis of many such problems is extremely difficult. Even computing the stresses in a human brachial artery when it has been compressed by a cuff to measure systolic pressure, appear, at the present time, to be virtually insurmountable. The deflections involved are almost twice the radius of the artery in its natural pre-stressed state, for much of the wall and the influence of the surrounding tissues, bones and ligaments cannot be estimated quantitatively. Thus we make no attempt to compute the quasi-static stresses in the artery, or to quantitatively relate the deformed configuration to the cuff pressure producing it. While many sophisticated methods for the "large" deflection analysis of shell type structures are currently available, the assumptions on which they are based are too far removed from the problem at hand to be physically meaningful. In shell theory we are almost always able to define an initial stress or strain free state and proceed systematically to derive the quasi-static prestress stresses and strains. In our problem it is not reasonable to define a known state, from which to initiate the analysis of the pre-stress state.

To make our problem tractable, we shall proceed as follows. It is well established that like almost all other arteries, the brachial is under considerable axial stretch with strains of order 0.2. We restrict our investigation of the quasi-static prestressed state to a definition of the transverse displacement, the (tensile) axial strain and the (compressive) lateral in-plane strain exhibited by a rectangular membrane. This highly idealized model infers that the cuff pressure transmitted by the tissue produces the lateral strain and displacements specified. However, because of the lack of the constitutive law, the relationship between the applied cuff pressure and the induced transverse displacement or lateral strain, is unknown. We rely on experimental evidence and the qualitative discussion in Section 1.8, to provide the connection between shape of the artery cross section and the cuff pressure. The experimental data obtained on a model of the brachial artery in [2], [3] and unpublished invivo studies show that the artery is virtually occluded at cuff pressures only slightly above systolic and provides the rationale for the choice of the theoretical model. We must now consider the response to small oscillatory perturbations superimposed on the quasi static transmural pressure.

1.3. Oscillations About the Deformed Equilibrium State.

Since we are studying the vibrations of the plate relative to the deformed position induced by the static transmural pressure, we must use geometrically non-linear plate theory. We assume that the $(\text{rotations})^2$ are negligible compared to unity and utilize the Karman equations which are well known to be (see [4], p. 417),

$$\nabla^4 F = \left[\left(\frac{\partial^2 w}{\partial x\, \partial y} \right)^2 - \frac{\partial^2 w}{\partial x^2} \frac{\partial^2 w}{\partial y^2} \right] \tag{1}$$

and

$$\nabla^4 w = \frac{h}{D} \left[\frac{q}{h} + \frac{\partial^2 F}{\partial y^2} \frac{\partial^2 w}{\partial x^2} + \frac{\partial^2 F}{\partial x^2} \frac{\partial^2 w}{\partial y^2} - 2 \frac{\partial^2 F}{\partial x \partial y} \frac{\partial^2 w}{\partial x \partial y} \right] \tag{2}$$

where

$$N_x = h \frac{\partial^2 F}{\partial y^2} \; ; \quad N_y = h \frac{\partial^2 F}{\partial x^2} \; ; \quad N_{xy} = -2h \frac{\partial^2 F}{\partial x\, \partial y} \quad .$$

Let us write $F = F^o + F^d$, $w = w^o + w^d$, where F^d and w^d are the stress function and transverse displacements induced by the pressure perturbations. The perturbation quantities are considered to be small enough for their products and those of their derivatives, to be neglected. Substituting into (1) and (2) and separating the "static" and "perturbed" equations we have for the former, the nonlinear equations for the static stresses, which will be ignored since they do not describe the physical situation, as previously mentioned.

The equations for the dynamic response follow immediately and are

$$\nabla^4 F^d = \left[2 \frac{\partial^2 w^o}{\partial x\, \partial y} \frac{\partial^2 w^d}{\partial x\, \partial y} - \frac{\partial^2 w^o}{\partial x^2} \frac{\partial^2 w^d}{\partial y^2} - \frac{\partial^2 w^o}{\partial y^2} \frac{\partial^2 w^d}{\partial x^2} \right] \tag{3}$$

and

$$\nabla^4 w^d = \frac{h}{D} \left[\frac{p^d}{h} - \rho \frac{\partial^2 w^d}{\partial t^2} + \frac{\partial^2 F^o}{\partial y^2} \frac{\partial^2 w^d}{\partial x^2} + \frac{\partial^2 w^o}{\partial x^2} \frac{\partial^2 F^d}{\partial y^2} + \frac{\partial^2 F^o}{\partial x^2} \frac{\partial^2 w^d}{\partial y^2} + \frac{\partial^2 w^o}{\partial y^2} \frac{\partial^2 F^d}{\partial x^2} - 2 \frac{\partial^2 F^o}{\partial x\, \partial y} \frac{\partial w^d}{\partial x\, \partial y} - 2 \frac{\partial^2 w^o}{\partial x\, \partial y} \frac{\partial^2 F^d}{\partial x\, \partial y} \right] . \tag{4}$$

Because the static stress system is independent of x, we have $\partial w^o/\partial x = 0$, which introduces considerable simplification into (3) and (4). Now we must consider the static stress resultants $N_y^o = h\partial^2 F^o/\partial x^2$ and $N_x^o = h\partial^2 F^o/\partial y^2$ which constitute the nonvanishing coefficients of (3) and (4).

To study the quasi-static strain distribution we simplify the very complex physical situation as follows. These stresses are taken to be independent of the axial coordinate and they are considered to consist of two components (i) axial stretch which is always tensile (ii) lateral in plane strain which is prescribed. For instabilities to develop, we expect large compressive lateral strains will be needed to overcome the influence of the axial stretch and the possibility of extremely large amplitude buckles arises. We invoke whatever tissue forces are required to maintain the plate in the position specified by w^o and the inplane strains ϵ_x^o and ϵ_y^o. This specification is admittedly somewhat fictitious but the actual situation is, as previously mentioned, beyond solution and it is convenient to postulate a quasi-static state in which the effects of prescribed inplane strains and transverse deflection are at least partially isolated. It is well known that extremely small "elastic foundations" forces can greatly stabilize plates.

Hence we assume that the quasi static deflection of the membrane can be represented by a half sine wave, namely $w^o = w_o \cos \pi y$ and $u^o = v_o \sin 2\pi y$. The relation between w_o and v_o can be obtained by noting ([4] p. 419) that the strain energy for a membrane subjected to a constant transverse force N_y^o is

$$V = \frac{1}{2(1-\nu^2)} \int_{-1/2}^{1/2} \left[\left(\frac{dv^o}{dy} \right)^2 + \frac{dv^o}{dy} \left(\frac{dw^o}{dy} \right)^2 + \frac{1}{4} \left(\frac{dw^o}{dy} \right)^4 \right] dy$$

$$+ N_y^o \int_{-1/2}^{1/2} \left[\frac{dv^o}{dy} + \frac{1}{2} \left(\frac{dw^o}{dy} \right)^2 \right] dy \quad .$$

Inserting the displacement expressions and carrying out the integrations we find

$$V = \frac{\pi^2}{2(1-\nu^2)} \left[2v_o^2 - \frac{\pi v_0 w_0^2}{2} + \frac{3\pi^2 w_0^4}{32} \right] + \frac{N_y^o \pi^2 w_0^2}{2} \quad .$$

Using theorem of Minimum Potential Energy we have

$$\frac{\partial V}{\partial v_0} = \frac{\pi^2}{2(1-\nu^2)} \left[4v_0 - \frac{\pi w_0^2}{2} \right] = 0 \quad .$$

Thus

$$v_0 = \frac{\pi w_0^2}{8} \quad .$$

From the stress-strain and strain-displacement laws we have

$$\left(\frac{\partial^2 F^o}{\partial y^2} - \frac{\nu \partial^2 F^o}{\partial x^2} \right) = \epsilon_x^o$$

and

$$\left(\frac{\partial^2 F^o}{\partial x^2} - \frac{\nu \partial^2 F^o}{\partial y^2} \right) = \frac{dv^o}{dy} + \frac{1}{2} \left(\frac{dw^o}{dy^2} \right)^2 + \epsilon_y^o = \frac{\pi^2 w_0^2}{2} \left(2 \cos 2\pi y + \sin^2 \pi y \right) + \epsilon_y^o$$

$$= \frac{\pi^2 w_0^2}{4} + \epsilon_y^o \quad .$$

Hence

$$\frac{\partial^2 F^o}{\partial y^2} = K_1 \qquad \text{and} \qquad \frac{\partial^2 F^o}{\partial x^2} = K_2 \tag{5}$$

where

$$K_1 = \frac{1}{(1-\nu^2)}\left[\epsilon_x^o + \nu\left(\epsilon_y^o + \frac{\pi^2 w_0^2}{4}\right)\right]$$

and

$$K_2 = \frac{1}{(1-\nu^2)}\left[\epsilon_y^o + \frac{\pi^2 w_0^2}{4} + \nu\epsilon_x^o\right]$$

This demonstrates that the static stress resultants are constants and substituting (5) into (3) and (4) and making use of the fact that $\partial w^o/\partial x = 0$ we see that (3) and (4) are simplified to

$$\nabla^4 F^d = -\frac{d^2 w^o}{d^2 y^2}\frac{\partial^2 w^d}{\partial x^2} \tag{6}$$

and

$$\nabla^2 w^d = \frac{h}{D}\left[\frac{p^d}{h} - \rho\frac{\partial^2 w^d}{\partial t^2} + K_1\frac{\partial^2 w^d}{\partial x^2} + K_2\frac{\partial^2 w^d}{\partial y^2} + \frac{d^2 w^o}{\partial y^2}\frac{\partial^2 F^d}{\partial x^2}\right] . \tag{7}$$

We note that each of these equations contain one variable coefficient and it does not appear feasible to simplify the equations further. These variable coefficient terms also provide the coupling between the two equations. The form of the solution is dictated, to a large extent by the equations of the fluid in contact with the walls. Let us consider the fluid motion.

1.4. Equations of the Fluid.

For the incompressible inviscid fluid flowing down the interior of the tube shown in Fig. 1, we have:

(i) Equation of Continuity

$$\nabla^2 \phi = 0 \tag{8}$$

(ii) Eulers equation for the pressure in linearize potential flow is

$$p = \rho_f \left(\frac{\partial \phi}{\partial t} + U \frac{\partial \phi}{\partial x}\right) . \tag{9}$$

If we assume that the fluid perturbation consists of a disturbance of frequency σ and wave number k, propagating in the axial direction, we can write the perturbation potential as:

$$\phi(x,y,z,t) = \Phi(y,z)\ \mathrm{Sin}(\sigma t - kx) . \tag{10}$$

Then, for the perturbing pressure we have,

$$\begin{aligned} p^d &= \rho_f\ \Phi(y,z)\ (\sigma - Uk)\ \mathrm{Cos}(\sigma t - kx) \\ &= 2\pi\ \rho_f\ \Phi(y,z)(f - U/\lambda)\mathrm{Cos}(\sigma t - kx) . \end{aligned} \tag{11}$$

Now the lower limit of the human audible range and hence Korotkoff sounds, is about 20 cps at it is shown in [1] that the dispersion relationship for this type of blood flow problem is $\bar{\lambda} \doteq \bar{c}_G/\bar{f}$ where the bars denote dimensional quantities.

$$(\bar{f}-\bar{U}/\bar{\lambda}) = \bar{f}(1-\bar{U}/\bar{c}_G) \tag{12}$$

where $\bar{U}/\bar{c}_G$ is the ratio of the blood velocity in the artery to that of the wave's group velocity, which is about one order of magnitude less than unity. Therefore we reduce (9) to

$$p^d = \rho_f \frac{\partial \phi}{\partial t} \quad . \tag{13}$$

This provides a simplification that will be discussed when we consider the stability boundary.

(iii) Kinematic boundary condition relating the fluid and wall velocities in the z direction

$$\frac{\partial w^d}{\partial t} = -\left(\frac{\partial \phi}{\partial z}\right)_{z=w^o \pm c/2} \tag{14}$$

Clearly (14) is approximate for large deflections, since the rigorously correct boundary condition involves velocities normal to the plate mid-surface. It is important to note that in the kinematic condition we are matching fluid and wall velocities at the deflected equilibrium position defined by $z = w^o \pm c/2$ for the upper and lower walls respectively.

(iv) The boundary condition at the rigid walls requires that the normal component of the fluid velocity vanish, i.e.,

$$\left(\frac{\partial \phi}{\partial y}\right)_{y=\pm 1/2} = 0 \tag{15}$$

Substituting (10) into (8) we obtain

$$\frac{\partial^2\Phi}{\partial y^2} + \frac{\partial^2\Phi}{\partial z^2} - k^2\Phi = 0 \ . \tag{16}$$

Let us put $\Phi(y,z) = Y(y)\,Z(z)$. Thus using the separation of variables in the usual manner, (16) can be written as

$$\frac{d^2Y/dy^2}{Y} = k^2 - \frac{d^2Z/dz^2}{Z} = -\Gamma^2 \tag{17}$$

where Γ^2 is a real positive constant, to be determined, and we may write

$$\phi(x,y,z,t) = (A_1 \operatorname{Cos} \Gamma y + B_1 \operatorname{Sin} \Gamma y)(A_2 \operatorname{Cosh} \Lambda z + B_2 \operatorname{Sinh} \Lambda z) \operatorname{Sin}(\sigma t - kx) \tag{18}$$

where $\Lambda = [\Gamma^2 + k^2]^{1/2}$ and A_i and B_i are arbitrary constants. If we put $B_2 = 0$, the potential is symmetric in z, while $A_2 = 0$ yields a solution antisymmetric in z.

1.5. Formulation of the Solution.

Having the form of the fluid potential function, we can now proceed to the corresponding plate motion.

Using (18) in the kinematic boundary condition, we see that the plate transverse displacement must satisfy

$$w^d(x,y,t) = \frac{\Lambda}{\sigma}\,(A_1 \operatorname{Cos} \Gamma y + B_1 \operatorname{Sin} \Gamma y)$$

$$\times \{A_2 \operatorname{Sinh} \Lambda(w^o + \tfrac{c}{2}) + B_2 \operatorname{Cosh} \Lambda(w^o + \tfrac{c}{2})\} \operatorname{Cos}(\sigma t - kx) \quad (19)$$

The four arbitrary constants in (18) and (19) must be reduced to one, prior to derivation of the eigenvalue problem. This is accomplished by distinguishing modes that are symmetric or antisymmetric about the x-y and x-z planes and considering each of the resulting four types of perturbations separately. Since w^o is a function of y, this expression is non-linear in y. However, the Galerkin method is to be used to reduce the final equations to a classic eigenvalue formulation.

Let us now turn our attention to demonstrating how the four arbitrary constants are reduced to one, depending on the symmetry of the particular fluid perturbation. To enforce the vanishing of the displacement (and fluid velocity) in the corners we must require that $w^d(x, y = \frac{1}{2}, t)$ equal zero.

$$\begin{bmatrix} \operatorname{Cos} \frac{\Gamma}{2} & \operatorname{Sin} \frac{\Gamma}{2} \\ \operatorname{Cos} \frac{\Gamma}{2} & -\operatorname{Sin} \frac{\Gamma}{2} \end{bmatrix} \begin{vmatrix} A_1 \\ B_1 \end{vmatrix} = \begin{vmatrix} 0 \\ 0 \end{vmatrix} \quad (20)$$

For non-trivial solutions we must have either $\Gamma = 2m\pi$ in which case, $A_1 = 0$ and the displacement is antisymmetric in y, or $\Gamma = (2m+1)\pi$ in which case, $B_1 = 0$ and the displacement is symmetric function of y. Thus we can consider four separate cases of fluid perturbations and the

resultant response, depending on which arbitrary constants are eliminated from the problem by the symmetry assumed. In each case we have only one arbitrary constant defining the perturbation fluid potential and plate displacement amplitudes. The form of the plate stress function F^d can be seen from (6) and (7) to be the same as w^d, except for a different arbitrary constant.

We are now at the stage where these expressions for ϕ, F^d and w^d must be substituted into (6) and (7) and Galerkins method used to obtain the frequency determinant. To do this it is convenient to consider the cases of $A_1 = 0$ and $B_1 = 0$ separately and it is useful to summarize the expressions that are to be substituted into (6) and (7)

$$
\begin{aligned}
w^d(x,y,t) &= B_1^* \Psi \text{ Sin } 2m\pi y \text{ Cos}(\sigma t - kx) && \text{for } A_1 = 0 \\
&= A_1^* \Psi \text{ Cos}(2m+1)\pi y \text{ Cos}(\sigma t - kx) && \text{for } B_1 = 0 \\
F^d(x,y,t) &= C_1^* \Psi \text{ Sin } 2m\pi y \text{ Cos}(\sigma t - kx) && \text{for } A_1 = 0 \\
&= D_1^* \Psi \text{ Cos}(2m+1)\pi y \text{ Cos}(\sigma t - kx) && \text{for } B_1 = 0 \qquad (21) \\
\phi(x,y,z,t) &= \frac{B_1^* \sigma}{\Lambda} \text{ Sin } 2m\pi y \{A_2 \text{ Cosh } \Lambda z + B_2 \text{ Sinh } \Lambda z\} \text{ Sin}(\sigma t, kx) && \text{for } A_1 = 0 \\
&= \frac{A_1^* \sigma}{\Lambda} \text{ Cos}(2m+1)\pi y \{A_2 \text{ Cosh } \Lambda z + B_2 \text{ Sinh } \Lambda z\} \text{ Sin}(\sigma t - kx) && \text{for } B_1 = 0
\end{aligned}
$$

where $\Psi = A_2 \text{ Sinh } \Lambda(\pm w^o \pm \frac{c}{2}) + B_2 \text{ Cosh } \Lambda(\pm w^o \pm \frac{c}{2})$ and we shall later use $\Omega = A_2 \text{ Cosh } \Lambda(\pm w^o \pm \frac{c}{2}) + B_2 \text{ Sinh } \Lambda(\pm w^o \pm \frac{c}{2})$.

Before we continue with our derivation of the frequency determinant, let us consider in a little more detail the differences that depend whether we admit perturbations that are symmetric or antisymmetric in z. In the former case $A_2 = 0$ and Ψ, takes on the form

$$\Psi = B_2 \text{ Cosh } \Lambda(\pm w^o \pm \frac{c}{2})$$

$$= B_2(\text{Cosh } \frac{\Lambda c}{2} \text{ Cosh } \Lambda w^o + \text{Sinh } \frac{\Lambda c}{2} \text{ Sinh } \Lambda w^o) \qquad (22a)$$

when the two signs are the same

$$= B_2(\text{Cosh } \frac{\Lambda c}{2} \text{ Cosh } \Lambda w^o - \text{Sinh } \frac{\Lambda c}{2} \text{ Sinh } \Lambda w^o) \qquad (22b)$$

when the two signs differ .

In both these situations the quasi static deflections are symmetric in z and (22b) is merely (22a) with a change of sign in w^o. Or saying this in another way (22a) represents outward deflection and (22b) an inward deflection. Thus ultilizing, say, (22a) for positive and negative w^o, yields all the solutions symmetric in z and either (22a) or (22b) satisfies the boundary conditions at both flexible walls.

The situation for solutions antisymmetric in z is entirely similar, as we can now demonstrate. Consider all four combinations of signs we have, for $B_2 = 0$,

$$\text{Sinh } \Lambda(w^o + \frac{c}{2}) = \text{Sinh } \frac{\Lambda c}{2} \text{ Cosh } \Lambda w^o + \text{Cosh } \frac{\Lambda c}{2} \text{ Sinh } \Lambda w^o \qquad (23a)$$

$$\text{Sinh } \Lambda(w^o - \frac{c}{2}) = -\text{Sinh } \frac{\Lambda c}{2} \text{ Cosh } \Lambda w^o + \text{Cosh } \frac{\Lambda c}{2} \text{ Sinh } \Lambda w^o \qquad (23b)$$

$$\text{Sinh } \Lambda(-w^o + \frac{c}{2}) = \text{Sinh } \frac{\Lambda c}{2} \text{ Cosh } \Lambda w^o - \text{Cosh } \frac{\Lambda c}{2} \text{ Sinh } \Lambda w^o \qquad (23c)$$

$$\text{Sinh } \Lambda(-w^o - \frac{c}{2}) = - \text{Sinh } \frac{\Lambda c}{2} \text{ Cosh } \Lambda w^o - \text{Cosh } \frac{\Lambda c}{2} \text{ Sinh } \Lambda w^o \quad . \qquad (23d)$$

Attempting to simultaneously satisfy the boundary conditions at both $w^o \pm \frac{c}{2}$, we do not obtain identical pairs as in the previous case but two terms that differ only in sign, as must occur for the antisymmetric situation. Combining (23a) and (23d) we have one pair and (23b) and (23c) constitute the other pair with a change of sign in w^o and again we need use only one form in the ensuing calculations and utilize positive and negative initial displacments to obtain all the solutions.

Substituting (21) into (6) and (7) we obtain for $A_1 = 0$

$$\left[k^4 + 2k^2 \Psi\left\{(2m\pi)^2 - \Lambda^2\left(\frac{dw^o}{dy}\right)^2\right\} \text{Sin } 2m\pi y - 2k^2 \Omega\Lambda \frac{d^2w^o}{dy^2} \text{ Sin } 2m\pi y \right.$$

$$\left. - 4k^2 \Omega(2m\pi) \Lambda \frac{dw^o}{dy} \text{ Cos } 2m\pi y + \Delta\right] C_1^* - Ek^2\Psi \frac{d^2w^o}{dy^2} \text{ Sin } 2m\pi y \bar{B}_1^* = 0$$

and

$$\frac{h}{D} k^2\Psi \frac{d^2w^o}{dy^2} \text{ Sin } 2m\pi y \, C_1^* + \left[k^4 + 2k^2 \Psi\left\{(2m\pi)^2 - \Lambda^2\left(\frac{dw^o}{dy}\right)^2\right\} \text{sin } 2m\pi y \right.$$

$$- 2k^2 \Omega\Lambda \frac{d^2w^o}{dy^2} \text{ Sin } 2m\pi y - 4k^2 \Omega(2m\pi)\Lambda \frac{dw^o}{dy} \text{ Cos } 2m\pi y + \Delta$$

$$- \frac{h}{D}\left\{\left(\frac{\rho_f}{\Lambda} + \rho\right) \sigma^2 \Psi \text{ Sin } 2m\pi y - K_1 k^2 \Psi \text{ Sin } 2m\pi y \right.$$

$$+ K_2 \left\langle\left(-(2m\pi)^2 \Psi + \Psi \Lambda^2 \left(\frac{dw^o}{dy}\right)^2 + \Omega\Lambda \frac{d^2w^o}{dy^2}\right) \text{Sin } 2m\pi y \right.$$

$$\left.\left.\left. + 2m\pi\Omega\Lambda \frac{dw^o}{dy} \text{ Cos } 2m\pi y\right\rangle\right\}\right] B_1^* = 0 \qquad (24)$$

where

$$\Delta = \Big\{(2m\pi)^4 \Psi - 6(2m\pi)^2 \Omega\Lambda \frac{d^2w^o}{dy^2} - 6(2m\pi)^2 \Psi\Lambda^2\Big(\frac{d^2w^o}{dy^2}\Big)^2 + 6\Omega\Lambda^3\Big(\frac{dw^o}{dy}\Big)^2 \frac{d^2w^o}{dy^2}$$

$$+ \Psi\Lambda^4\Big(\frac{dw^o}{dy}\Big)^4 + 3\Psi\Lambda^2\Big(\frac{d^2w^o}{dy^2}\Big)^2 + 4\Psi\Lambda^2 \frac{dw^o}{dy}\frac{d^2w^o}{dy^2} + \Omega\Lambda \frac{d^2w^o}{dy^4}\Big\} \operatorname{Sin} 2m\pi y$$

$$+ \Big\{-4(2m\pi)^3 \Omega\Lambda \frac{dw^o}{dy} + 4(2m\pi)\Omega\Lambda^3\Big(\frac{dw^o}{dy}\Big)^3 + 12(2m\pi)\Psi\Lambda^2 \frac{dw^o}{dy}\frac{d^2w^o}{dy^2}$$

$$+ 4(2m\pi)\Psi\Lambda \frac{d^3w^o}{dy^3}\Big\} \operatorname{Cos} 2m\pi y \quad .$$

If, in the above expressions we put $B_2 = 0$ we obtain the solution that is symmetric in z (see (21)). Likewise $A_2 = 0$ yields the solution anitsymmetric in z. In writing down the frequency equation we shall assume the former choice is used, but we note that to obtain the latter solution we just replace $\operatorname{Sinh}(\Lambda c/2)$ by $\operatorname{Cosh}(\Lambda c/2)$ and vice versa, wherever they appear.

Ot obtain the frequency determinant, multiply (24) by $\operatorname{Sin} 2m\pi y$ and integrate from $-1/2$ to $+1/2$. This step leads to many integrals of which the following may be considered typical,

$$\int_{-1/2}^{1/2} \operatorname{Sin}^2 2m\pi y \operatorname{Cosh} \Lambda(w^o + \frac{c}{2})\, dy$$

$$= \operatorname{Cosh} \frac{\Lambda c}{2} \int_{-1/2}^{1/2} \operatorname{Sin}^2 2m\pi y \operatorname{Cosh} \Lambda w^o\, dy + \operatorname{Sinh} \frac{\Lambda c}{2} \int_{-1/2}^{1/2} \operatorname{Sin}^2 2m\pi y \operatorname{Sinh} \Lambda w^o\, dy.$$

We deal with these integrals by noting that [5]

$$\text{Cosh } \Lambda w^{o} = \text{Cosh}(\Lambda w_0 \text{ Cos } \pi y)$$

$$= \sum_{n=0,2,4,\ldots}^{\infty} (2n+1) \left(\frac{\pi}{2\Lambda w_0}\right)^{1/2} I_{n+1/2}(\Lambda w_0)\, P_n(\text{Cos } \pi y)$$

and

$$\text{Sinh } \Lambda w^{o} = \text{Sinh}(\Lambda w_0 \text{ Cos } \pi y)$$

$$= \sum_{n=1,2,5,\ldots}^{\infty} (2n+1) \left(\frac{\pi}{2\Lambda w_0}\right)^{1/2} I_{n+1/2}(\Lambda w_0)\, P_n(\text{Cos } \pi y)$$

where $(\pi/2\Lambda w_0)^{1/2} I_{n+1/2}(\Lambda w_0)$ are Modified Spherical Bessel functions of the first kind and $P_n(\text{Cos } \pi y)$ are the Legendre polynomials. Thus we can write, for example

$$\int_{-b/2}^{b/2} \text{Sin}^2 2m\pi y \text{ Cosh } \Lambda(w^{o} + \frac{c}{2})\, dy = I_1 \text{ Cosh } \frac{\Lambda c}{2} + I_2 \text{ Sinh } \frac{\Lambda c}{2}$$

where

$$I_1 = \sum_{n=0,2,4,\ldots}^{\infty} (2n+1) \left(\frac{\pi}{2\Lambda w_0}\right)^{1/2} I_{n+1/2}(\Lambda w_0) \int_{-1/2}^{1/2} \text{Sin}^2 2m\pi y\, P_n(\text{Cos } \pi y)dy$$

and

$$I_2 = \sum_{n=1,3,5,\ldots}^{\infty} (2n+1) \left(\frac{\pi}{2\Lambda w_0}\right)^{1/2} I_{n+1/2}(\Lambda w_0) \int_{-1/2}^{1/2} \text{Sin}^2 2m\pi y\, P_n(\text{Cos } \pi y)dy.$$

The infinite sums in the I_j integrals must be truncated in all numerical calculations and fortunately it can be shown that the convergence is quite rapid over the range of Λw_0 with which we are concerned. Expanding the Modified Spherical Bessel functions we have, for example

$$\left(\frac{\pi}{2\Lambda w_0}\right)^{1/2} I_{1/2}(\Lambda w_0) = 1 + \frac{(\Lambda w_0)^2}{6} + \frac{(\Lambda w_0)^4}{120} + \frac{(\Lambda w_0)^6}{5040} + \frac{(\Lambda w_0)^8}{362,880} + \cdots$$

$$\left(\frac{\pi}{2\Lambda w_0}\right)^{1/2} I_{11/2}(\Lambda w_0) = \frac{(\Lambda w_0)^5}{10,395} + \frac{(\Lambda w_0)^7}{270,270} + \cdots \quad .$$

Since Λ is order ten or less and $w_0 < 0.3$ in the work presented, the expansions for the M.S.B.F. were truncated at $(\Lambda w_0)^8$ and only three terms were considered in each of the summations for the I_j integrals. A few check cases showed the stability boundaries were insensitive to these numerical approximations.

There are in fact eighteen such integrals that arise in this problem, many of which are functions of m, nine involving the even Legendre polynomials and nine the odd. The nine integrals involving y will be denoted by $I^*_{2j+1}(m,n)$ where $j = 0, 1, 2, \ldots, 8$ and are

$$I^*_1(m,n) = \int_{-1/2}^{1/2} \mathrm{Sin}^2\, 2m\pi y\, P_n(\mathrm{Cos}\, \pi y)\, dy$$

$$I^*_3(m,n) = \int_{-1/2}^{1/2} \mathrm{Sin}^2\, 2m\pi y\, \mathrm{Sin}^2\, \pi y\, P_n(\mathrm{Cos}\, \pi y)\, dy \qquad (25)$$

$$I^*_5(m,n) = \int_{-1/2}^{1/2} \mathrm{Sin}^2\, 2m\pi y\, \mathrm{Cos}\, \pi y\, P_n(\mathrm{Cos}\, \pi y)\, dy$$

$$I_7^*(m,n) = \int_{-1/2}^{1/2} \text{Sin } 2m\pi y \text{ Cos } 2m\pi y \text{ Sin } \pi y \; P_n(\text{Cos } \pi y)\, dy$$

$$I_9^*(m,n) = \int_{-1/2}^{1/2} \text{Sin}^2 2m\pi y \text{ Sin}^2 \pi y \text{ Cos } \pi y \; P_n(\text{Cos } \pi y)\, dy$$

$$I_{11}^*(m,n) = \int_{-1/2}^{1/2} \text{Sin}^2 2m\pi y \text{ Sin}^4 \pi y \; P_n(\text{Cos } \pi y)\, dy$$

$$I_{13}^*(m,n) = \int_{-1/2}^{1/2} \text{Sin}^2 2m\pi y \text{ Cos}^2 \pi y \; P_n(\text{Cos } \pi y)\, dy \qquad (25)$$

$$I_{15}^*(m,n) = \int_{-1/2}^{1/2} \text{Sin } 2m\pi y \text{ Cos } 2m\pi y \text{ Sin}^3 \pi y \; P_n(\text{Cos } \pi y)\, dy$$

$$I_{17}^*(m,n) = \int_{-1/2}^{1/2} \text{Sin } 2m\pi y \text{ Cos } 2m\pi y \text{ Sin } \pi y \text{ Cos } \pi y \; P_n(\text{Cos } \pi y)\, dy \; .$$

Now we may write the final two equations as

$$\Big[\langle k^4 + 2k^2(2m\pi)^2\rangle \{I_1S + I_2C\} - 2(\alpha\pi\Lambda w_0)^2 \{I_3S + I_4C\} + 2(k\pi)^2 \Lambda w_0\{I_5C + I_6S\}$$

$$\overline{\oplus}\, 2(2m\pi)\, \pi\Lambda w_0 \{I_7C + I_8S\} + (2m\pi)^4 \{I_1S + I_2C\} - 6(2m\pi)^2 (\pi\Lambda w_0)^2 \{I_3S + I_4C\}$$

$$+ (\pi\Lambda w_0)^4 \{I_{11}S + I_{12}C\} + 3\pi^4(\Lambda w_0)^2 \{I_{13}S + I_{14}C\} - 4\pi^4(\Lambda w_0)^2 \{I_3S + I_4C\}$$

$$+ 6(2m\pi)^2 \pi^2 \Lambda w_0\{I_5C + I_6S\} - 6\pi^4(\Lambda w_0)^3 \{I_9C + I_{10}S\} + \pi^4 \Lambda w_0\{I_5C + I_6S\}$$

$$\overline{\oplus}\, 4(2m\pi)^3\, \pi\Lambda w_0\{I_7C + I_8S\} \overline{\oplus}\, 4(2m\pi)\, \pi^3(\Lambda w_0)^3 \{I_{15}C + I_{16}S\}$$

$$\overset{+}{\ominus}\, 12(2m\pi)\, \pi^3(\Lambda w_0)^2 \{I_{16}S + I_{18}C\} \overset{+}{\ominus}\, 4(2m\pi)\, \pi^3 \Lambda w_0\{I_7S + I_8C\}\Big]\, C_1^*$$

$$+ (k\pi)^2\, w_0\{I_5S + I_6C\}\, B_1^* = 0$$

where we have utilized the shorthand S for Sinh(Λc/2) and C for Cosh(Λc/2). The second (equilibrium) equation is

$$\Big[(\text{coefficient of } C_1^* \text{ in the above eq.}) - \frac{h}{D}\Big(\Big(\frac{\rho_f}{\Lambda} + \rho\Big)\sigma^2\{I_1C + I_2S\}$$

$$- K_1k^2\{I_1S + I_2C\} + K_2\langle -(2m\pi)^2\{I_1S + I_2C\} + \pi^2(\Lambda w_0)^2\{I_3S + I_4C\}$$

$$- \pi^2\Lambda w_0\{I_5C + I_6S\} \oplus 2(2m\pi)\pi\Lambda w_0\{I_7C + I_8S\}\rangle\Big)\Big] B_1^*$$

$$- \frac{h}{D}(k\pi)^2 w_0\{I_5S + I_6C\} C_1^* = 0 \quad .$$

There appears to be no hope for a closed form solution of the frequency determinant and a digital computer program must be relied upon to perform the bulk of the arithmetic. The procedure is as follows:

(i) Choose a value of m and insert the appropriate I_j integrals.

(ii) With $\sigma^2 = 0$, solve the determinant for a succession of values of k, taking note of those values for which the determinant vanishes. They provide the stability boundary for perturbations antisymmetric in y and symmetric z. The background to using $\sigma^2 = 0$ as a stability criterion is reviewed in [1].

Next we must consider the case of perturbations that are symmetric functions of y, namely $\Gamma = (2m+1)\pi$, which is very similar to the previous case with the following exceptions:

(i) Replace Sin(2mπy) and Cos(2mπy) by Cos(2m+1)πy and Sin(2m+1)πy respectively wherever they occur. This affects only the $I_j^*(m,n)$ integrals.

(ii) Replace $(2m\pi)$ by $(2m+1)\pi$ wherever it occurs.

(iii) There are six sign changes in the determinant indicated by a circle around the sign underneath that for $\Gamma = 2m\pi$ which must be accounted for.

To obtain the solutions that are antisymmetric in z, we just replace $\mathrm{Sinh}(\Lambda c/2)$ by $\mathrm{Cosh}(\Lambda c/2)$ wherever they appear. The four cases that must be investigated separately can be described as follows:

Case 1: Antisymmetric in y and Symmetric in z

Case 2: Symmetric in y and Symmetric in z

Case 3: Antisymmetric in y and Antisymmetric in z

Case 4: Symmetric in y and Antisymmetric in z.

1.6. Relationship Between Frequency and Wavelength of the Perturbations.

The dispersion relationship is well known to be $\bar{f} = \bar{c}_G/\bar{\lambda} = \bar{c}_G\,\bar{k}/2\pi$. If we assume, as a first rough approximation, that the group velocity does not change with artery cross section and utilize $\bar{c}_G = 500$ cm/sec from [1], we obtain $\bar{f} = 80\,\bar{k}$. In nondimensionalizing the equations we have taken $\bar{b}$ as the basic length. Thus the total circumference of the artery is $2\bar{b}(1+c)$ and assuming a radius of the brachial artery in its natural condition of 0.4 cm we have $2\bar{b}(1+c) = 2\pi(0.4)$, i.e., $\bar{b}(1+c) = 1.26$ cms. Thus for $c = 0.5$ we take $\bar{b} = 0.84$ cm, for $c = 0.25$, $\bar{b} = 1.0$ cm. Clearly the relationship between frequency and wave number is a function of the parameter c defining the ratio of the sides of the rectangular cross section used in the theory, but as an approximate relation we take $\bar{b}$ as

unity and hence $\bar{f} \cong 80\,\bar{k}$. This is used to provide an approximate dimensional frequency scale on the curves.

1.7. Presentation of the Results.

Before considering the strictly physiological implications let us note some of the stability boundary characteristics and the manner in which certain parameters influence them.

1.7.1. Perturbations antisymmetric in y and symmetric in z. The stability boundaries for a typical set of parameters are shown in Fig. 2 as a function of the quasi static strains and deflection, with a negative deflection being inward. Thus for $c = 0.5$, $w_0 = -0.25$ and for $c = 0.25$, $w_0 = -.125$ correspond to the two flexible plates being in contact with each other at the midpoints. Even though it is very doubtful that plate theory is applicable for such highly curved configurations we include the corresponding results with this reservation in mind. From Fig. 2 it is clear that the stability boundaries change character rather significantly as the artery walls are allowed, by decreasing the cuff pressure or increasing the intraluminal pressure to move outwards. This is particularly true for $w_0 \leq -.10$. Otherwise, we have only relatively small changes in the stability boundaries. For large outward deflections, the artery cross section will become more rounded and the "sides" will cease to be rigid, thus violating one of our basic assumptions.

In all the data presented here, the change from stability to instability occurred very suddenly. Using $\sigma^2 = -10^4$ yields stability

boundaries that cannot, to within graphical accuracy, be distinguished from those for $\sigma^2 = 0$. The results for all four types of perturbations exhibited this characteristic. The fact that there is virtually no change in the boundaries for large negative values of σ^2 tends to corroborate the experimental evidence that the change from stable (silent) to unstable (audible) conditions is quite sudden. Anliker and Raman [1] have expounded in considerable detail on the mechanism by which the inaudible pressure fluctuations in the arterial flow are amplified into the audible range by the cuff-induced instability, and we refer the reader to that work. It suffices to say here that the disturbance is amplified by $\exp|\sigma|\tau$ as it passes through the unstable artery segment, where τ is the lesser of the instability duration or the time taken for it to travel through the cuff.

When the two opposite plates are not close together, say $w_0/c \geq -0.25$ the consistent negative slope of the stability boundaries in Fig. 2 is intuitively reasonable. They indicate that for a prescribed axial stretch the system is stable when the lateral strain is tensile, or if compressive, of a sufficiently small value. Only when the lateral compressive strain exceeds a certain limit does the system become unstable. When the plates have a relatively large inward deflection the situation is markedly different, as typified by the top of Fig. 2 which illustrates the characteristic behavior. There is a "separation" wavelength that divides two entirely different modes of behavior. On the high frequency or high wave number side of this critical wavelength, the character of the stability boundaries can be explained by the argument presented above.

However, at the frequencies below this critical one, the behavior is somewhat different. The distinguishing characteristic is that in this wavelength regime, for a prescribed axial stretch, an increase in the absolute value of the compressive strain stabilizes the system.

In an attempt to explain this, the wall thickness of the artery was changed by fifty percent and a number of calculations redone. The value of the separation frequency and the general character of the stability boundaries remained unchanged as shown in Fig. 6. Similarly a twenty percent change in fluid density produced virtually identical stability boundaries as the data presented. These simple attempts to isolate whether the phenomenon was primarily due to structural or fluid behavior thus failed to shed any light to the problem. It should be recalled that the equilibrium configuration of the plate is a highly curved surface for which the applicability is questionable. The essential behavior of the stability boundaries shown in Fig. 2 could always be observed for any value of m considered.

As is to be expected, the quasi static strains exercise a dominant influence on the frequency range in which perturbations are amplified. While ϵ_x^o, the axial stretch of the artery, remains fairly constant during blood pressure measurements, this is not true for ϵ_y^o since the cross section undergoes very significant changes, and the lateral strain varies markedly along the circumference and with time. This is discussed further when the physiological implications are reviewed.

The influence of the transverse wavelength, manifested in the parameter m, is relatively insignificant and the general result is that

the character of the boundaries is only weakly dependent on m, at least for m less than five. No attempt was made to obtain data for larger values of this parameter.

In the theoretical model, the rather complex cross section of the artery has been replaced by a rectangle having one pair of sides rigid and the other able to deflect. Theory provides no guide as to the most realistic ratio of the sides, i.e., the parameter c. It is clear from the equations that stability boundaries are independent of c, for $w_0 = 0$, and the differences which do occur for the relatively small deflections are not significant.

1.7.2. Case 2. Perturbations symmetric in y and symmetric in z. The general pattern of the stability boundaries is similar to that of Case 1. When the flexible artery walls are close together we have again two separate regions of instability which merge into one as w_0 tends to zero. The influence of the number of transverse waves is small.

1.7.3. Case 3. Perturbations antisymmetric in y and antisymmetric in z. Perturbations that are antisymmetric in z exhibit behavior somewhat different from the symmetric, as can be seen in Fig. 3. For $c = 0.5$ and small lateral strain, a large range of disturbances is being amplified even when the two flexible walls are in contact. However, for $c = 0.25$ there is no "separation" frequency and the theory predicts that unless the absolute value of the compressive lateral strain is much smaller than the axial strain, we would expect to hear a range of low frequency perturbations amplified for all positions of the artery wall. This evidence tends

to suggest that Korotkoff sounds due to this mode may be audible when the opposite walls of the artery are just in contact at the midpoint of the flexible sides. The wall on either side of this contact point is perfectly free to oscillate.

1.7.4. Case 4. Perturbations symmetric in y and antisymmetric in z. These are very similar to those of Case 3 and will not be discussed further.

1.7.5. Further discussion of the stability boundaries. In summarizing we note that the stability boundaries are highly dependent upon the quasi static prestress as would be expected. The transition from stable to unstable conditions is very clearly defined in that $\sigma^2 = 0$ and $\sigma^2 = -10^4$ yield virtually identical boundaries showing that the system changes rapidly from a stable one to a highly unstable one. This supports the evidence of a sudden onset of Korotkoff sounds at systole. It must be noted that at the large axial strains representative of the brachial artery in situ, the compressive strains needed to produce the instabilities are an order of magnitude larger than those usually considered in the analysis of metallic structures.

1.8. Discussion of the Results and Their Relationship to the Physiological Phenomena Occurring at Systole.

The fluid-shell instability mechanism postulated by Anliker and Raman [1] for Korotkoff sounds at diastole, is extended to the systolic case for which the cross section is no longer a circle.

We have discussed the four types of behavior that depend on the symmetries of the motions relative to the major axes of the cross sections. It is pertinent to question whether any of these modes are more likely than the others to be the major cause of the Korotkoff sounds. In attempting to answer this question it eases the discussion if we refer to Fig. 7 which illustrates the motions involved in the four cases. Since the artery is surrounded by virtually incompressible fluid-filled tissues which are being compressed by the cuff, the resistance to the deformations of Case 2 are considerable since it involves a net change of artery cross sectional area. In Case 4 there is a movement of the artery center of gravity in the z direction which would necessitate some fluid motion outside the artery from the positive z, to negative z sides and back, during each cycle. This could not occur very easily in the arm under a cuff. On the other hand Cases 1 and 3 do not involve a change in cross sectional area. This suggests that they are less restrained by either the tissues or cuff and, therefore, are more likely to participate in the generation of the Korotkoff sounds. For this reason attention will be restricted in what follows to the two Cases 1 and 3 whose motions are antisymmetric in the y coordinate. While bearing in mind what has just been said about the stability boundaries predicted by the theory, let us consider what happens as the cuff pressure is raised to well above the systolic pressure and then is gradually released, as during the auscultatory blood pressure measurement. In doing this let us focus attention on the history of the quasi static lateral strain. Initially, the cuff pressure is markedly greater than the intraluminal pressure and the artery is almost completely occluded as sketched in Fig. 8a. Simple statics

analysis shows that the quasi static stress is compressive in the artery walls at all points well removed from the region of very large curvature. The magnitude of the compressive stress is approximately the pressure difference. It is worth noting that in the theoretical model the concave inward wall is in tension when the cuff pressure exceeds the intraluminal, as the flexible walls are simply supported at fixed corners. This must be borne in mind when interpreting the results. Also, the theory is not applicable and also we do not expect to hear any sounds when large portions of the opposite walls are in contact with each other.

As the cuff pressure is decreased below the maximum intraluminal pressure, as shown in Fig. 8b, the initial deflection pattern will intermittently exhibit complete separation of the walls. In this situation simple equilibrium considerations of the membrane indicate that there are three contributions to the lateral stress in the wall at the point M. One is simply $(p_i - p_e)$ regardless of whether the walls are in contact or not. The second occurs only when the walls separate and is $(p_i - p_e)\, d/h$ where d is the gap between the walls and h their thickness. The third and for our purposes the most important component is due to the curvature of the artery wall. If it is assumed that the points L and M do not move, the wall element between them is subjected to a stress of $(p_e - p_i)\, R/h$ when the radius of curvature is of constant magnitude R. Therefore

$$\epsilon_y^o = \frac{(p_i - p_e)}{E}\left(1 + \frac{d}{2h} - \frac{R}{h}\right) \quad \text{for} \quad w_o < 0 \qquad (27)$$

and the sign of this quasi static strain is of paramount importance in our analysis. As previously stated, the theory becomes questionable for large deflections and in certain cases the stability boundaries have a peculiar character when the initial curvature is large. As of now these peculiarities cannot be explained in terms of physical considerations. A separate investigation is needed to explain them. However, the results depicted in Fig. 4b for Case 3 are consistently in agreement with our intuition even when the initial displacements are large and we shall base much of the ensuing discussion on these curves. It is clear that to explain Korotkoff sounds by the theory presented, large quasi static compressive strains must occur. Let us consider in some detail what happens when the cuff pressure is in the neighborhood of systolic pressure and let us hypothesize how the Korotkoff sounds are being generated.

It has been well established experimentally [2] that Korotkoff sounds are not audible until the walls have separated as shown in Fig. 7b. During the time the artery is virtually occluded the proximal peak pressure builds up to a value somewhat in excess of the normal peak pressure that would exist in the absence of the cuff. As the artery walls separate due to a lowering of the cuff pressure, a large compressive strain is produced as soon as the cuff pressure drops below the intraluminal pressure. This large compressive strain is due to the "curvature" of the wall and is represented by the last term of (27). As the inrushing blood attempts to distend the artery, the inertia and elastic forces in the surrounding medium and the cuff inhibit such distension. Thus the points L and N in Fig. 8b can be considered as essentially stationary, while the flexible wall acts as an arch.

To quantise the level of lateral strain that may occur, let us take the situation when the intraluminal pressure exceeds that in the cuff of 5mm Hg, $E = 10^6$ dynes/cm^2, $h = d = 1$ mm and $R = 2.0$ cm. Then (27) yields $\epsilon_y^o = -.10$. Since the axial stretch in an artery is at least 0.2, this is seen from Fig. 4b, to be a little too small to explain Korotkoff sounds at systole, but it is off the right order of magnitude. But increasing the pressure difference to 10 mm Hg or increasing R provides a situation where the theory predicts amplification of the low frequency perturbations when $\epsilon_x^o = 0.2$.

The large compressive quasi static strain state postulated need exist for only about a tenth of a cardiac cycle or less due to the high amplification factor which is of order exp. 30 (see [1]). Another important aspect is that it takes a finite time to amplify the perturbations inherent in the arterial flow to an audible level. If the time duration of the prestress required to produce instability is less than that needed to amplify the perturbations to the audible level so sounds are heard. Thus when $p_e < p_i$ for a sufficiently small time duration, the human ear will not detect sounds. This suggests that the auscultatory systolic peak will be slightly below the peak intraluminal pressure. On the other hand, and as previously mentioned, while the brachial artery is occluded the pressure builds up the systolic peak proximal to the cuff to a level markedly greater than when the cuff is removed. Experimental evidence suggests that the latter influence is the more significant and the auscultatory technique generally leads to an upper bound of the systolic pressure.

The hypothesis presented appears to support many of the facets evidenced in experiments [2] and [6] in which measurements were made of the quasi static pressure and of the Korotkoff sounds generated in a physical model of the brachial artery. Figure 8 gives a diagram of the experimental setup and tracings of representative sounds and pressure recordings and shows the microphone sensed fluctuations prior to the human ear. This seems to support the contention that it takes a finite time for the perturbations to be amplified to the audible level and the microphone responds at a lower level of amplification than the ear. Another very interesting facet illustrated in Fig. 8 is that the distal (downstream) pressure measurement F exhibits high frequency fluctuations for cuff pressures above systolic while that at the proximal end of the cuff model at C shows them only very slightly. This tends to support the idea of the cuff acting as a mechanical amplifier which magnifies the perturbations as they propagate through the segment of the artery affected by the cuff. If the Korotkoff sounds were due to a sudden collapse of the artery wall, the response would be equally strong at point C as at point F.

As the cuff pressure is reduced the duration of the cardiac cycle in which the intraluminal pressure exceeds that of the cuff is increased as indicated in Fig. 8c. This should lead to an increase in the Korotkoff sound intensity as is indeed observed, clinically and experimentally.

Thus far we have restricted the discussion to that part of the cardiac cycle when w_0 is less than zero and the intraluminal pressure exceeds that in the cuff. For w_0 greater than zero the artery becomes

approximately elliptic in cross section and the quasi lateral strain in the artery is compressive only during that phase of the cardiac cycle in which the cuff pressure exceeds the intraluminal pressure. Once the artery takes on this shape the theory and intuition lead us to expect audible pressure fluctuations only during the downstroke from the systolic peak of the cardiac cycle. Looking at Fig. 9, we see this is precisely what happens. The initial sounds recorded by the microphone occur just at the peak of the quasi static pressure at F, measured downstream of the cuff. If we superimposed on the recording of F a sinusoidal wave to approximate the quasi static pressure of the cardiac cycle as it would be without the modulation we see that as the cuff pressure is reduced, the Korotkoff sounds are generated progressively further along the downstroke from the systolic peak. Explaining the behavior when the cuff pressure approaches the average of the cardiac cycle is beyound the scope of this investigation.

In trying to assess the influence of the arterial stiffness on the systolic pressure, it appears that a reduction in the axial stretch leads to an increase in the systolic pressure measured by the auscultatory technique. To illustrate this, let us assume, as a rough approximation that for a prescribed deflected shape of the flexible wall, that the lateral quasi static strain is directly related to the cuff pressure and for illustrative purposes only, focus attention on the curves for $w_0 = -0.10$ in Fig. 4b. If we have $\epsilon_x^o = 0.35$ and $\epsilon_y^o = -0.20$ or less, we have no perturbations amplified and we conclude the cuff pressure is above systolic. If instead, we take $\epsilon_x^o = 0.2$, a range of frequencies is amplified and if sufficiently so, we are lead to believe that the

cuff pressure is below systolic. This reduced axial stretch leads to increased levels of systolic pressure measured by the auscultatory technique.

The influence of thickening of the arteries can be inferred from Fig. 6, from which we note that the range of frequencies that are amplified by the instability is reduced. This means that a thicker artery is either stable or has a smaller region of instability which results in a slight reduction in the systolic pressure. Therefore, the two effects that can occur in older persons, namely stiffening of the artery wall and reduction in axial stretch tend to have opposite effects on the measurements of systolic pressure by the auscultatory technique. This may mean the method's accuracy is maintained regardless of age provided the two influences mentioned are reasonably well balanced.

1.9. Conclusions.

The simple theoretical model of the brachial artery subjected to a cuff pressure, predicts amplification of a range of the lower frequency perturbations inherent in the arterial blood flow. Several aspects of the hypothesis put forward to explain the Korotkoff sounds at systole as an example of fluid-shell instability induced by the cuff pressure are in substantial agreement with available experimental evidence. For cuff pressures well above systolic the artery is virtually occluded and the theory is not applicable. As the cuff pressure drops below the intraluminal peak a range of low frequency perturbations is amplified due

to the instability caused by large compressive strains. As the cuff pressure decreases, the duration of the instability increases, leading to more intense Korotkoff sounds.

It is shown that decreasing the axial stretch of the artery can lead to increased systolic pressures measured by the auscultatory technique while increasing the artery stiffness reduces the high frequency content of the initial Korotkoff sounds.

The pecular behavior of some of the predicted stability boundaries for certain mode shapes and the artery walls which are strongly deflected by the cuff pressure cannot be satisfactorily explained. While these discrepancies occur outside the range of strict applicability of the plate theory utilized and only for certain modes, it is not clear why the stability boundaries exhibit intuitively reasonable behavior for some types of perturbations but not for others. This behavior must be investigated more deeply in a separate analysis.

It is considered that there is much evidence to support the hypothesis that the Korotkoff sounds at systole are also a manifestation of dynamic instability which amplifies the perturbations above the audible level.

NOTATION

$\bar{b}$	Width of the rectangular tube model of the artery
$c = \bar{c}/\bar{b}$	Nondimensional depth of the rectangular tube model of the artery
$c_G = \bar{c}_G/\bar{\omega}_0\bar{b}$	Nondimensional group velocity
$D = h^2/12(1-\nu^2)$	Nondimensional bending stiffness of the artery wall
$\bar{E}$	Young's modulus of the artery wall
$F = \bar{F}/\bar{E}\bar{b}^2$	Nondimensional stress function
$f = 2\pi\bar{f}/\bar{\omega}_0$	Nondimensional frequency
$h = \bar{h}/\bar{b}$	Nondimensional artery thickness
I_j, $I^*_{j,k}$	Integrals defined in equ. (25)
K_1, K_2	Nondimensional static prestresses in the artery
$k = 2\pi/\lambda$	Wave number
m	Number of half waves in the y direction
N_x, N_y, N_{xy}	Nondimensional stress resultants in the artery

$P_n(\cdot)$	Legendre polynomial
$p = \bar{p}/\bar{E}$	Nondimensional pressure
$q = \bar{q}/\bar{E}$	Nondimensional transverse force
$t = \bar{\omega}_0\bar{t}$	Nondimensional time
$U = \bar{U}/\bar{b}\bar{\omega}_0$	Nondimensional blood velocity
$w = \bar{w}/\bar{b}$	Nondimensional transverse displacement of the artery
$x,y,z = \bar{x}/\bar{b},\ \bar{y}/\bar{b},\ \bar{z}/\bar{b}$	respectively, the nondimensional coordinates
Γ	$2m\pi/b$ for perturbations antisymmetric in y $(2m+1)\pi/b$ for perturbations symmetric in y
Λ	$[\Gamma^2+k^2]^{1/2}$
$\lambda = \bar{\lambda}/\bar{b}$	Nondimensional wavelength
ν	Poisson's ratio
$\rho = \bar{b}^2\ \bar{\omega}_0^2\ \bar{\rho}/\bar{E}$	Nondimensional density of the artery
$\rho_f = \bar{b}^2\ \bar{\omega}_0^2\ \bar{\rho}/\bar{E}$	Nondimensional density of the blood
$\phi = \bar{\phi}/\bar{b}^2\ \bar{\omega}_0$	Nondimensional fluid perturbation potential
$\sigma = \bar{\sigma}/\bar{\omega}_0$	Nondimensional circular frequency
$\bar{\omega}_0 = [\bar{E}/\bar{\rho}_0\ \bar{b}^2(1-\nu^2)]^{1/2}$	The normalizing frequency
$\bar{\cdot}$	Denotes a dimensional quantity

REFERENCES

[1] Anliker, M. and Raman, K. R., "Korotkoff Sounds at Diastole - A Phenomenon of Dynamic Instability of Fluid-Filled Shells", International Journal of Solids of Structures 2, No. 3, 467-491 (1966).

[2] Raman, K. R., "Experimental Study of the Mechanical Behavior of Flexible Fluid Filled Tube, Simulating Arteries", Engineers Thesis, Stanford University, 1964.

[3] Raman, K. R., "Korotkoff Sounds at Systole--A Phenomenon of Dynamic Instability", Vidya Report No. 214, February 1966.

[4] Timoshenko, S. and S. Woinowsky-Krieger, Theory of Plates and Shells, McGraw-Hill, Inc., 1959.

[5] Abramowitz, M. and I. A. Stegun, "Handbook of Mathematical Functions", NBS Applied Math. Series No. 55, U.S. Government Printing Office 1964, pp. 445.

[6] Sacks, A. H., K. R. Raman, and J. A. Burnell, "A Study of Auscultatory Blood Pressure in Simulated Arteries, Part 4", Proc. 4th Int. Congr. on Rheology, edited by A. L. Copley, pp. 215-230, Interscience, 1965.

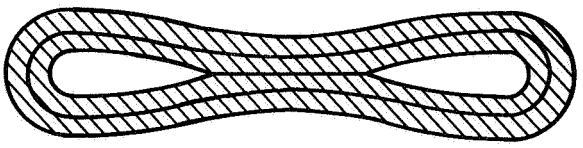

Fig. 1a. Sketch of the Brachial Artery Cross Section at Cuff Pressures Just Above Systolic

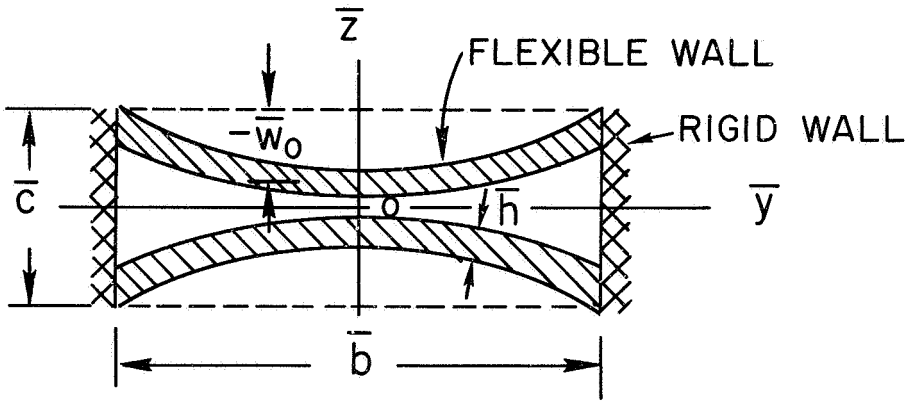

Fig. 1b. Model of the Artery Cross Section Used in the Analysis

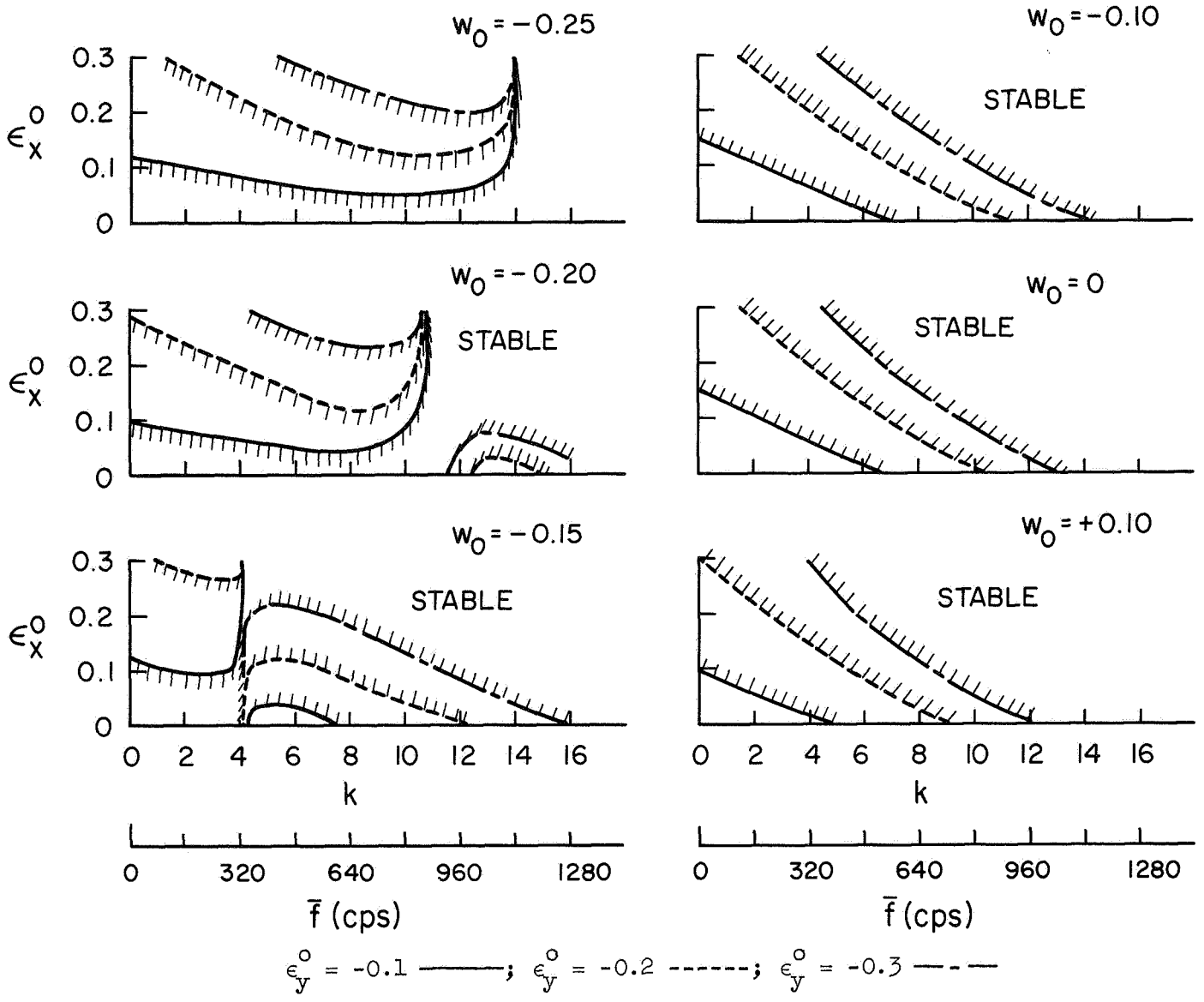

Fig. 2a. Stability Boundaries for Case 1, m = 1
Perturbations for c = 0.5

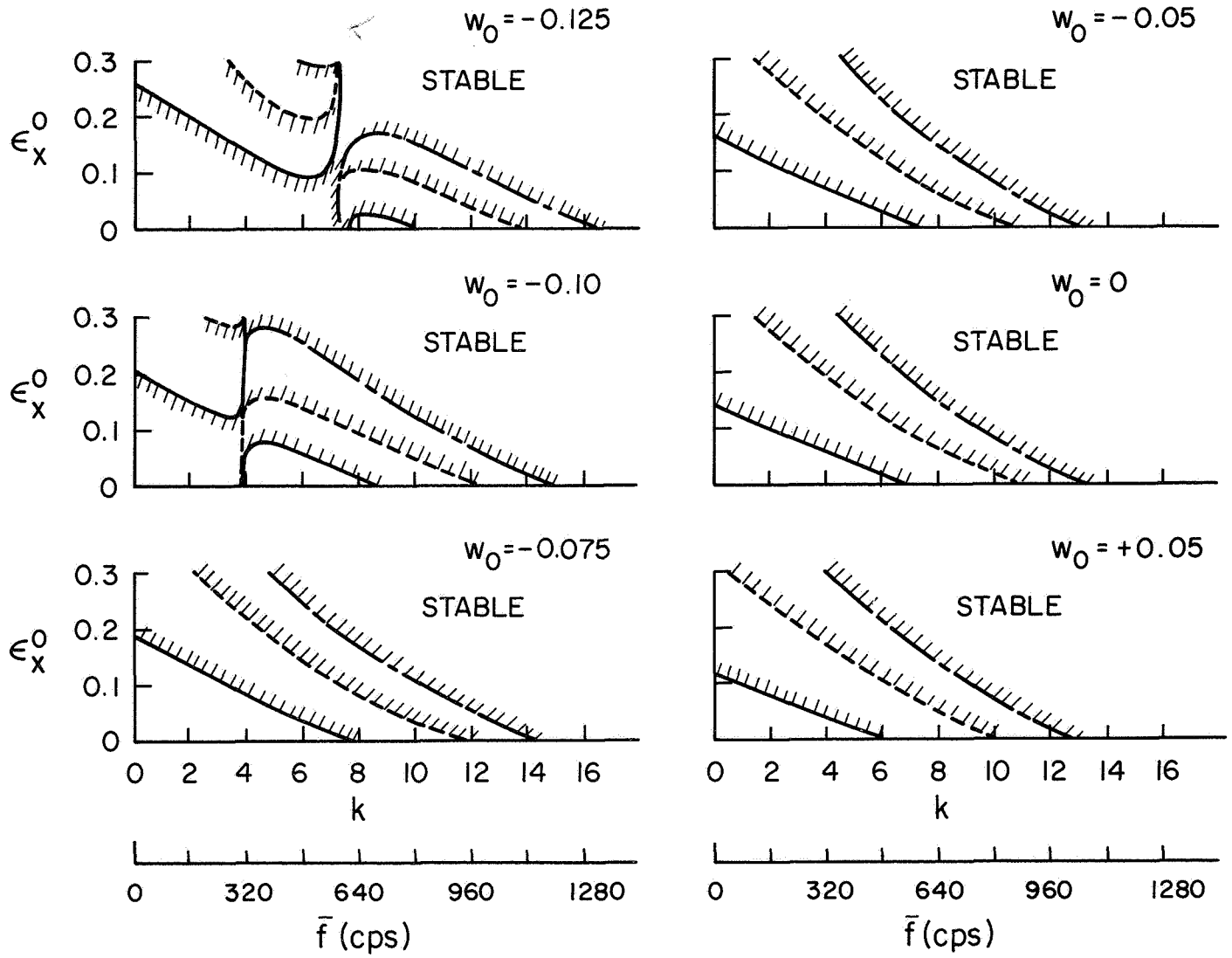

Fig. 2b. Stability Boundaries for Case 1, m = 1
Perturbations for c = 0.25

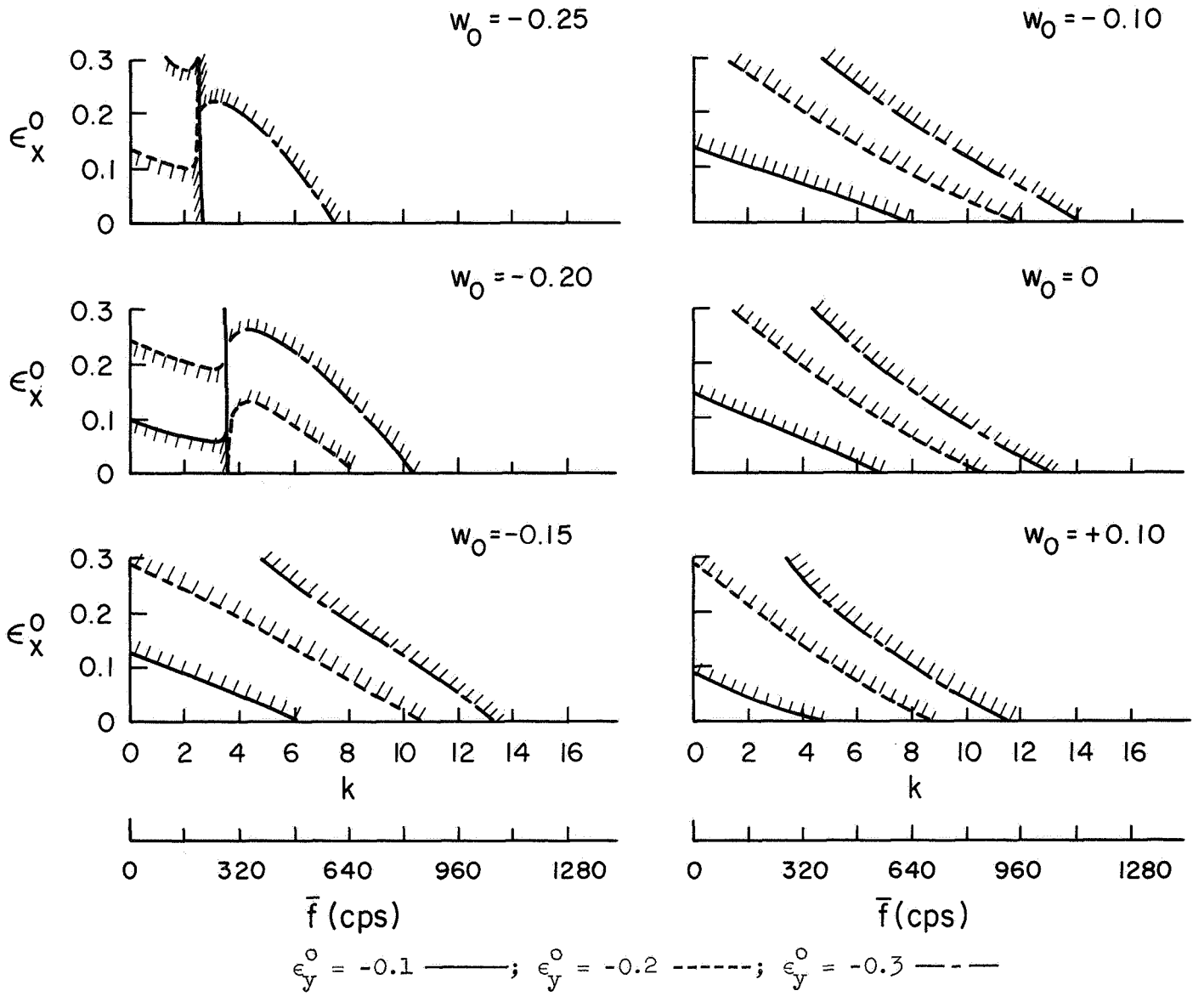

Fig. 3a. Stability Boundaries for Case 2, m = 0
Perturbations for c = 0.5

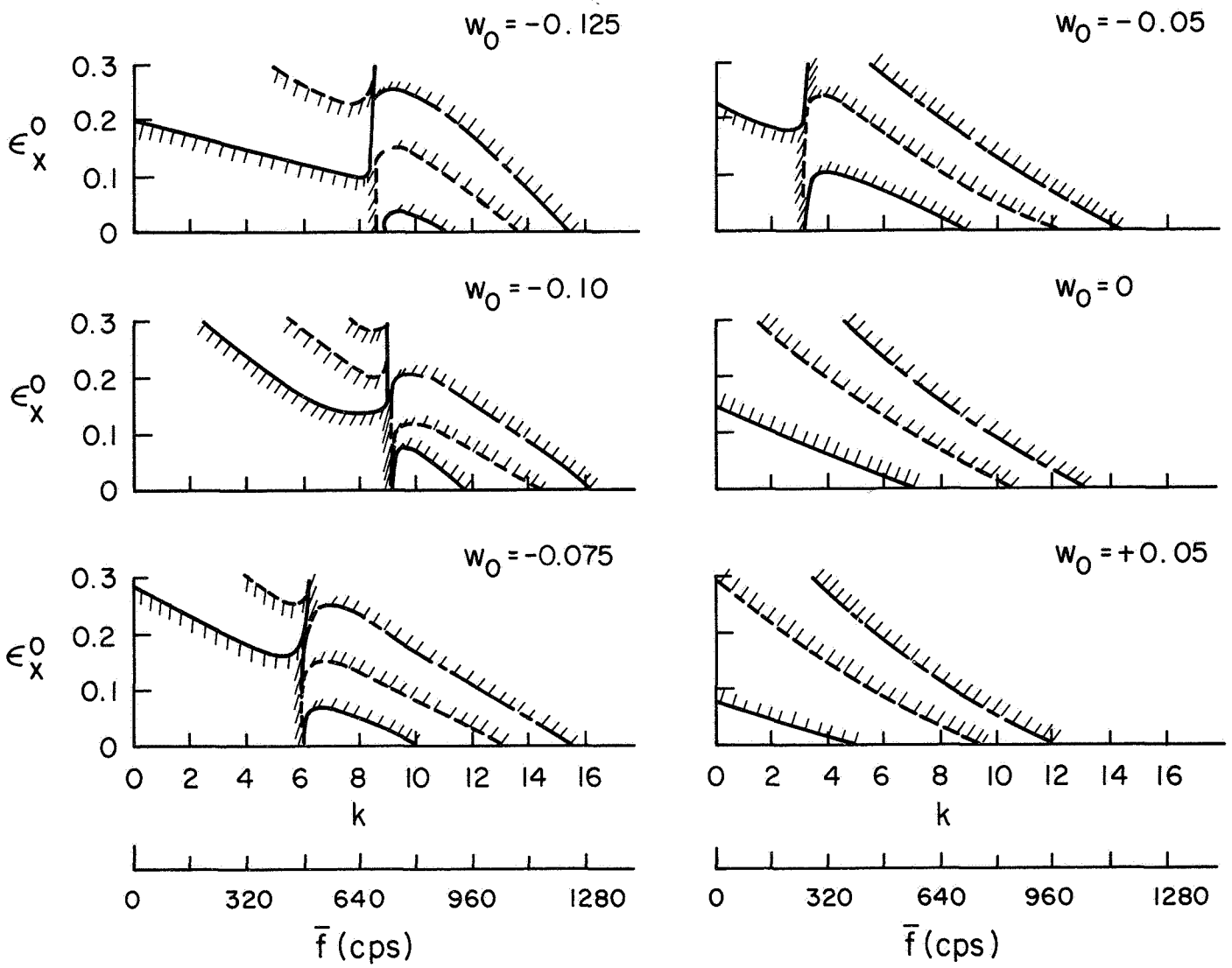

$\epsilon^0 = -0.1$ ———; $\epsilon_y^0 = -0.2$ ------; $\epsilon_y^0 = -0.3$ — - —

Fig. 3b. Stability Boundaries for Case 2, m = 0
Perturbations for c = 0.25

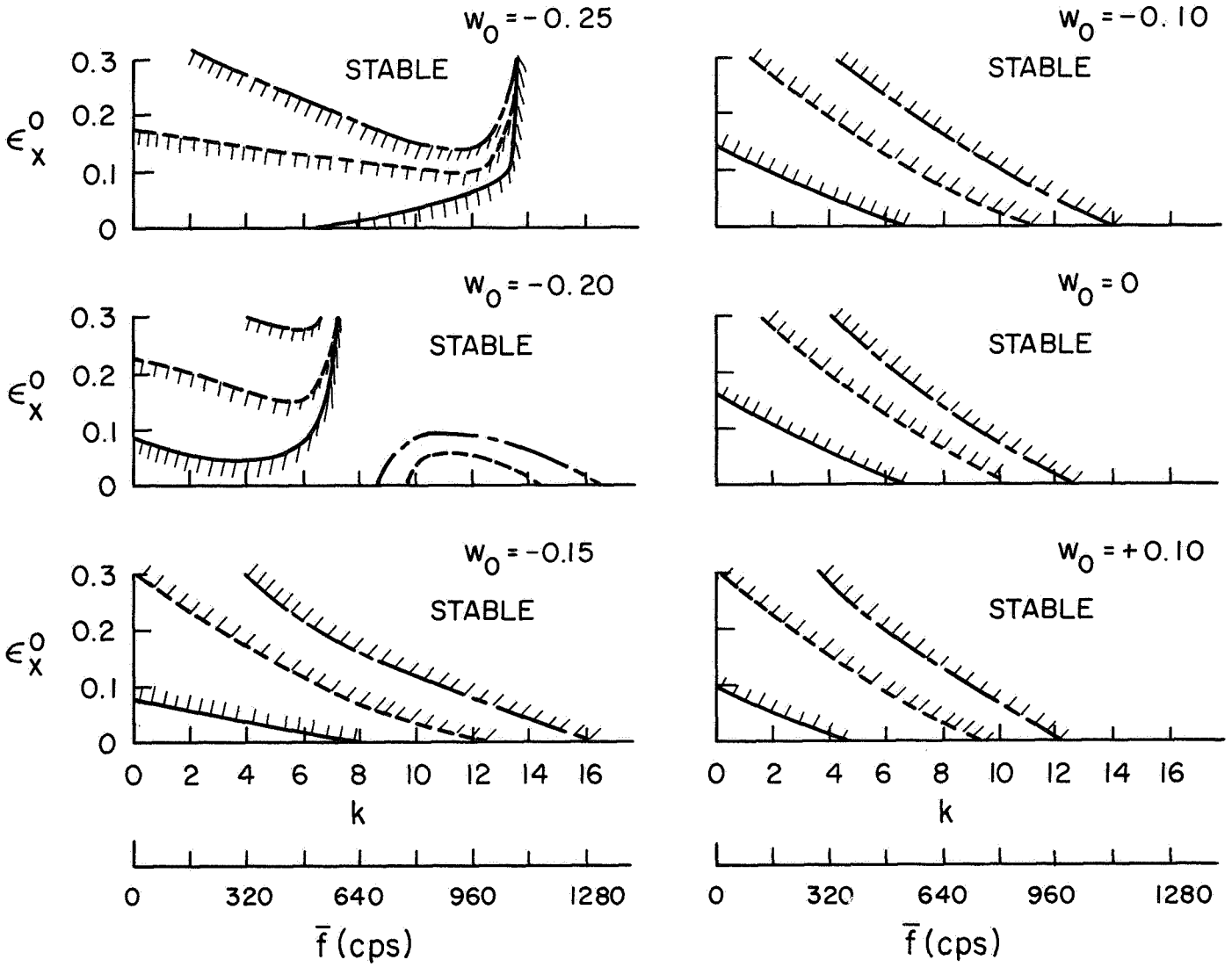

Fig. 4a. Stability Boundaries for Case 3, m = 1
Perturbations for c = 0.50

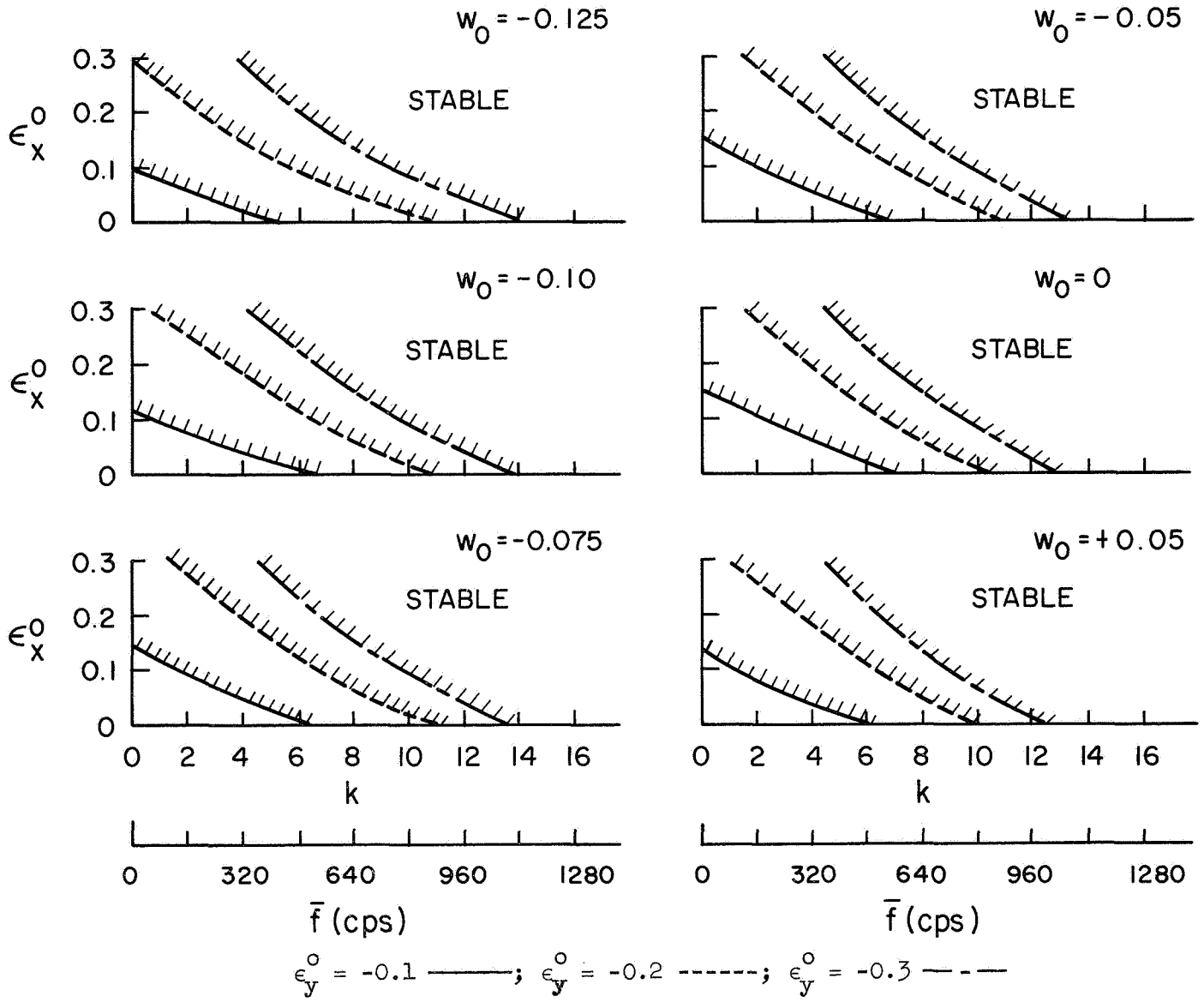

Fig. 4b. Stability Boundaries for Case 3, m = 1
Perturbations for c = 0.25

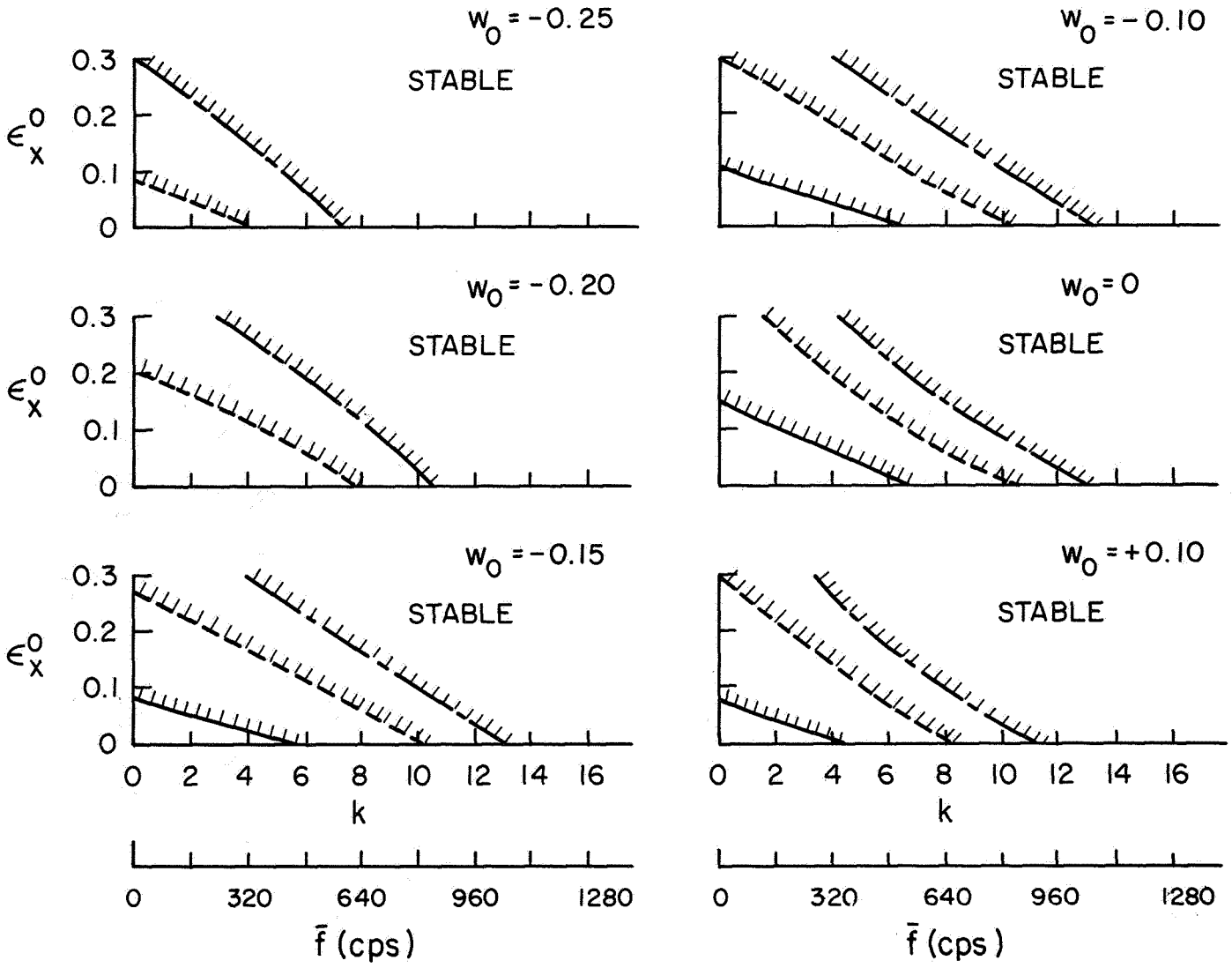

Fig. 5a. Stability Boundaries for Case 4, m = 0
Perturbations for c = 0.50

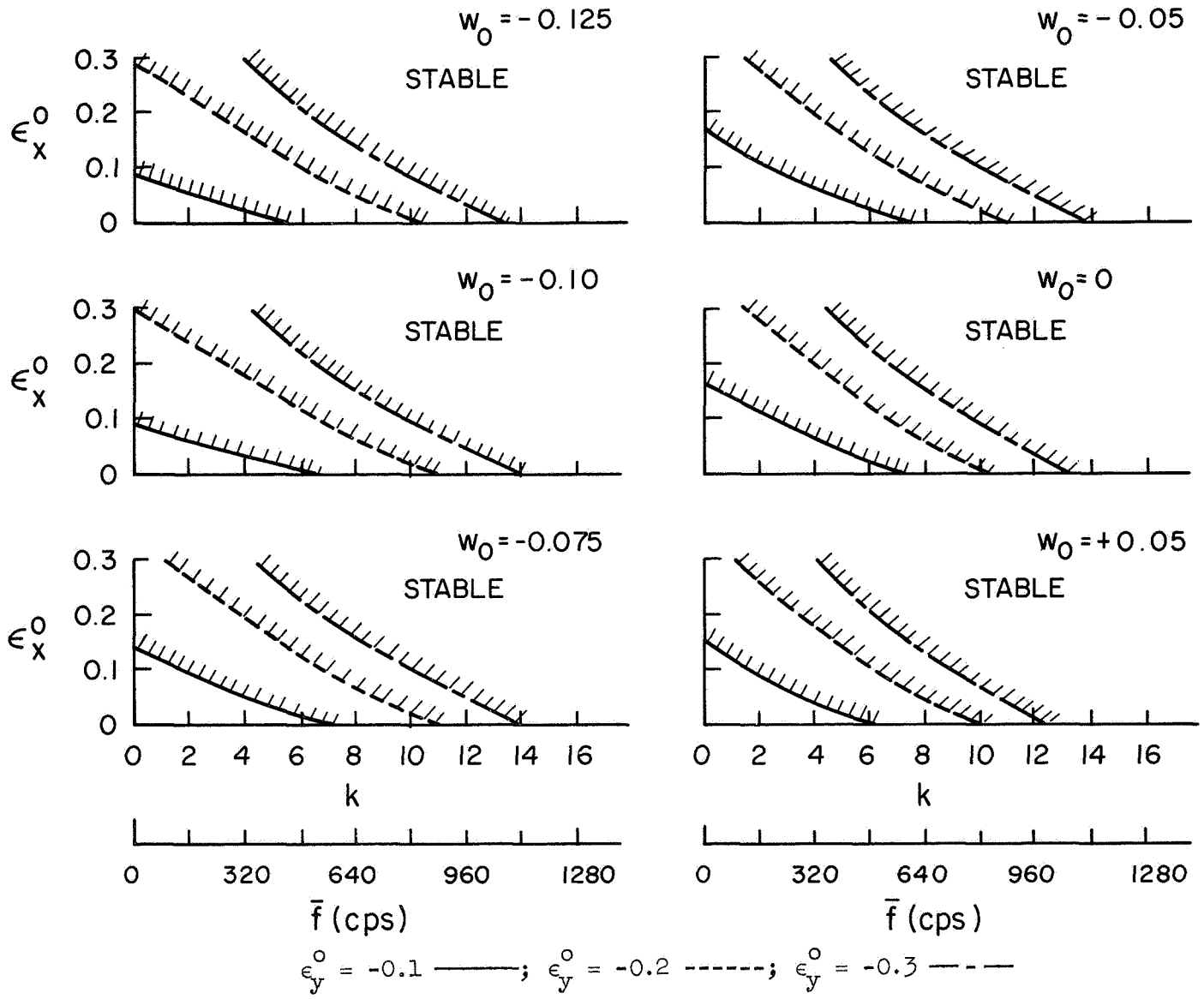

Fig. 5b. Stability Boundaries for Case 4, m = 0
Perturbations for c = 0.25

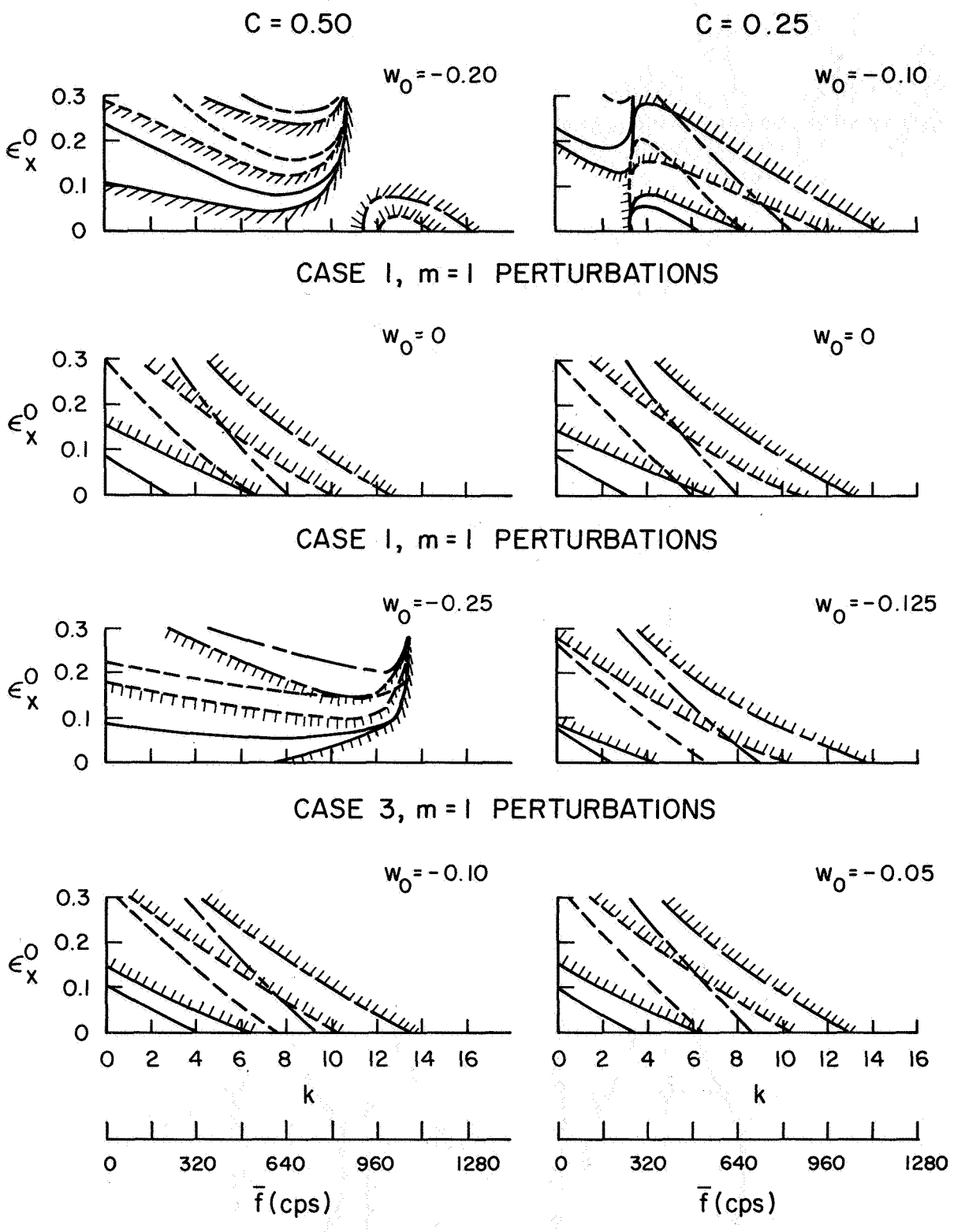

$\epsilon_y^0 = -0.1$ ———; $\epsilon_y^0 = -0.2$ ------; $\epsilon_y^0 = -0.3$ — - —

The boundaries for h = 0.1 are cross hatched on the stable side. Those for h = 0.15 are not cross hatched.

Fig. 6. Influence of Wall Thickness on the Stability Boundaries

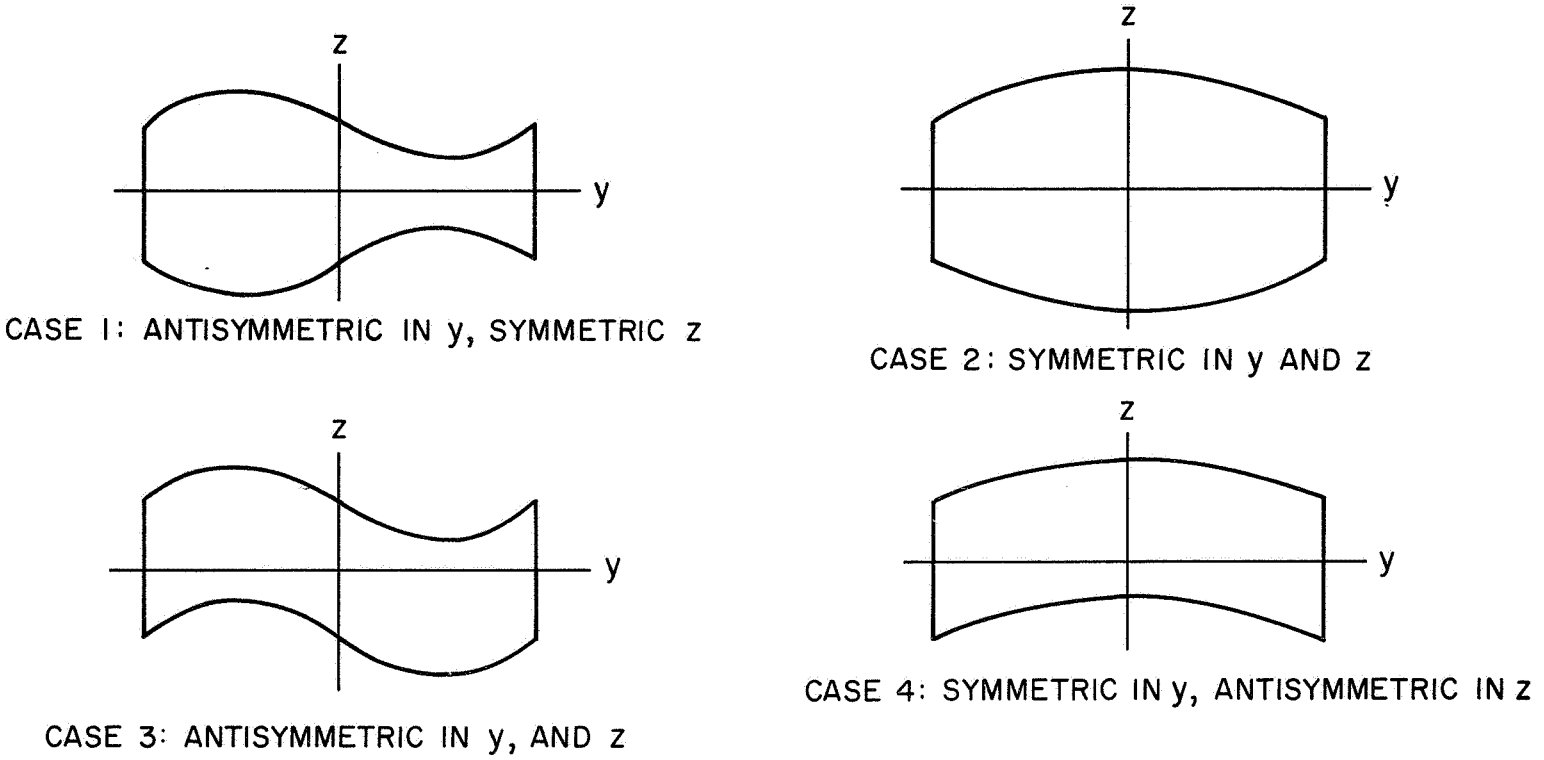

Fig. 7. Deformation Mode Shapes of the Four Cases of Instability when $w_0 = 0$

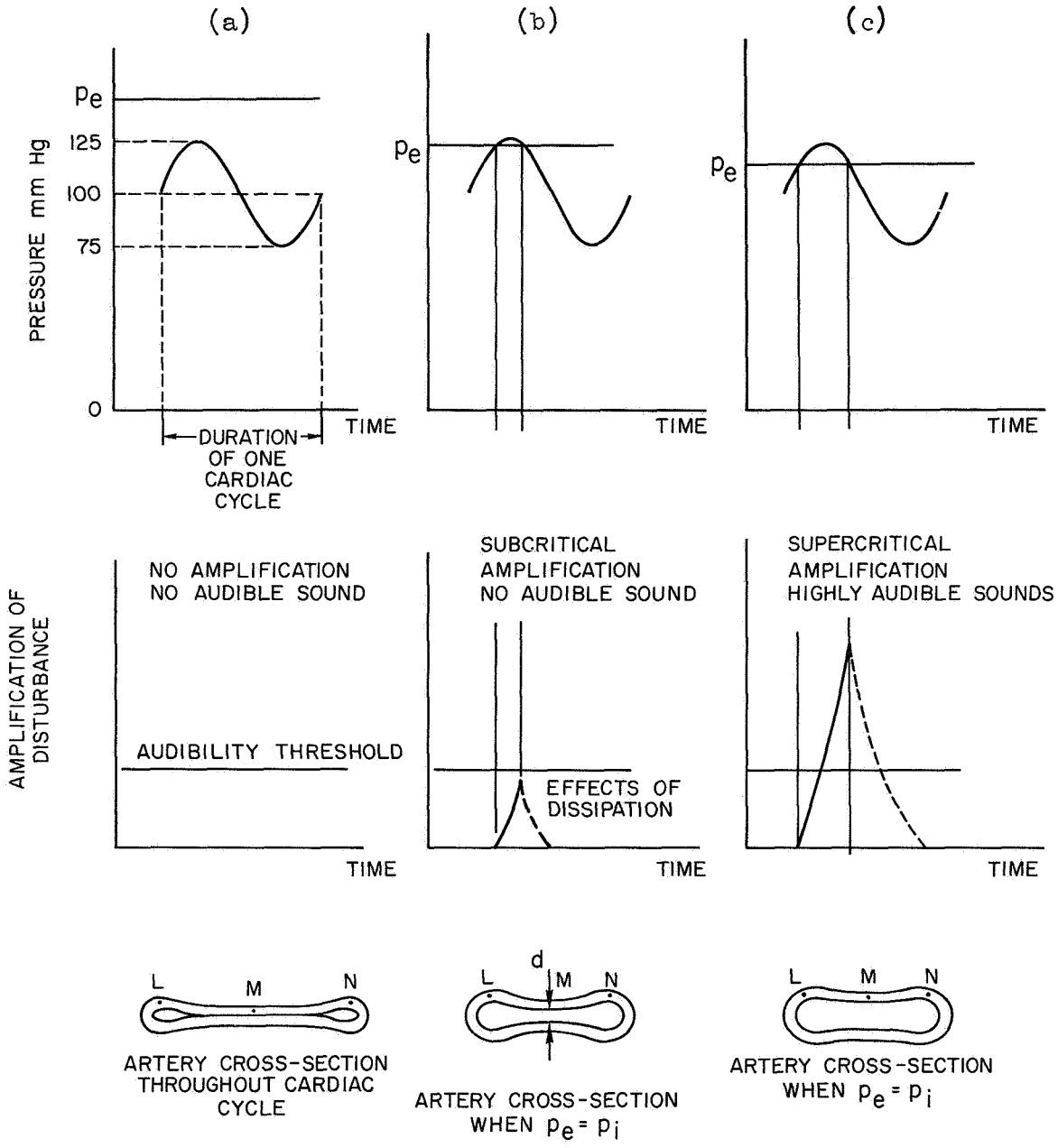

(a) $p_e > p_i$ and no amplification;

(b) $p_e < p_i$ and insufficient amplification for audibility;

(c) $p_e < p_i$ and clearly audible sounds.

Fig. 8. Relationship Between Cuff Pressure, Intraluminal Pressure, Artery Cross Section and the Generation of Korotkoff Sounds

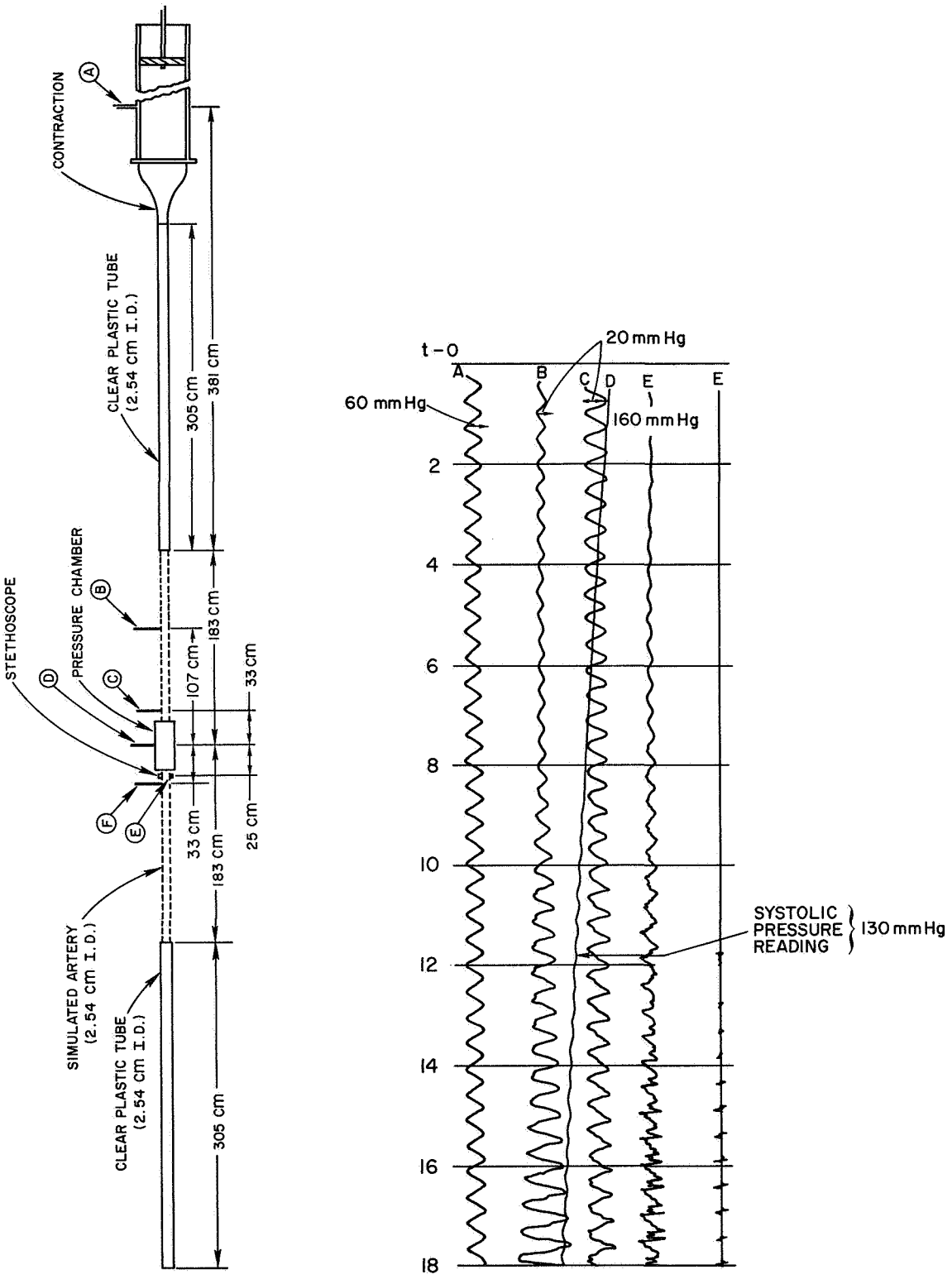

Fig. 9. Experimental Record of Pressures Along the Test Section as the Cuff Pressure Approaches Systolic

CHAPTER II

AXISYMMETRIC WAVES IN THICK WALLED CYLINDERS CONTAINING AN INVISCID INCOMPRESSIBLE FLUID

2.1. Introduction.

The study of waves along thin tubes containing various fluids allowing for viscosity, compressibility, a non-Newtonian constitutive law for the fluid and viscoelastic behavior of the walls has become a subject of widespread interest. The literature, much of it devoted to promoting a deeper understanding of the flow of blood in arteries, is fairly extensive and making no pretense of being complete we mention [1] to [8], as being typical. One thing that all these analyses have in common is that they assume the thickness of the arterial wall to be small compared to its radius and use thin shell theory based on the Kirchoff-Love hypothesis. Apart from the intrinsic interest in relaxing this assumption and representing the wall by the equations of the three dimensional theory of elasticity, this type of analysis has applications in biomechanics. It is important to know the effect of thickness on wave speeds. While the arteries are known to consist of three layers, it will be assumed that the elastic properties and densities are the same in each layer. It may well turn out that viscoelastic behavior will have to be allowed for, to yield more satisfactory descriptions of these phenomena, but the present analysis may serve as a first step in such analyses. Maxwell and Anliker [4] show that the type I waves (i.e., involving large radial displacements for all but very low frequencies) with which we are primarily concerned, the viscoelastic properties of the vessel wall have little effect on the phase

velocity, but a strong influence on the dissipation. However, in experiments on living animals it is difficult to isolate the dissipative forces in the vessel wall from those of the surrounding tissue, unless the tissue is removed. Klip [9], [10] Mirsky [11] have relaxed the thin shell assumption, but not attempted to solve the problem of interest to us.

2.2. Equations of the Elastic Continuum.

The linear displacement equations of motion for thick orthotropic cylinders are well known. We intend to restrict the analysis by introducing three assumptions. Firstly, we consider transversely isotropic (i.e., cylindrically anistropic) bodies which introduces into Hookes law

$$\begin{vmatrix} \sigma_{rr} \\ \sigma_{\theta\theta} \\ \sigma_{xx} \end{vmatrix} = \begin{bmatrix} C_{11} & C_{12} & C_{13} \\ C_{12} & C_{22} & C_{23} \\ C_{13} & C_{23} & C_{33} \end{bmatrix} \begin{vmatrix} \epsilon_{rr} \\ \epsilon_{\theta\theta} \\ \epsilon_{xx} \end{vmatrix}$$

$$\tau_{rx} = C_{44}\,\gamma_{rx}, \quad \tau_{r\theta} = C_{55}\,\gamma_{r\theta}, \quad \tau_{x\theta} = C_{66}\,\gamma_{x\theta}$$

the following simplifications

$$C_{13} = C_{23}, \quad C_{22} = C_{11} \quad \text{and} \quad C_{55} = C_{44}\,.$$

Secondly, all motions are restricted to being rotationally symmetric and having zero circumferential displacement, i.e., $v = \partial/\partial\theta = 0$, and finally the analysis is restricted to the case of zero prestresses. Thus the

equilibrium equations become

$$C_{11}\left(\frac{\partial^2 w}{\partial r^2}+\frac{1}{r}\frac{\partial w}{\partial r}-\frac{w}{r^2}\right)+C_{44}\frac{\partial^2 w}{\partial x^2}+(C_{13}+C_{44})\frac{\partial^2 u}{\partial r\partial x}=\rho\frac{\partial^2 w}{\partial t^2}$$

$$(C_{13}+C_{44})\left(\frac{\partial^2 w}{\partial r\partial x}+\frac{1}{r}\frac{\partial w}{\partial x}\right)+C_{44}\left(\frac{\partial^2 u}{\partial r^2}+\frac{1}{r}\frac{\partial u}{\partial r}\right)+C_{33}\frac{\partial^2 u}{\partial x^2}=\rho\frac{\partial^2 u}{\partial t^2}\ . \tag{1}$$

The solution of coupled equations of this type are most conveniently accomplished by the introduction of displacement potentials and following Prasad and Jain [12] we introduce the following forms for the displacements in a body of infinite length, undergoing steady harmonic oscillations propagating along the axis

$$w(x,r,t)=\frac{d\Phi}{dr}\,\mathrm{Sin}(\alpha x-\omega t)$$

$$u(x,r,t)=U\,\mathrm{Cos}(\alpha x-\omega t)\ . \tag{2}$$

In terms of Φ and U, functions of r only in this case, the equations of motion are:

$$\frac{d}{dr}\left[C_{11}\nabla^2\Phi+\lambda_1\Phi-\mu U\right]=0 \tag{3}$$

and

$$\mu\nabla^2\Phi+C_{44}\nabla^2 U+\lambda_2 U=0 \tag{4}$$

where

$$\nabla^2 = \frac{d^2}{dr^2} + \frac{1}{r}\frac{d}{dr}; \quad \lambda_1 = (\rho\omega^2 - c_{44}\alpha^2); \quad \lambda_2 = (\rho\omega^2 - c_{33}\alpha^2)$$

and

$$\mu = (c_{13} + c_{44})\alpha \ .$$

To obtain uncoupled equations for Φ and U we take $(d/dr + 1/r)$ operating on (3) to obtain

$$c_{11}\nabla^4\Phi + \lambda_1\nabla^2\Phi - \mu\nabla^2 U = 0 \ . \tag{5}$$

Multiplying (5) by c_{44} and (4) by μ and adding, we obtain

$$U = \frac{-1}{\lambda_2\mu}\left[c_{11}\, c_{44}\, \nabla^2\Phi + (\lambda_1\, c_{44} + \mu^2)\, \nabla^2\Phi\right] \ . \tag{6}$$

Substituting (6) into (5) we obtain

$$\nabla^2[c_{11}\, c_{44}\, \nabla^4\Phi + (\mu^2 + \lambda_1\, c_{44} + \lambda_2\, c_{11})\, \nabla^2\Phi + \lambda_1\lambda_2\Phi] = 0 \ . \tag{7}$$

Prasad and Jain [12] showed how Bessel Functions can be used to solve equations of which (7), involving even integral powers of the Laplacian operator, is a typical example. To be complete, we give a brief introduction of their technique. In cylindrical polar coordinates the equation

$$\nabla^2\Phi = -p^2\Phi$$

has for $p^2 > 0$ solutions of the form

$$\Phi(r) = AJ_0(pr) + BY_0(pr) \quad .$$

Since (7) is a quadratic in the Laplacian operator we may replace $\nabla^2\Phi$ by $-p^2\Phi$ and write the solution of (7) as

$$\Phi(r) = \sum_{i=1}^{2} \{A_i J_0(p_i r) + B_i Y_0(p_i r)\} \tag{8}$$

and

$$U(r) = \sum_{i=1}^{2} F_i\{A_i J_0(p_i r) + B_i Y_0(p_i r)\} \tag{9}$$

where

$$F_i = \frac{1}{\lambda_2 \mu} [(\lambda_1 C_{44} + \mu^2) p_i^2 - C_{11} C_{44} p_i^4]$$

and p_i^2 are the roots of

$$C_{11} C_{44} p^4 - \{\mu^2 + \lambda_1 C_{44} + \lambda_2 C_{11}\} p^2 + \lambda_1\lambda_2 = 0 \tag{10}$$

Since the zero roots of (7) do not contribute to the solution they are not considered further.

Clearly it is not necessary that the solutions of (10) for p^2 be either real or greater than zero. For that range of parameters which yield $p^2 < 0$, the method mentioned above is valid if we just replace the Bessel functions by Modified Bessel functions and the minus sign in (10) by a plus. For problems to be studied here, the discriminant is always greater than zero, so we need not be concerned with Bessel functions of complex argument.

Solution of the problem necessitates that the boundary conditions on the inner and outer surfaces of the thick shells be specified. Before doing this it is convenient to express the displacements in terms of the Bessel Functions, so they will be available for future use. Substituting (8) into (9) and (2) we find for the displacements w and u the expressions

$$w(x,r,t) = \{\Gamma^1_{11}(r)\, A_1 + \Gamma^1_{12}(r)\, B_1 + \Gamma^2_{11}(r)\, A_2 + \Gamma^2_{12}(r)\, B_2\} \operatorname{Sin}(\alpha x - \omega t) \quad (11)$$

$$u(x,r,t) = \{\Gamma^1_{21}(r)\, A_1 + \Gamma^1_{22}(r)\, B_1 + \Gamma^2_{21}(r)\, A_2 + \Gamma^2_{22}(r)\, B_2\} \operatorname{Cos}(\alpha x - \omega t) \quad (12)$$

in which we have introduced the following shorthand notation for the eight functions of r. For $p_i^2 > 0$

$$\Gamma^i_{11}(r) = -p_i\, J_1(p_i r) \qquad \Gamma^i_{12}(r) = -p_i\, Y_1(p_i r)$$

$$\Gamma^i_{21}(r) = F_i\, J_0(p_i r) \qquad \Gamma^i_{22}(r) = F_i\, Y_0(p_i r)\ .$$

For $p_i^2 < 0$

$$\Gamma^i_{11}(r) = p_i\, I_1(p_i r) \qquad \Gamma^i_{12}(r) = -p_i\, K_1(p_i r)$$

$$\Gamma^i_{21}(r) = F_i\, I_0(p_i r) \qquad \Gamma^i_{22}(r) = F_i\, K_0(p_i r)\ .$$

2.3. Boundary Conditions.

We shall consider only one type of condition on the surfaces of the thick shell, namely, stress specified on the surfaces.

The fluid pressure must equal the radial direct stress at the contact surface and at stress free boundaries they obviously vanish. Hence, $\sigma_{rr} = 0$ and $\tau_{rx} = 0$ at $r = b$. When the inviscid fluid is in contact with the inner surface, $\tau_{tx} = 0$ and $\sigma_{rr} = -\rho_f \partial\phi/\partial t$ at $r = 1$. Introducing the displacement functions we have

$$\sigma_{rr} = C_{11} \frac{\partial w}{\partial r} + C_{12} \frac{w}{r} + C_{13} \frac{\partial u}{\partial x}$$

$$= \{\Omega^i_{11}(r)\, A_1 + \Omega^i_{12}(r)\, B_1 + \Omega^2_{11}(r)\, A_2 + \Omega^2_{12}(r)\, B_2\} \operatorname{Sin}(\alpha x - \omega t)$$

where for $p_i^2 > 0$

$$\Omega^i_{11}(r) = \frac{C_{11}\, p_i^2}{2} \{J_2(p_i r) - J_0(p_i r)\} - \frac{C_{12}\, p_i}{r} J_1(p_i r) - C_{13}\, \alpha\, F_i J_0(p_i r)$$

$$\Omega^i_{12}(r) = \frac{C_{11}\, p_i^2}{2} \{Y_2(p_i r) - Y_0(p_i r)\} - \frac{C_{12}\, p_i}{r} Y_1(p_i r) - C_{13}\, \alpha\, F_i Y_0(p_i r)$$

and for $p_i^2 < 0$

$$\Omega^i_{11}(r) = \frac{C_{11}\, p_i^2}{2} \{I_2(p_i r) + I_0(p_i r)\} + \frac{C_{12}\, p_i}{r} I_1(p_i r) - C_{13}\, \alpha\, F_i\, I_0(p_i r)$$

$$\Omega^i_{12}(x) = \frac{C_{11}\, p_i^2}{2} \{K_2(p_i r) + K_0(p_i r)\} - \frac{C_{12}\, p_i}{r} K_1(p_i r) - C_{13}\, \alpha\, F_i\, K_0(p_i r)\ .$$

For the shear stress, we find

$$\tau_{rx} = C_{44}\left(\frac{\partial u}{\partial r} + \frac{\partial w}{\partial x}\right)$$

$$= \{\Omega_{21}^{1}(r)\, A_1 + \Omega_{22}^{1}(r)\, B_1 + \Omega_{21}^{2}(r)\, A_2 + \Omega_{22}^{2}(r)\, B_2\} \cos(\alpha x - \omega t) \quad (14)$$

where, for $p_i^2 > 0$

$$\Omega_{21}^{i}(r) = -C_{44}(F_i + \alpha)\, p_i\, J_1(p_i r)$$

$$\Omega_{22}^{i}(r) = -C_{44}(F_i + \alpha)\, p_i\, Y_1(p_i r)$$

and for $p_i^2 < 0$

$$\Omega_{21}^{i}(r) = C_{44}(F_i + \alpha)\, p_i\, I_1(p_i r)$$

$$\Omega_{22}^{i}(r) = -C_{44}(F_i + \alpha)\, p_i\, K_1(p_i r) \ .$$

These two relations for the stresses give us the two stress boundary conditions which will be used later in the formulation of the frequency determinant.

2.4. Perturbation Pressure Applied by the Fluid to the Shell Inner Surface.

According to linear potential flow theory, the pressure p at the inner surface of the shell is given by

$$p = \rho_f\left(\frac{\partial \phi}{\partial t} + V\,\frac{\partial \phi}{\partial x}\right)_{r=1}$$

where ϕ is the velocity potential, V the flow velocity and ρ_f is the fluid density.

In many investigations involving blood flow in the cardiovascular system the flow velocity V is sufficiently small for us to neglect $V\partial\phi/\partial x$ compared to $\partial\phi/\partial t$.

To arrive at the eigenvalue problem, we must express ϕ in terms of the four unknown constants A_i and B_i introduced in the solution for the thick shell equations. This is accomplished as follows. The fluid potential function satisfies the continuity equation

$$\left\{ \frac{\partial^2\phi}{\partial r^2} + \frac{1}{r}\frac{\partial\phi}{\partial r} - \alpha^2\,\phi \right\} \mathrm{Cos}(\alpha x - \omega t) = 0 \quad .$$

Since ϕ is finite along the axis of the cylinder, the solution of this equation is

$$\phi(x,r,t) = HI_0(\alpha r)\ \mathrm{Cos}(\alpha x - \omega t)$$

where $I_0(\alpha r)$ is the zero order modified Bessel function of the first kind. The constant H is obtained by satisfying the kinematic boundary condition

$$\left.\frac{\partial w}{\partial t}\right|_{r=1} = -\left.\frac{\partial\phi}{\partial r}\right|_{r=1}$$

which yields

$$H = \frac{\omega}{\alpha I_1(\alpha)} \left[\Gamma^1_{11}(1)\ A_1 + \Gamma^1_{12}(1)\ B_1 + \Gamma^2_{12}(1)\ A_2 + \Gamma^2_{12}(1)\ B_2\right] .$$

Therefore we can write for the velocity potential

$$\phi(x,r,t) = \frac{\omega I_0(\alpha r)}{\alpha I_1(\alpha)} \left[\Gamma^1_{11}(1)\, A_1 + \Gamma^1_{12}(1)\, B_1 + \Gamma^2_{11}(1)\, A_1 + \Gamma^2_{12}(1)\, B_2\right] \mathrm{Cos}(\alpha x - \omega t) \tag{16}$$

and for the perturbation pressure

$$p(1,x,t) = \left[\Gamma^1_{11}(1)\, A_1 + \Gamma^1_{12}(1)\, B_1 + \Gamma^2_{11}(1)\, A_2 + \Gamma^2_{12}(1)\, B_2\right] m\omega^2 \,\mathrm{Sin}(\alpha x - \omega t) \tag{17}$$

where $m = \rho_f\, I_0(\alpha)/\alpha\, I_1(\alpha)$.

2.5. Formulation of the Eigenvalue Problem.

By enforcing the stress boundary conditions at the inner and outer surfaces of the shell we obtain a classical eigenvalue problem. Clearly the two boundary conditions on the inner surface must now reflect the vanishing of the shear stress and the radial stress being equal to the fluid perturbation pressure. Those on the outer surface enforce the vanishing of both stress components. Hence the eigenmatrix is

$$\begin{bmatrix} \Omega^1_{21}(1) & \Omega^1_{22}(1) & \Omega^2_{21}(1) & \Omega^2_{22}(1) \\ m\omega^2\Gamma^1_{11}(1)+\Omega^1_{11}(1) & m\omega^2\Gamma^1_{12}(1)+\Omega^1_{12}(1) & m\omega^2\Gamma^2_{11}(1)+\Omega^2_{11}(1) & m\omega^2\Gamma^2_{12}(1)+\Omega^2_{12}(1) \\ \Omega^1_{11}(b) & \Omega^1_{12}(b) & \Omega^2_{11}(b) & \Omega^2_{12}(b) \\ \Omega^1_{21}(b) & \Omega^1_{22}(b) & \Omega^2_{21}(b) & \Omega^2_{22}(b) \end{bmatrix} \begin{Vmatrix} A_1 \\ B_1 \\ A_2 \\ B_2 \end{Vmatrix} = 0 \tag{18}$$

2.6. Numerical Solution of the Eigenvalue Problem.

To obtain satisfactory accuracy for the mode shapes it is necessary to exercise considerable ingenuity in the extraction of the eigenvalues and eigenvectors from (17). Firstly, it is not adequate to use what may be described as "commerically available" Bessel function routines and special techniques were used. The Bessel functions $J_n(x)$, $Y_n(x)$ and $I_n(x)$ for $n = 0, 1$ and 2 are computed by the ascending series for small x and asymptotic series for large x. The Bessel function $K_n(x)$ for $n = 0$ and 1 is computed by ascending series for $x < 10$, an integral for $10 \leq x \leq 40$ and the asymptotic series for $x > 40$. The recurrence formula is used for $n = 2$. The computer subroutines are double precision arithmetic for the series summation. The series are terminated when the current term does not contribute any information to the single precision part of the summation.

Secondly, finding the zeros or roots of the determinant was accomplished with the aid of the following technique using also double precision arithmetic. A special form of two word arithmetic is used throughout the root finder. The double precision value of the function is converted to a single precision word which has been scaled to be between 0.5 and 1.0. The second word is an integer number which represents the power of two scale factors. Arithmetic overflow or underflow is thereby eliminated and no further scaling is required.

A lower and upper bound of the range in which the roots are sought is supplied as part of the input data. Two initial guesses are obtained using the lower bound and 1.1 times the lower bound. Linear

interpolation is used to compute the next estimate and it is examined for convergence. If it satisfies the convergence criterion $(x_i - x_{i+1})/x_{i+1} < 10^{-6}$, a zero has been computed. If not, the estimate $F(x_{i+1})$ is tested for a sign change. If the sign has not changed, the linear interpolation procedure is repeated using the two latest estimates. If the sign has changed, a root has been bracketed. Of the three available estimates the two which maintain the bracketing and are closest to the root are chosen for the next linear interpolation. If convergence is not obtained within five iterates, the bracketed region is halved and the process repeated. Convergence is thereby virtually guaranteed.

If the linear interpolation yields an estimate outside the bounded region it is discarded. The bounded region is searched at twenty intervals for an estimate which will be suitable to restart the linear interpolation.

Each zero is numerically divided out at each iteration, thereby preventing its calculation a second time. After the requested number of roots have been computed or the bounded region searched at twenty steps, the function is examined for the changes in sign at ten equal steps between each root. A sign change of the function indicates one or more roots remain to be computed.

After the first root has been found, the next initial estimate is chosen to be .8 times the previous root or 1.5 times the lower bound. It is desirable to find the roots in ascending order and not to miss any of them. This procedure could skip single roots in groups of two or skip multiple roots. In practice this problem is minimized by chosing small bounded regions to search and using as an initial estimate a smaller value than the previous root computed.

The linear interpolation method theoretically will not converge to multiple roots but in practice it is successful due to the inaccuracies in each computed root and the truncative computer arithmetic.

2.7. Presentation of the Results.

The influences of wall thickness and anisotropy are presented separately for each of the two types of waves. The waves referred to as Type I are those whose modes involve large radial displacements at the higher frequency, but in the limit of zero frequency the radial displacement vanishes. They are also frequently referred to as the "pressure" modes since at the higher frequencies they are associated with strong pressure fluctuations. The Type III waves involve predominantly axial displacements at all but the lowest frequencies and are not significantly affected by the presence of an inviscid fluid.

2.7.1. Type I waves for isotropic walls. The phase velocity as a function of frequency is shown in Figure 1. The results of this analysis and those based on thin shell (Kirchoff-Love hypothesis) theory for the Type I phase velocity are rather similar at least for $h/a \leq 0.2$, with the latter yielding a slightly lower velocity. Both theories show a minimum velocity at $\omega \simeq 0.6$, and a very similar effect of thickness that is virtually independent of frequency. The variation of phase velocity with thickness follows very closely the classic Moens-Korteweg relationship, insofar as it increases like the square root of the ratio of wall thickness to mean radius.

The mode shape predictions, as a function of frequency, based on thin shell theory are also quite well substantiated by the theory of elasticity analysis given here. As examples, the mode shapes have been plotted in Figure 2 for two values of the nondimensional frequency. Since the spatial distribution of displacement cannot be defined in terms of the values at the mean radius, the comparison with thin shell theory is not completely straight-forward. For $\omega = 0.1$, thin shell theory [4] predicts that the modal amplitudes of the axial and radial displacements at the middle surface will be almost the same. This is corroborated by the elasticity solution shown in Figure 2a. We note that the modal amplitudes do not change significantly with thickness or as we traverse the wall of prescribed thickness. The thin shell analysis predicts for $\omega = 0.5$ a radial displacement of the middle surface which is approximately eight times the axial displacement, for $h/a = 0.1$. For the elasticity solution, this factor is about ten. However, at this frequency both the effect of wall thickness and the variation of modal amplitude as a function of the radius are much more pronounced. In particular, it is clear that at this higher frequency the axial displacement is considerably less at the outer and hence visible surface than it is at the inner surface where it is in contact with the fluid. The thinner the wall, the less is the motion visible from the outside.

2.7.2. Type III waves in isotropic walls. The elasticity solutions for these waves shows that the thin shell theory underestimates the phase velocity by about eight percent for all frequencies when the wall thickness

to mean radius ratio is 0.1. As we raise the wall thickness the waves become slightly dispersive with a phase velocity that decreases with increasing frequency while thin shell theory predicts a very small increase in the phase velocity as the wall is thickened at least for h/a less than 0.2. The modal amplitudes are shown in Figure 3 which confirms that radial displacements are very small in comparison with the axial displacements. We note that, as in contrast to Type I waves, the maximum radial displacements are at the outer surface. The smallness of the radial displacements confirms the experimental observation [13] that axial waves are associated with extremely small pressure perturbations.

2.7.3. Material properties of transversely isotropic vessel walls. The restriction of the wall equation of state to transverse isotropy means that it is possible to select five elastic parameters. This was done by choosing the three elastic moduli, the shear modulus and one Poisson's ratio and utilizing the equations of [14]. To keep the Poisson's ratios no greater than 0.5 it is necessary to restrict the radial modulus to be reasonably close to the circumferential value. For convenience they were restricted to being the same.

Of the resulting elastic constants, C_{11} which exercises a dominant influence on the Type I waves, is approximately equal to 1.4 times the modulus ratio. On the other hand, C_{33} and C_{44} which have a marked effect on the axial waves, vary much less as a function of the modulus ratio and in fact the former decreases when this ratio increases.

The constant C_{44} can be specified independently of the others and a variation of C_4 from 0.33 (the value for an isotropic wall with $\nu = 0.5$) to 0.2 produced a virtually negligible change in the results.

2.7.4. Type I waves for transversely isotropic vessel walls. The significant influence of this particular type of orthotropic material on the phase velocity of Type I waves is shown in Figure 4, for the case of a relatively thin wall with $h/a = 0.1$. The low frequency regime is the one of primary physiological importance and at zero frequency, the phase velocity is proportional to $(E_\theta/E_x)^{1/2}$. The reason for this is the large change in C_{11} mentioned previously. The marked change in the modal displacements is illustrated in Figure 5. The axial displacement for the low frequency situation ($\omega = 0.1$) and the radial for the high frequency case ($\omega = 0.5$) are hardly affected but for each frequency the smaller of the two displacements is heavily dependent upon the ratio of the moduli. As the modulus ratio increases, the radial displacement amplitude decreases for the low frequency case. This sensitivity of the mode shape to modulus ratio could be utilized to assess the degree of anisotropy.

2.7.5. Type III waves in transversely isotropic vessel walls.

The small reduction in phase velocity of the Type III waves, as the modulus ratio increases is to be expected from the small reduction in C_{33} that has been discussed previously.

2.8. Comparison of the Theory with Experimental Data.

Recently obtained experimental results, such as those by Moritz [13] on the wave speeds in the corotid arteries of anesthetized dogs is reproduced here as Figure 6. The first prerequisite, before a comparison can be made between theory and experiment is to reduce his results to nondimensional form. This is considerably facilitated because the Type III waves are so insensitive to the moduli. The square of the nondimensional wave speed is given as

$$c^2 = \bar{c}^2 \, \bar{\rho}/\bar{E}_x \quad .$$

Moritz has measured $\bar{c}$ for Type III waves as about 30 meters/sec, $\bar{\rho}$ is close to 1.0, g/cm^3, c can be taken as unity and (18) yields a value of 9×10^6 dynes/cm^2 for $\bar{E}_x$. Taking Moritz's value of 0.225 cm for $\bar{a}$ and using the definition of $\bar{\omega}_0$, we obtain $\omega = \bar{\omega}/1.3 \times 10^4$. This completes the reduction of Moritz's data to nondimensional form and the scales have been added to Figure 6.

We note that a frequency of 100 Hz corresponds to an extremely small nondimensional frequency and we are able to use the zero frequency phase velocities for comparison with the experimental results. The nondimensional phase velocity for the pressure waves, from Moritz's experiments is approximately 0.4. Hence, the ratio of the elastic moduli is $E_\theta/E_x = (0.4/0.225)^2 = 3.16$. This suggests that the carotid artery of dogs are significantly anisotropic and we would expect to find the circumferential modulus about three times the axial modulus. However, it must

be remembered that the curves presented are limited to transverse isotropy with equal radial and circumferential moduli. To our knowledge no experimental evidence is available on the radial modulus and it would be very difficult to obtain.

2.9. Conclusions.

Using the equations of elasticity for an unprestressed, transversely isotropic circular cylinder to represent the walls of blood vessels, we have shown the importance of both wall thickness and anisotropy. The axial waves are but little influenced by either wall thickness or anisotropy of the types considered. However, the pressure or "Type I" waves are significantly affected by both. Increasing the wall thickness raises this phase velocity by approximately the ratio of $(h/a)^{1/2}$ as could be expected on the basis of the classic Meons-Korteweg equation. For a mean radius to wall thickness ratio of ten, the phase velocity predicted by the thin shell analysis is about ten percent less than that corresponding to the elasticity solution. The influence of wall thickness on mode shape agrees at least qualitatively with the thin shell approximation.

Increasing the circumferential and radial elastic moduli, relative to the axial, produces very little change in the phase velocity of axial waves. For the pressure waves the phase velocity is approximately proportional to the square root of the ratio of the circumferential to axial moduli. The mode shapes are also markedly affected by the wall properties.

A comparison of the theory with recent experimental results for the speed of axial and pressure waves in corotid arteries of anesthetized dogs suggests that the carotid wall is transversely isotropic with a circumferential moduls three times the axial.

NOTATION

A_i	Arbitrary constants in the solution of the equations of motion
$\bar{a}$	Inner radius of the shell and normalizing geometric dimension
a	Nondimensional mean radius of the shell
B_i	Arbitrary constants in the solution of the equations of motion
$b = \bar{b}/\bar{a}$	Nondimensional outer radius of the thick shell
$C_{ij} = \bar{C}_{ij}/\bar{E}_x$	Nondimensional elastic constants of the thick shell
$c = \bar{c}/[\bar{E}/\bar{\rho}]^{1/2}$	Nondimensional phase velocity
$\bar{E}_x$	Normalizing (axial) Young's Modulus
$\bar{E}_\theta$	Circumferential Young's modulus
I_i, J_i, K_i, Y_i	Bessel functions of integer order
$m =$	$\rho_f I_0(\alpha)/\alpha I_1(\alpha)$
p_i	Roots of equation (6a)
$p, \bar{p}/\bar{E}_x$	Nondimensional fluid pressure on shell inner surface
$r = \bar{r}/\bar{a}$	Nondimensional radial coordinate

t, $\bar{w}_0\bar{t}$	Nondimensional time
U	Displacement potential introduced in equation (2)
V, $\bar{V}/\bar{a}\ \bar{\omega}_0$	Nondimensional fluid velocity
u, $\bar{u}/\bar{a}$	Nondimensional axial displacement
w, $\bar{w}/\bar{a}$	Nondimensional radial displacement
x, $\bar{x}/\bar{a}$	Nondimensional axial coordinate
α, $2\pi/\lambda$	Nondimensional wave number
Γ^i_{jk}	Functions introduced in equation (7)
γ_{ij}	Shear strain
ϵ_{jj}	Direct strain
λ, $\bar{\lambda}/\bar{a}$	Nondimensional wavelength
$\lambda_1 =$	$(\rho\omega^2 - C_{44}\,\alpha^2)$
$\lambda_2 =$	$(\rho\omega^2 - C_{33}\,\alpha^2)$
$\mu =$	$(C_{13} + C_{44})\alpha$
ν	Poisson's ratio
ρ, $\bar{a}^2\,\bar{\omega}_0^2\bar{\rho}/\bar{E}_x$	Nondimensional density of the shell wall
ρ_f, $\bar{a}^2\bar{\omega}_0^2\bar{\rho}_f/\bar{E}_x$	Nondimensional fluid density

$\sigma_{jj} = \bar{\sigma}_{jj}/\bar{E}_x$	Nondimensional axial stress
Φ	Displacement potential function introduced in equation (2)
ϕ	Fluid potential function introduced in equation (9)
τ, $\bar{\tau}/\bar{E}$	Nondimensional shear stress
$\omega = \bar{\omega}/\bar{\omega}_0$	Nondimensional frequency
$\bar{\omega}_0$, $[\bar{E}_x/\bar{\rho}\bar{a}^2]^{1/2}$	Normalizing frequency
	Denotes a dimensional quantity

REFERENCES

[1] McDonald, D. A., "Blood Flow in Arteries", Williams and Wilkins Co., Baltimore, 1960.

[2] Womersley, J. R., "An Elastic Tube Theory of Pulse Transmission and Oscillatory Flow in Mammalian Arteries", WADCTR-56-614, 1957.

[3] Morgan, G. W., and W. R. Ferrante, "Wave Propagation in Elastic Tubes Filled with a Streaming Liquid", J. Acoust. Soc. Am. 27, 715 (1955).

[4] Maxwell J. A. and M. Anliker, "Dispersion and Dissipation of Waves in Blood Vessels", Biophysical J. 8, No. 8, pp. 925-950

[5] Atabek, H. B., and H. S. Lew, "Wave Propagation Through a Viscous Incompressible Fluid Contained in an Initially Stressed Elastic Tube", Biophysical J. 6, pp. 481-503 (1966).

[6] Fox, E. A., and E. Saibel, "Attempts in the Mathematical Analysis of Blood Flow," Trans. Soc. Rheol. 7, 25 (1963).

[7] Jones, E., M. Anliker, I-Dee Chang, "Effects of Viscosity and External Constraints on Wave Transmission in Blood Vessles", SUDAAR No. 344, 1968.

[8] Fung, Y. C., "Biomechanics, Its Scope, History and Some Problems of Continuum Mechanics in Physiology", J. App. Mech. Rev. 21 (1) (1968).

[9] Klip, W., Velocity and Damping of the Pulse Wave, Martinus Nijhoff, The Hague, 1962.

[10] Klip, W., Von Loon, P., and Klip, D., "Formulas for Phase Velocity and Damping of Longitudinal Waves in Thick-Walled Viscoelastic Tubes", J. App. Phys. 38 (9) pp. 3745-3755 (1967).

[11] Mirsky, I., "Pulse Velocities in Initially Stressed Cylindrical Rubber Tubes", Bull. of Math. Biophysics 30, No. 2, pp. 299-308 (1968).

[12] Prasad, C. and R. K. Jain, "Vibrations of Transversely Isotropic Cylindrical Shells of Finite Length", J. Ac. Soc. Am. 37, pp. 1006-1009 (1965)

[13] Moritz, W., "Transmission Characteristics of Distension, Torsion and Axial Waves in Arteries", SUDAAR No. 373, May 1969.

[14] Mirsky, I., "Vibrations of Orthotropic, Thick Cylindrical Shells", J. Ac. Soc. Am. 36, pp. 41-51 (1964).

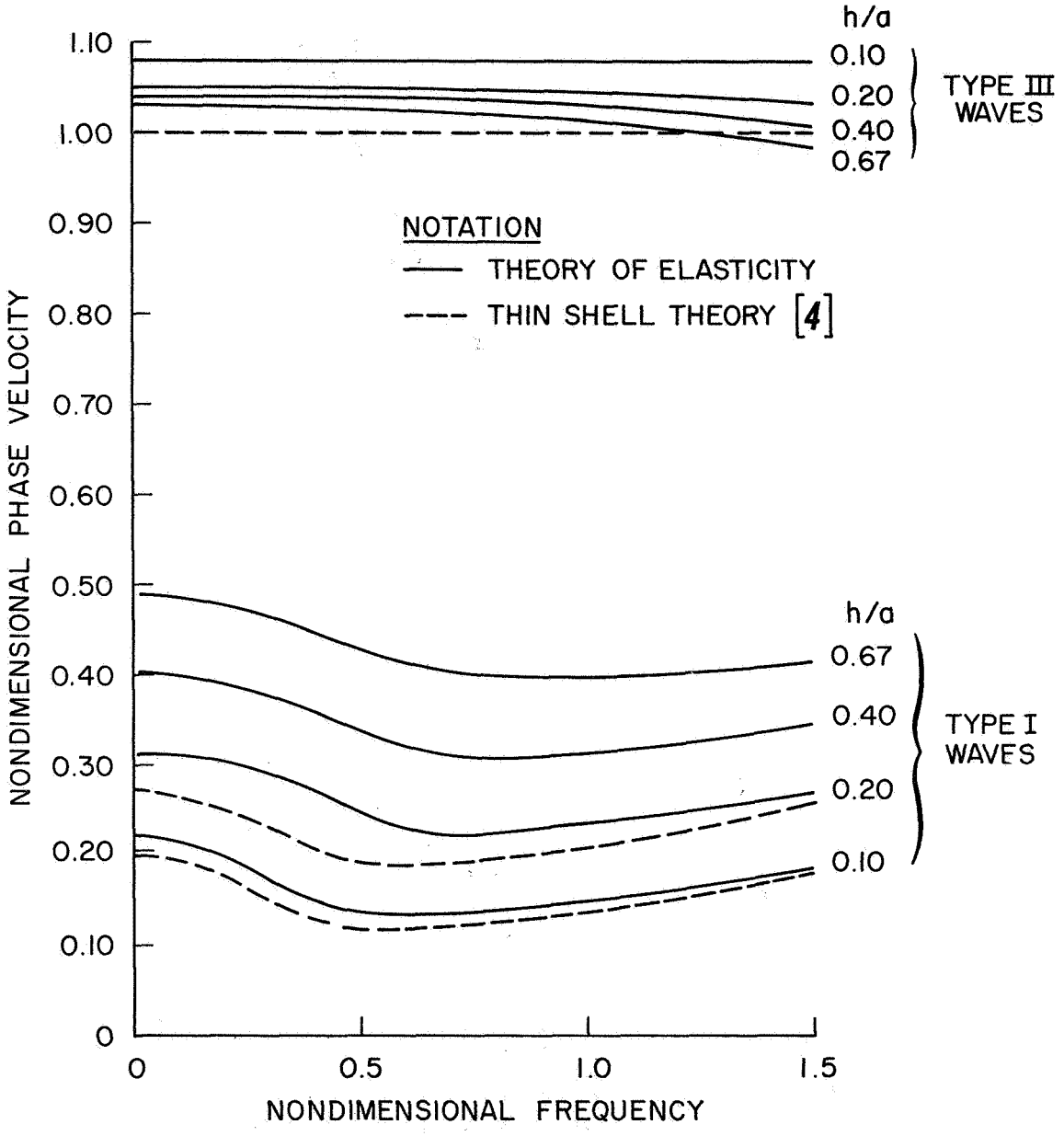

Fig. 1. Influence of Wall Thickness on Phase Velocity for an Isotropic Shell

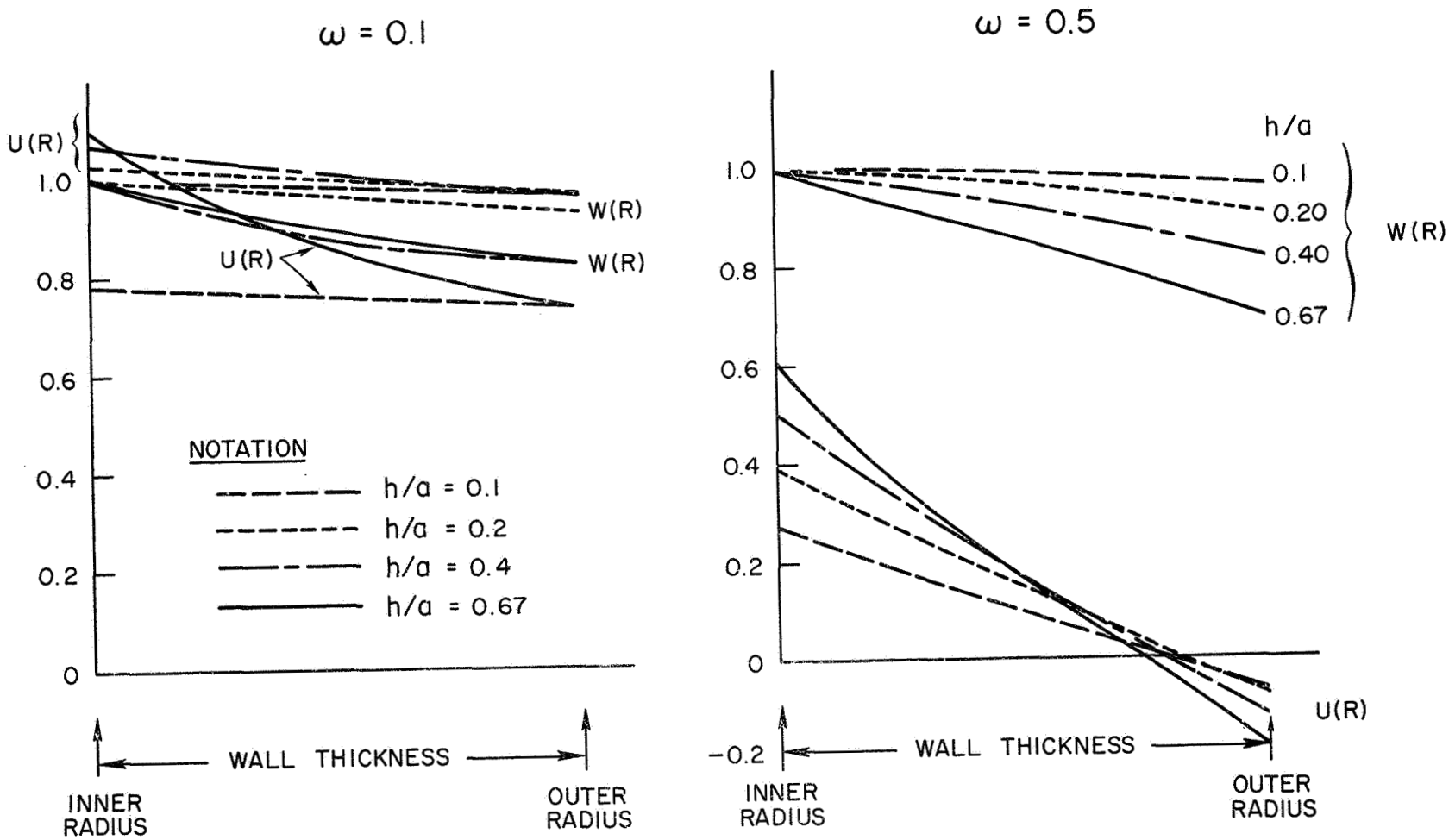

Fig. 2. Modal Amplitudes as Functions of Wall Thickness for Type I Waves in an Isotropic Shell

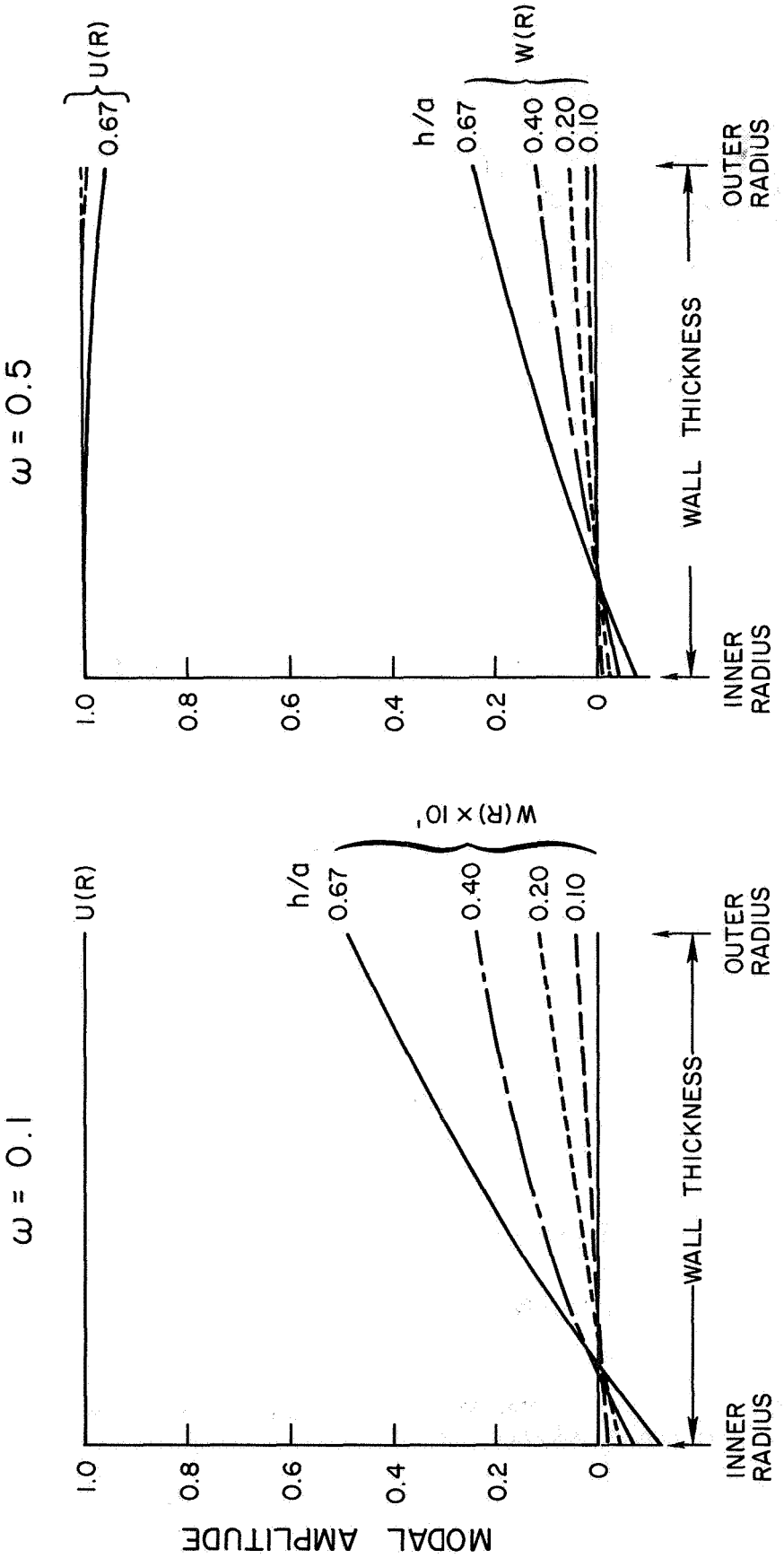

Fig. 3. Modal Amplitudes as Functions of Wall Thickness for Type III Waves in an Isotropic Shell

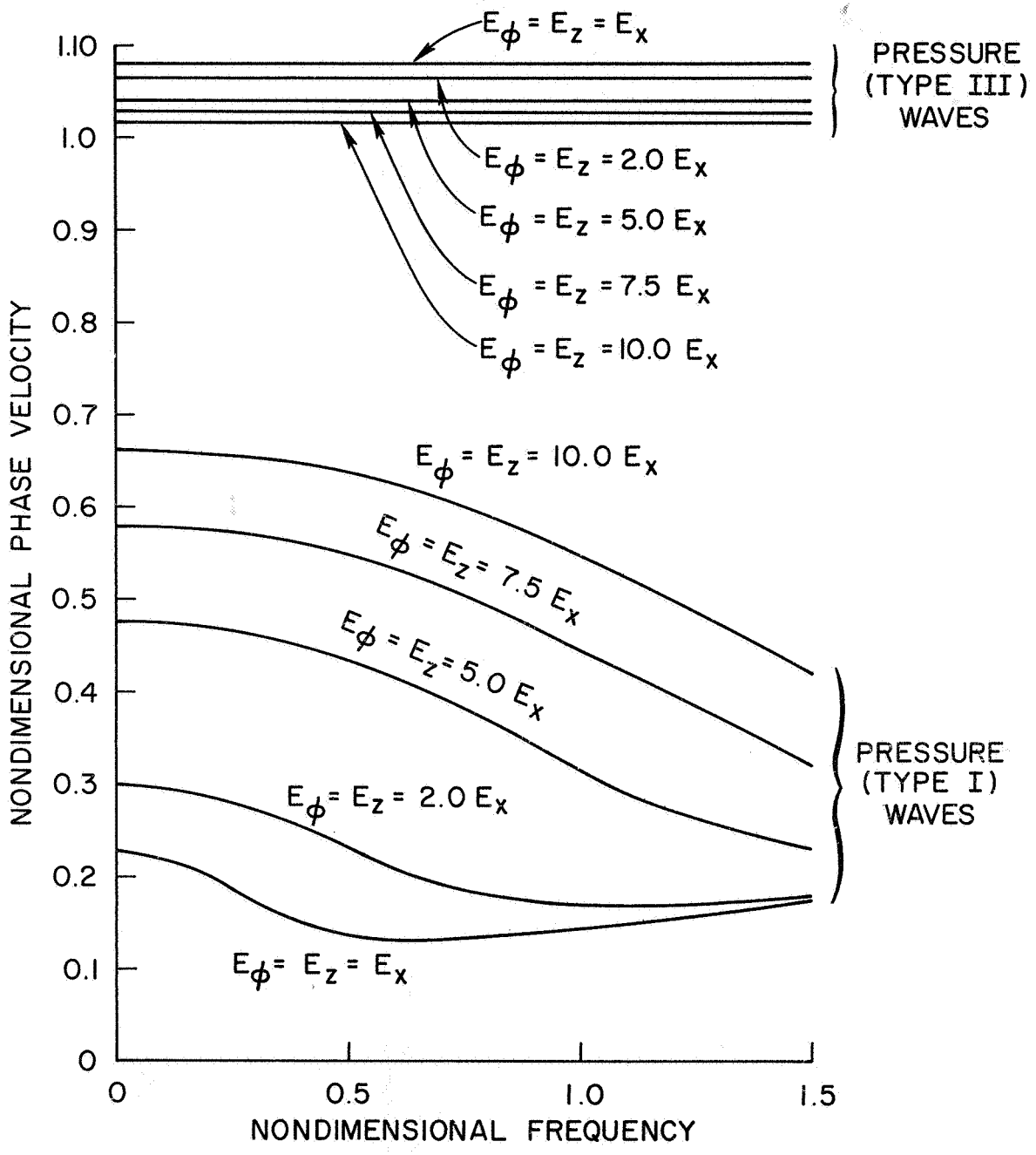

Fig. 4. Influence of Transversely Isotropic Wall Moduli on the Phase Velocity

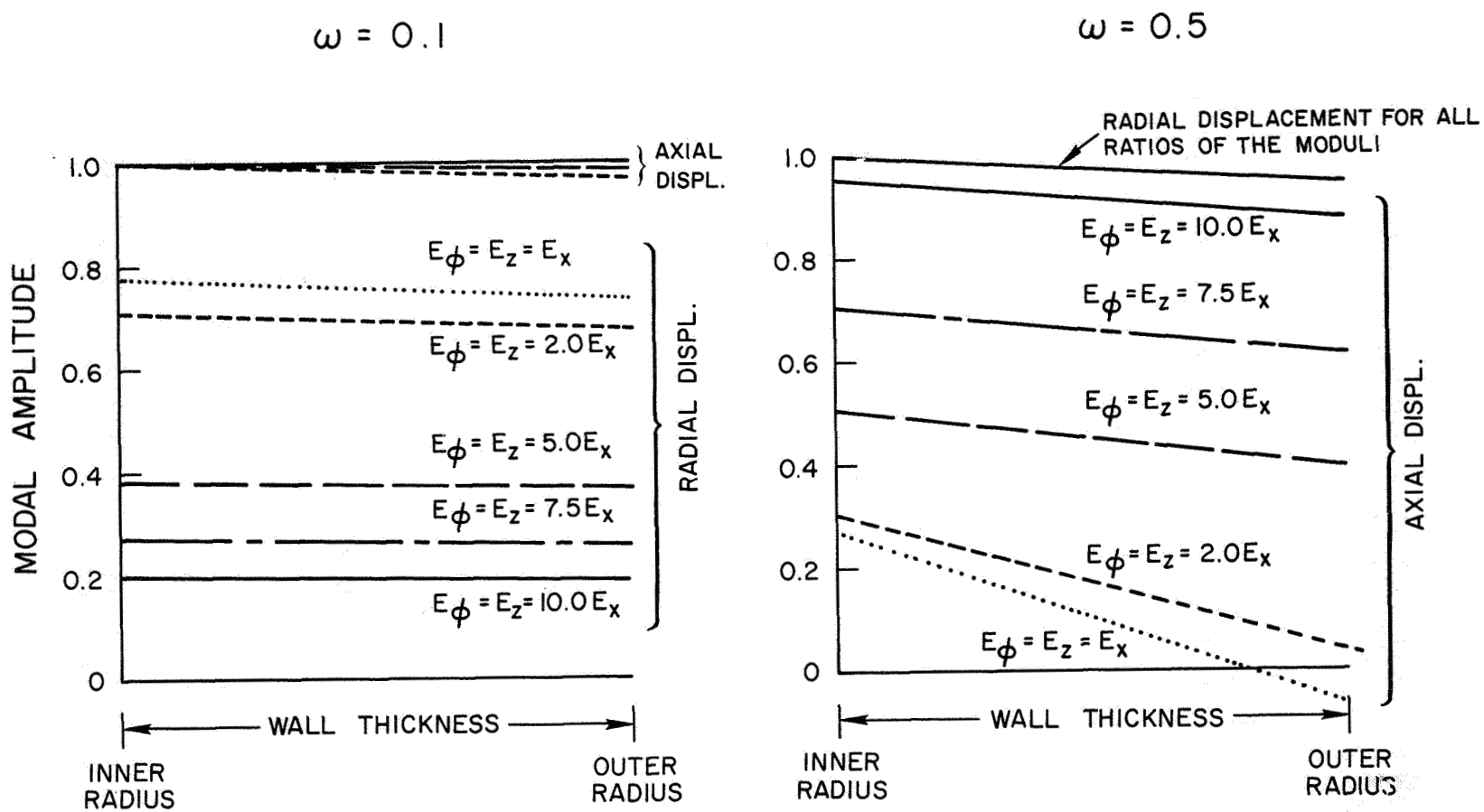

Fig. 5. Modal Amplitudes as Functions of the Wall Moduli for Type I Waves

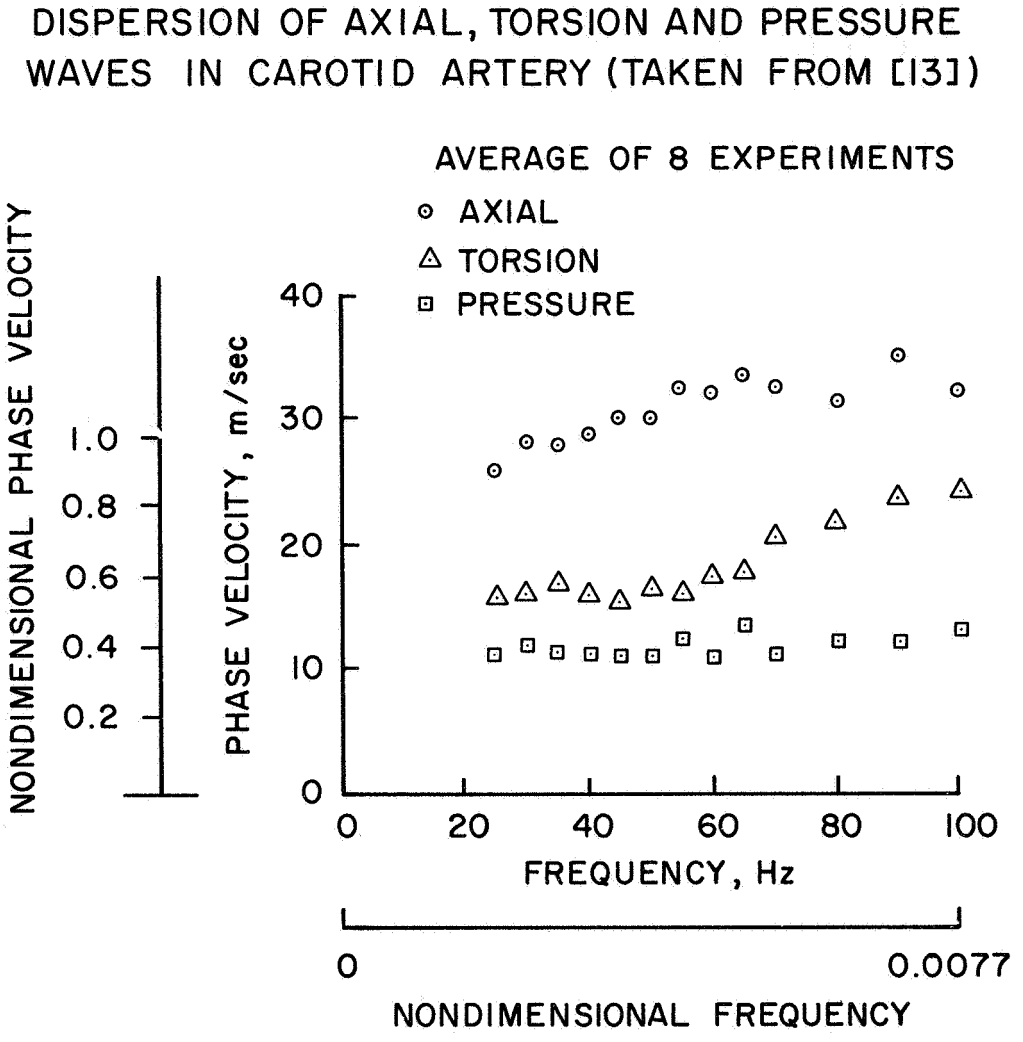

Fig. 6. Dispersion of Axial, Torsion and Pressure Waves in Carotid Artery

CHAPTER III

DISPERSION OF PRESSURE WAVES IN FLUID FILLED CYLINDERS OF ELLIPTIC CROSS SECTION

3.1. Introduction.

A review of the literature on the flow of blood in arteries and veins as well as that devoted to wave propagation in thin shells, suggests that an overwhelming majority of investigations have focused on blood vessels with a circular cross section. In fact, we are not aware of any numerical computation of the wave speeds in a prestressed shell of elliptic cross section, other than that by Kresch [1] who used electric circuit analogies to show that the cross section shape exercises a very small influence on the phase velocity of the pressure waves. The approach taken here is that of engineering mechanics and follows quite closely the work of Anliker and Maxwell [2].

One significant complication of a blood vessel whose cross section is noncircular is that, in general, the quasi static transmural pressure distorts the cross section to a different shape and induces bending stresses. In this investigation we restrict the transmural pressure to be that which produces a membrane prestress state. It is also assumed that the constitutive equation for the vessel wall is that of an isotropic and linearly elastic body. Since we are only concerned with local behavior over a small range of the stress, strain curve, this is a tenable assumption. The purpose of the investigation is to check whether deviations from a circular cross section can account for a definite pattern in the transmission of pressure waves in blood vessels.

3.2. Fluid Motion and its Relationship to the Shell Motion.

For an incompressible, inviscid fluid flowing irrotationally in an elliptic cylinder as shown in Figure 1, the equation of continuity in terms of the velocity potential function Φ is,

$$\nabla^2\Phi + \frac{\partial^2\Phi}{\partial x^2} = 0 \qquad (1)$$

where ∇^2 is the two dimensional Laplacian operator in the elliptic coordinates (ξ, η) which are related (see [3]) to the Cartesian coordinates y and z by

$$y = e \text{ Sinh } \xi \text{ Sin } \eta \quad \text{and} \quad z = e \text{ Cosh } \xi \text{ Cos } \eta \ . \qquad (2)$$

In the limit, as the eccentricity tends to zero and the ellipse becomes a circle, ξ and η reduce to the cylindrical polar coordinates. All the geometric variables are nondimensionalized by dividing by the semi-major axis length.

Considering wave propagation along the axis of the cylinder, we assume that the velocity potential function has the form

$$\Phi(\xi, \eta, x, t) = \psi(\xi,\eta) \text{ Cos}(\sigma t - kx) \ . \qquad (3)$$

Substitution of (3) into (1) yields the equation for ψ as

$$\nabla^2\psi - k^2\psi = 0 \qquad (4)$$

Writing (4) in the elliptic coordinates we find (p. 173 of [3])

$$\frac{\partial^2\psi}{\partial\xi^2} + \frac{\partial^2\psi}{\partial\eta^2} - 2q(\text{Cosh } \xi - \text{Cos } \eta)\psi = 0 \tag{5}$$

in which $q = k^2e^2/4$.

If we now separate variables by assuming $\psi(\xi,\eta) = X(\xi)\,\Theta(\eta)$ and introduce this into (5) we find

$$\begin{aligned} &\frac{\partial^2\Theta}{\partial\eta^2} + (a + 2q\ \text{Cos } 2\eta)\Theta = 0 \\ &\frac{\partial^2 X}{\partial\xi^2} - (a + 2q\ \text{Cosh } \xi)X = 0 \quad . \end{aligned} \tag{6}$$

These are respectively the well known Mathieu and Modified Mathieu equations. In our case, q is negative. It is clear that we are concerned with only periodic solutions in η; the nonperiodic solution being untenable on physical grounds for a complete elliptic shell. We assume that the fluid perturbations satisfy (6) and study the phase velocity for each perturbation of interest.

The relationship between the fluid velocity normal to the shell surface and the shell velocity in this direction is prescribed by the kinematic boundary condition which is somewhat more involved than for a circular cross section.

The kinematic boundary condition is (see eg. [4])

$$\left.\frac{\partial R}{\partial n}\right|_{\xi=\xi_0} \left.\frac{\partial\Phi}{\partial n}\right|_{\xi=\xi_0} = -\left(\frac{\partial w}{\partial t} + U\frac{\partial w}{\partial x}\right) \quad . \tag{7}$$

In regions where the shell curvature does not change too drastically we can replace $\partial R/\partial n$ by unity and $\partial\Phi/\partial n$ by $\partial\Phi/\partial r$, but we shall retain (7).

The fluid perturbation can have any required symmetry about the major axes of the ellipse provided we choose appropriate Mathieu and Modified Mathieu functions. To clarify the technique we shall restrict ourselves to the case of a perturbation symmetric about both axes and by using (6) and (3) we have

$$\Phi_{2m}(\xi,\eta,x,t) = H\, Ce_{2m}(\xi,-q)\, ce_{2m}(\eta,-q)\, \mathrm{Cos}(\omega t - kx) \tag{8}$$

where H is an arbitrary constant, to be determined. To obtain other types of symmetries we just replace $Ce_{2m}(\xi,-q)$ by $Ce_{2m+1}(\xi,-q)$ or $Se_{2m+1}(\xi\ -q)$ and so forth.

If we utilize elliptic coordinates in (7) we can write

$$\frac{1}{B^2}\frac{\partial R}{\partial \xi}\bigg|_{\xi=\xi_0}\frac{\partial \Phi_{2m}}{\partial \xi}\bigg|_{\xi=\xi_0} = -\left(\frac{\partial w}{\partial t} + U\frac{\partial w}{\partial x}\right) \tag{9}$$

where, according to [3]

$$R = e\left[\frac{\mathrm{Cosh}\ 2\xi_0 + \mathrm{Cos}\ 2\eta}{2}\right]^{1/2}$$

and

$$B = e\left[\frac{\mathrm{Cosh}\ 2\xi_0 - \mathrm{Cos}\ 2\eta}{2}\right]^{1/2}$$

We note that the Lamé coefficient B, of the first fundamental form equals R only when $\text{Cos } 2\eta \ll \text{Cosh } 2\xi_0$ which occurs when the shell cross section is reasonably close to being circular.

Substituting (8) into (9) and assuming for the transverse displacement of the shell an expression of the form

$$w(\eta,x,t) = C\ ce_{2m}(\eta,-q)\ \text{Sin}(\sigma t - kx) \tag{10}$$

we obtain

$$\frac{H\sqrt{2}\ \text{Sinh } 2\xi_0}{e\beta^{3/2}(1-\theta)(1+\theta)^{1/2}} \frac{d\ Ce_{2m}(\xi,-q)}{d\xi}\bigg|_{\xi=\xi_0} ce_{2m}(\eta,-q)$$

$$= -\ (\sigma - kU)\ C\ ce_{2m}(\eta,-q) \tag{11}$$

where $\theta = \text{Cos } 2\eta/\beta$ is less than unity for elliptic cylinder except in the pathological case of the ellipse degenerating into the interfocal line. As the ellipse tends to a circle, the Modified Mathieu function tends to a Modified Bessel function, while the Mathieu function tends to a Cosine and the two arbitrary constants H and C can be immediately determined. In the general situation the problem is more complex and we choose to solve (11) by a Galerkin procedure in that we multiply both sides of the equation by $ce_{2m}(\eta_1,-q)$ and integrate from 0 to 2π. In doing this, the degree to which the binomial expansions in θ are carried out is important. Since $\beta = (2/e^2-1)$, the larger the eccentricity, the

more terms are needed in the expansion to achieve a desired accuracy. We shall restrict ourselves to relatively small eccentricities and the first power of θ in the binomial expansion. In other words we retain β^{-1} compared to unity but neglect all higher order terms. We note that $\beta = 49$ for $e = 0.2$ and $\beta \simeq 21$ for $e = 0.3$ so the influence of ellipticity can be detected by the analysis.

From (11) we obtain

$$\frac{\sqrt{2}\ \text{Sinh}\ 2\xi_0}{e\ \beta^{3/2}} \left.\frac{d\ Ce_{2m}(\xi,-q)}{d\xi}\right|_{\xi=\xi_0} \int_0^{2\pi} \left(1 + \frac{\theta}{2}\right) ce_{2m}^2(\eta,-q)\ d\eta\ H$$

$$= -\ (\sigma - kU)\ C \int_0^{2\pi} ce_{2m}(\eta,-q)\ d\eta \quad . \tag{12}$$

This ensures the normal fluid and shell wall velocities are equal, in the Galerkin sense and we are in a position to consider the fluid pressure exerted on the elastic shell. Introducing the shorthand M and N for the integrals on the left and right sides, respectively of (12), we have

$$H = -\ (\sigma - kU)\ \frac{N}{M} \cdot \frac{e\ \beta^{1/2}}{2^{1/2}} \frac{\text{Cosh}\ 2\xi_0}{\text{Sinh}\ 2\xi_0} \cdot \frac{1}{\left.\frac{d\ Ce_{2m}(\xi,-q)}{d\xi}\right|_{\xi=\xi_0}} \cdot C \quad .$$

For linearized potential flow, the pressure is given by

$$p = \rho_f\left(\frac{\partial\Phi}{\partial t} + U\frac{\partial\Phi}{\partial x}\right)$$

$$= C\,\rho_f(\sigma-kU)^2\,\frac{N}{M}\,\frac{e\,\beta^{1/2}}{2^{1/2}}\,\frac{\text{Cosh } 2\xi_0}{\text{Sinh } 2\xi_0}\cdot\left.\frac{Ce_{2m}(\xi,-q)}{\frac{d\,Ce_{2m}(\xi,-q)}{d\xi}}\right|_{\xi=\xi_0} ce_{2m}(\eta_1,-q)\,\text{Sin}(\sigma t-kx)\ .$$

For negative values of q the Modified or Radial Mathieu functions are expressible in terms of Modified Bessel functions (see eg. [3] p. 165) as

$$Ce_{2m}(\xi,-q) = (-1)^m\,ce_{2m}(0,q)\sum_{r=0}^{\infty}(-1)^r\,A_{2r}^{2m}\,I_{2r}(\gamma)$$

$$\frac{d\,Ce_{2m}(\xi,-q)}{d\xi} = (-1)^m\,ce_{2m}(0,q)\,2(q)^{1/2}\,\text{Sinh}\,\xi\sum_{r=0}^{\infty}(-1)^r\,A_{2r}^{2m}\,I'_{2r}(\gamma)$$

in which $\gamma \equiv 2|q|^{1/2}\,\text{Cosh}\,\xi$ and where $I'_{2r}(\cdot)$ denotes derivatives with respect to the argument. Putting $n = 0$ in the above expression we obtain

$$\left.\frac{Ce_0(\xi,-q)}{\frac{d\,Ce_0}{d\xi}(\xi,-q)}\right|_{\xi=\xi_0}$$

$$= \frac{A_0^0\,I_0(\tilde{\gamma}) - A_2^0\,I_2(\tilde{\gamma}) + A_4^0\,I_4(\tilde{\gamma})\cdots}{2|q|^{1/2}\,\text{Sinh}\,\xi_0[A_0^0\,I_1(\tilde{\gamma}) - A_2^0\{I_1(\tilde{\gamma}) + I_3(\tilde{\gamma})\}/2 + A_4^0\{I_3(\tilde{\gamma}) + I_5(\tilde{\gamma})\}/2\cdots]}$$

where $\tilde{\gamma} = 2|q|^{1/2}\,\text{Cosh}\,\xi_0$.

3.3. Shell Theory.

Since the prestress due to axial stretch and the quasi static pressure difference across the shell wall are known to be significant in wave propagation problems it is essential to utilize shell theory that contains such terms. This subject is reviewed in Chapter IV where it is shown that utilizing Washizu's [5] theory we can write the following equation of motion

$$[L_{ij}] \begin{vmatrix} u \\ v \\ w \end{vmatrix} + \rho \begin{vmatrix} \ddot{u} \\ \ddot{v} \\ \ddot{w} \end{vmatrix} - \begin{vmatrix} 0 \\ 0 \\ p \end{vmatrix} = 0 \tag{13}$$

where

$$L_{11} = (1 + N_{\alpha}^{o}) \frac{\partial^2}{\partial x^2} + \{\frac{(1-\nu)}{2} + N_{\beta}^{o}\} \frac{1}{B^2} \frac{\partial^2}{\partial \eta^2}$$

$$L_{12} = L_{21} = \frac{(1+\nu)}{2B} \frac{\partial^2}{\partial x \partial \eta}$$

$$L_{31} = - L_{13} = \frac{\nu}{R} \frac{\partial}{\partial x}$$

$$L_{22} = \frac{(1+N_{\beta}^{o})}{B^2} \frac{\partial^2}{\partial \eta^2} + \{\frac{(1-\nu)}{2} + N_{x}^{o}\} \frac{\partial^2}{\partial x^2} - \frac{N_{\beta}^{o}}{R^2} + \frac{h^2}{12R^2} \{2(1-\nu) \frac{\partial^2}{\partial \alpha^2} + \frac{R}{B^2} \frac{\partial^2}{\partial \eta^2} (\frac{\cdot}{R})\}$$

$$L_{23} = - \frac{1}{B} \frac{\partial}{\partial \eta} (\frac{\cdot}{R}) - \frac{2N_{\beta}^{o}}{RB} \frac{\partial}{\partial \eta} + \frac{h^2}{12R^2} \{\frac{1}{B^3} \frac{\partial^3}{\partial \eta^3} + \frac{(2-\nu)}{B} \frac{\partial^3}{\partial x^2 \partial \eta}\}$$

$$L_{32} = \frac{1}{RB}\frac{\partial}{\partial\eta} + \frac{2N_\beta^o}{B}\frac{\partial}{\partial\eta}\left(\frac{\cdot}{R}\right) - \frac{h^2}{12B^2}\left\{\frac{1}{B^2}\frac{\partial^3}{\partial\eta^3}\left(\frac{\cdot}{R}\right) + (2-\nu)\frac{\partial}{\partial\eta}\left(\frac{1}{R}\frac{\partial^2}{\partial\alpha^2}\right)\right\}$$

$$L_{33} = -\frac{(1+N_\beta^o)}{R^2} + N_\alpha^o\frac{\partial^2}{\partial x^2} + \frac{N_\beta^o}{B^2}\frac{\partial^2}{\partial\eta^2} - \frac{h^2}{12}\nabla^2\nabla^2 \quad .$$

In the general case all that remains is to assume suitable functions similar to (10) for the axial and circumferential displacements, substitute them into (13) utilize Galerkins method and after a considerable number of algebraic manipulations, the analysis is reduced to that of a classic eigenvalue problem. To illustrate the technique and provide the numerical data for the case of greatest physiological significance we shall consider the lowest doubly symmetric mode, namely that which degenerates into rotationally symmetric case for the circular shell. This is accomplished by putting the subscript equal to zero in all the equations.

While this method of using the Mathieu functions reduces the solution to a third order eigenvalue problem, the algebra involved is tedious and we shall omit it. We assume for the displacements, the form

$$u(\eta,x,t) = A\ ce_0(\eta,-q)\ \mathrm{Cos}(\varrho t - kx) \qquad (14)$$

and similar expressions for the other two displacements. Since we are concerned only with small values of q, we truncate the Mathieu functions at the third term of the expansion. Thus we have, from [3], for example

$$ce_0(\eta,-q) \simeq A_0^o + A_2^o\ \mathrm{Cos}\ 2\eta + A_4^o\ \mathrm{Cos}\ 4\eta \qquad (15)$$

where $A_0^o = 1$, $A_2^o = (q/2)\,(1 - 7q^2/56)$, $A_4^o = (q^2/32)\,(1 - 40q^2/163)$. The influence of terms of higher order than q^4 on the eigen solutions was negligible.

Substituting (15) into (14) and then into (13) and using Galerkins method, we obtain the terms in the eigenmatrix as

$$L_{11}^* = (1+N_x^o)\,k^2 N + \{\frac{(1-\nu)}{2} + N_\beta^o\}\,(\frac{2}{e^2\beta})\left[4(A_2^o)^2 + 16(A_4^o)^2 + \frac{4A_2^o(1+5A_4^o/2)}{\beta}\right]$$

$$L_{12}^* = -\frac{(1+\nu)}{2}\,k\left(\frac{2^{1/2}}{e\,\beta^{1/2}}\right)\left[2A_2^o + 4A_4^o B_4^2 + \frac{(1+A_2^o B_4^2 + A_4^o/2)}{\beta}\right]$$

$$L_{21}^* = -\frac{(1+\nu)}{2}\,k\left(\frac{2^{1/2}}{e\,\beta^{1/2}}\right)\left[2A_2^o + 4A_4^o B_4^2 + \frac{(A_4^o + A_2^o B_4^2/2)}{\beta}\right]$$

$$L_{13}^* = L_{31}^* = \nu\left(\frac{2^{1/2}}{e\,\beta^{1/2}}\right)k\left[N - \frac{A_2^o(1 + A_4^o)}{\beta}\right]$$

$$L_{22}^* = (1+N_\beta^o)\,\frac{2}{e^2\beta}\left[4 + 16(B_4^2)^2 - \frac{2B_4^2}{\beta}\right] + \{\frac{(1-\nu)}{2} + N_x^o\}\,k^2 M + N_\beta^o\left(\frac{2}{e^2\beta}\right)\left[M + \frac{B_4^2}{\beta}\right]$$

$$+ \frac{h^2}{12}\left(\frac{2}{e^2\beta}\right)\left\{2(1-\nu)\,k^2\left[M + \frac{B_4^2}{\beta}\right] + \left(\frac{2}{e^2\beta}\right)\left[4 + 16(B_4^2)^2 + \frac{5B_4^2}{\beta}\right]\right\}$$

$$L_{23}^* = -\frac{2}{e^2\beta}\left[2A_2^o + 4A_4^o B_4^2 - \frac{(1-A_4^o/2 + A_2^o B_4^2/2)}{\beta}\right] + 2N_\beta^o\left(\frac{2}{e^2\beta}\right)[2A_2^o - 4A_4^o B_4^2]$$

$$- \frac{h^2}{12}\left(\frac{2}{e^2\beta}\right)\left[\left(\frac{2}{e^2\beta}\right)^8\left\{A_2^o + 8A_4^o B_4^2 + \frac{(4A_4^o + A_2^o B_4^2)}{\beta}\right\} + (2-\nu)\,k^2(2A_2^o + 4A_4^o B_4^2)\right]$$

$$L^*_{32} = -\frac{2}{e^2\beta}\left[2A_2^o + 4A_4^oB_4^2\right] + 2N_\beta^o\left(\frac{2}{e^2\beta}\right)\left[2A_2^o - 4A_4^oB_4^2 - \frac{(1+A_4^o+3A_2^oB_4^2/2)}{\beta}\right]$$

$$- \frac{h^2}{12}\left(\frac{2}{e^2\beta}\right)\left[\left(\frac{2}{e^2\beta}\right)^8\left\{A_2^o + 8A_4^oB_4^2 + \frac{(\frac{3}{2} + 4A_4^oB_4^2 + A^o/4)}{\beta}\right\}\right.$$

$$\left. + (2-\nu)\,k^2(2A_2^o + 4A_4^o\,B_4^2)\right]$$

$$L^*_{33} = (1+N_\beta^o)\left(\frac{2}{e^2\beta}\right)\left[N + \frac{A_2^o(2+A_4^o)}{\beta}\right] + N_x^o\,k^2\,N - N_\beta^o\left(\frac{2}{e^2\beta}\right)\left[4(A_2^o)^2+16(A_4^o)^2\right.$$

$$\left. - \frac{A_4^o(4-10_2^o)}{\beta}\right] + \frac{h^2}{12}\left\{k^4N + \frac{2k^2}{e^2\beta}\left[4(A_2^o)^2 + 16(A_4^o)^2 + \frac{A_2^o(4+10A_4^o)}{\beta}\right]\right.$$

$$\left. + \frac{4}{e^4\,\beta^2}\left[16(A_2^o)^2 + 256(A_4^o)^2 + \frac{32A_2^o + 256A_4^o + 272A_2^o\,A_4^o}{\beta}\right]\right\} .$$

3.4. Discussion of the Results.

The eigenvalue problem was solved by using a digital routine capable of handling nonsymmetric matrices and by defining all the parameters except σ^2, which is the eigenvalue. It is noted that the elements of the matrix are nonsymmetric only with respect to terms that are of order β^{-1}. Clearly these terms are of questionable accuracy and when deleted the change in the eigenvalues was entirely negligible. It is also self evident that the approximations introduced preclude the use of this work for very large eccentricities. A check of all cases with a two term solution of (15) was made by taking $A_4^o = 0$. It was found that adequate accuracy was achieved for eccentricities up to 0.5 but for higher

values the results are suspect. Noting the interdependence of β and e, this is not at all surprising.

On reviewing the equations, it takes little effort to show that the theory does indeed converge to the results for a circular cross section as the eccentricity tends to zero. This is amply demonstrated by the results in Table 1. In this table we see a very small effect of eccentricity on the phase velocities for all three types of waves. The circumferential prestress due to uniform internal pressure in a cylinder of noncircular cross section is not a simple problem in membrane theory. Therefore this preliminary study of the effects of ellipticity of the cross section on the wave transmission characteristics was restricted to zero circumferential prestress. In Chapter IV, it is shown that the displacements and rotations of the circumferential prestress resultants must be accounted for to obtain physically meaningful results.

3.5. Conclusion.

The influence of eccentricity on the phase velocities of perturbations represented by the zeroth order Mathieu functions are, for eccentricities less than 0.5, very small.

N_x^o	Wave Mode	e	k	σ	c	k	σ	c	k	σ	c
	Type I	0	0.5	.0942	.1884	1.0	.1781	.1781	2.0	.3046	.1523
	or	0.1		.0943	.1887		.1785	.1785		.3061	.1530
	Pressure	0.3		.0947	.1895		.1800	.1800		.3087	.1543
		0.5		.0910	.1820		.1821	.1821		.3176	.1588
	Type II	0		.2500	.5000		.5000	.5000		1.0000	.5009
0	or	0.1		.2504	.5008		.5008	.5008		1.0018	.5009
	Torsion	0.3		.2484	.4969		.4989	.4989		.9981	.4991
		0.5		.2316	.4632		.4884	.4884		.9701	.4850
	Type III	0		.5030	1.0060		1.0055	1.0055		2.0078	1.0039
	or	0.1		.5031	1.0062		1.0055	1.0055		2.0079	1.0040
	Axial	0.3		.5034	1.0086		1.0067	1.0067		2.0103	1.0052
		0.5		.5135	1.0269		1.0157	1.0157		2.0283	1.0142
	Type I	0		.1055	.2110		.2147	.2147		.4551	.2276
	or	0.3		.1007	.2014		.2063	.2063		.4417	.2208
	Pressure	0.5		.1002	.2005		.2075	.2075		.4413	.2206
	Type II	0		.3354	.6708		.6708	.6708		1.3416	.6708
0.2	or	0.3		.3342	.6684		.6700	.6700		1.3403	.6702
	Torsion	0.5		.3207	.6414		.6577	.6577		1.3196	.6598
	Type III	0		.5031	1.0062		1.0055	1.0055		2.0078	1.0039
	or	0.3		.5511	1.1022		1.1007	1.1007		2.1992	1.0996
	Axial	0.5		.5596	1.1193		1.1090	1.1090		2.2157	1.1078

Table I: Influence of Eccentricity on the Phase Velocities of Waves Defined by the Zeroth Order Mathieu Function.

NOTATION

$\underline{a}$	Characteristic number of the Mathieu Function
$\bar{a}$	Semi major axis of the ellipse and normalizing geometric dimension
A_{2r}^{2m}, B_{2r}^{2m}	Coefficients of the Mathieu and Modified (Radial) Mathieu Functions
A, B	Lamé parameters of the shell midsurface
$Ce_{2m}(\xi, -q)$	Modified (radial) Mathieu Function of order 2m, with negative q
$ce_{2m}(\eta, -q)$	Mathieu Function of order 2m with negative q
$\bar{E}$	Young's modulus
e	Eccentricity of the ellipse
$h = \bar{h}/\bar{a}$	Nondimensional shell thickness
L_{ij}	Differential operators of the displacement equilibrium equations
k	Nondimensional wave number
M, N	Integrals defined in (12)
N_{α}^{o}, N_{β}^{o}	Nondimensional prestress resultants
n	Coordinate normal to the shell midsurface
$p = (1-\nu^2)\bar{p}/\bar{E}h$	Nondimensional pressure

$q =$	$k^2e^2/4$
R	Nondimensional radial coordinate
$t = \bar{\sigma}_0 \bar{t}$	Nondimensional time
U	Nondimensional fluid velocity
u, v, w	Nondimensional shell midsurface displacements
x, y, z	Cartesian coordinates
$\beta =$	$(2/e^2-1)$
$\gamma =$	$2\lvert q\rvert^{1/2} \cosh \xi$
ν	Poissons ratio
ξ, η	Elliptic coordinates
ρh	Nondimensional shell wall density, which is unity because of the choice of normalizing constants
ρ_f	Nondimensional fluid density
$\sigma = \bar{\sigma}/\bar{\sigma}_0$	Nondimensional frequency
$\bar{\sigma}_0 = \left[\frac{\bar{E}}{\bar{\rho}\,\bar{a}^2(1-\nu^2)}\right]^{1/2}$	Normalizing frequency
$\Phi = \bar{\Phi}/\bar{a}^2\,\bar{\sigma}_0$	Nondomensional fluid potential function
$\bar{\cdot}$	Bar over a symbol denotes a dimensional quantity

REFERENCES

[1] Kresch, E. N., "Design of a Nonlinear Electric Model for Veins", University of Pennsylvania Dissertation, 1968.

[2] Anliker, M. and J. E. Maxwell, "The Dispersion of Waves in Blood Vessels", Biomechanics Symposium, ASME, New York, pp. 47-67 (1967).

[3] McLachlan, N. W., "Theory and Application of Mathieu Functions, Dover, Inc., New York, 1964.

[4] Bisplinghoff, R. H. and H. Ashley, Principles of Aeroelasticity, John Wiley, New York, pp. 79-80, 1962.

[5] Washizu, K., "Some Considerations of Shell Theory, A.S.R.L., Rept. 1001, M.I.T., October 1960.

CHAPTER IV

APPLICATION OF VARIOUS SHELL THEORIES TO BLOOD FLOW PROBLEMS

4.1. Introduction.

In many situations involving the flow of blood within the vascular system, as in the case of primary arteries, it is essential to account for the significant prestressed state, about which the pulsations take place. In addition to this, it is clearly established that the constitutive law of any tissue is very complex and there is evidence, e.g., [1], [2] that arteries and veins, over their full range, including the excised state, exhibit some of the characteristics of locking solids [3]. However for a number of investigations we are primarily concerned with the behavior of the vessel in a small neighborhood of a quasi-static prestressed state. For such cases the perturbation strains of interest are small and it is reasonable, at least as a first approximation, to treat the vessel wall material as perfectly elastic and consider the prestressed state as given. Once this is done the equations of elastic shell theory become applicable to blood vessels and we shall now discuss certain facets of this theory, as it applies to cylinders, in particular those of circular cross section.

In reviewing the well known literature, e.g., [4] to [13] of this type of problem it is immediately obvious, as in many other fields of shell analysis, that the equations used by the various authors do not agree in all respects. Another subject of considerable interest is to note that

unlike metal structures, the strains induced by the prestress in the primary arteries are not negligible compared to unity. Furthermore Biot showed in 1938 [14] and reviewed in his book [15] the fact that the stress-strain law for the incremental deformations, relative to the prestress state is, in rectangular Cartesian coordinates, non-symmetric, for prestress states which are not hydrostatic. The same conclusion is reached by Pflüger [16]. Therefore it is desirable to review the cylindrical elastic shell equations for linearized perturbations about a given prestressed state, in an attempt to illustrate some of the questions raised. Since many of the points we wish to make can be illustrated using cylinders of circular cross section we shall take advantage of the algebraic simplicity of having the second Lamé coefficient equal to the constant radius of the shell, in certain investigations while retaining general cross sections in others.

4.2. Bolotins Dynamic Stability Equations for a Circular Cylinder.

Since the dynamic stability of shells has been a research topic of considerable interest over the past decade and is likely to remain so for many years, it is tempting to utilize the equations presented in a well known text. As an example there is [7], in which Bolotin considers the dynamic stability of circular cylinders and gives the differential equations describing small perturbations about a prestressed state:

$$[L_{ij}] \begin{vmatrix} u \\ v \\ w \end{vmatrix} + \begin{vmatrix} X \\ Y \\ Z \end{vmatrix} = 0 \qquad (1)$$

in which, after correcting some typographical errors in [7]

$$L_{11} = \frac{\partial^2}{\partial x^2} + \frac{(1-\nu)}{2R^2} \frac{\partial^2}{\partial \phi^2}$$

$$L_{12} = L_{21} = \frac{(1+\nu)}{2R} \frac{\partial^2}{\partial x \partial \phi} + \frac{(N_x^o - N_\phi^o)}{R} \frac{\partial^2}{\partial x \partial \phi}$$

$$L_{13} = - \frac{\nu}{R} \frac{\partial}{\partial x} - \frac{(N_x^o - N_\phi^o)}{R} \frac{\partial}{\partial x}$$

$$L_{22} = \frac{1}{R^2} \frac{\partial^2}{\partial \phi^2} + \frac{(1-\nu)}{2} \frac{\partial^2}{\partial x^2}$$

$$L_{23} = - L_{32} = - \frac{1}{R^2} \frac{\partial}{\partial \phi}$$

$$L_{31} = \frac{\nu}{R} \frac{\partial}{\partial x}$$

$$L_{33} = d^2 \nabla^2 \nabla^2 + N_x^o \frac{\partial^2}{\partial x^2} + \frac{N_\phi^o}{R^2} \left(\frac{\partial^2}{\partial \phi^2} - 1 \right)$$

and X, Y and Z are the applied midsurface loads per unit area. One of the most interesting aspects of these operators is that L_{13} is not the adjoint of L_{31} except when $N_x^o = N_\phi^o$ in which case the only "prestress term" appears in operator L_{33}.

Reviewing Bolotin's derivation we see that it is based on the determination of certain "reduced (membrane) loads". These are obtained by writing the linear membrane equations in terms of the Lamé coefficients and then replacing these by their values in the deformed state, to obtain a set of geometrically non-linear (large displacement) membrane equations.

This technique does not produce the same large displacement membrane equations as those described by other authors. Also, Bolotin's equations exhibit non-self adjointness in one of the operator pairs even though his theory is based on the assumption of small strains. It is well known that all linear differential equations derivable from a variational principle must be self adjoint. Hence his equations for the incremental reduced loads should be scrutinized. The basic idea of using the large deflection membrane equations to obtain the membrane prestress terms is valid, but obtaining these equations by replacing in the linear equations A by $A(1 + \ell_{11})$ and B by $B(1 + \ell_{22})$ is not satisfactory as we shall now demonstrate.

If we restrict ourselves to $N^{o}_{\alpha\beta} = 0$ for this purpose, Washizu's membrane equations [12] for cylinders with $A = 1$ and $R_{\alpha}^{-1} = 0$, we can write

$$\frac{\partial}{\partial\alpha}\{N_{\alpha}(1 + \ell_{11})\} + \frac{1}{B}\frac{\partial}{\partial\beta}(N_{\beta}\,\ell_{12}) + X = 0$$

$$\frac{1}{B}\frac{\partial}{\partial\beta}\{N_{\beta}(1 + \ell_{22})\} + \frac{\partial}{\partial\alpha}(N_{\alpha}\,\ell_{21}) - \frac{N_{\beta}\,\ell_{32}}{R_{\beta}} + Y = 0 \qquad (2)$$

$$\frac{\partial}{\partial\alpha}(N_{\alpha}\,\ell_{31}) + \frac{1}{B}\frac{\partial}{\partial\beta}(N_{\beta}\,\ell_{32}) + \frac{N_{\beta}}{R_{\beta}}(1 + \ell_{22}) + Z = 0$$

where the ℓ_{ij} are the linear strains and rotations, namely

$$\ell_{11} = \partial u/\partial\alpha; \quad \ell_{12} = (1/B)\,\partial u/\partial\beta; \quad \ell_{21} = \partial v/\partial\alpha$$

$$\ell_{22} = (1/B)\,\partial v/\partial\beta - w/R_{\beta}; \quad \ell_{31} = \omega_{\beta} = \partial w/\partial\alpha$$

$$\ell_{32} = \omega_{\alpha} = v/R_{\beta} + (1/B)\,\partial w/\partial\alpha.$$

The technique for obtaining the equations for the incremental or "reduced" forces due to the prestress (labelled by some authors as variational equations) is to express each dependent variable as the sum of the value corresponding to the zeroth (basic membrane) state plus a perturbation. Then we make use of the fact that the shell is in equilibrium in the zeroth state and retain only those terms that are of the first power in the perturbation quantities. To simplify the algebra without deleting anything significant for our demonstration, let us restrict ourselves to cylinders in which $B = R_\beta$, $N^o_{\alpha\beta} = 0$ and the membrane prestress resultants, N^o_α and N^o_β are constants. Then we have

$$N^o_\alpha \frac{\partial^2 u}{\partial \alpha^2} + \frac{N^o_\beta}{R_\beta} \frac{\partial}{\partial \beta}\left(\frac{1}{R_\beta}\frac{\partial u}{\partial \beta}\right) + X' = 0$$

$$\frac{N^o_\beta}{R_\beta}\frac{\partial}{\partial \beta}\left(\frac{1}{\beta}\frac{\partial v}{\partial \beta}\right) + N^o_\alpha \frac{\partial^2 v}{\partial \alpha^2} - \frac{N^o_\beta v}{R^2_\beta} - \frac{N^o_\beta}{R_\beta}\left\{\frac{\partial}{\partial \beta}\left(\frac{w}{R_\beta}\right) + \frac{1}{R_\beta}\frac{\partial w}{\partial \beta}\right\} + Y' = 0 \qquad (3)$$

$$\frac{N^o_\beta}{R_\beta}\left\{\frac{\partial}{\partial \beta}\left(\frac{v}{R_\beta}\right) + \frac{1}{R_\beta}\frac{\partial v}{\partial \beta}\right\} + N^o_\alpha \frac{\partial^2 w}{\partial \alpha^2} + \frac{N^o_\beta}{R_\beta}\left\{\frac{\partial}{\partial \beta}\left(\frac{1}{R_\beta}\frac{\partial w}{\partial \beta} - \frac{w}{R_\beta}\right)\right\} + Z' = 0 .$$

These equations are self adjoint in contrast to those given by Bolotin.

While this review of Bolotin's equations may be of interest, it does not help explain the differences in the equations proposed by other authors. Many have used the principles of virtual work or minimum potential energy, but the results depend on the strain displacement relations utilized. For theories applicable primarily to metal shells, the neglection of the nonlinear terms involving the inplane displacements in

these relations has been proven permissible. However we shall retain these terms to study their effects in the case of blood vessels and present Washizu's [12] theory for a cylinder of general cross section.

4.3. Equations for Cylindrical Shells Under Initial Stress when the Strains are Negligible Compared to Unity.

Let us now restrict our attention to those sets of equations in which the strains are considered negligible compared to unity, while retaining all terms involving the prestress resultants, but relax the assumption that the cross section is circular. Once this particular small strain assumption is invoked, Washizu's equations [12] can be utilized directly and the matrix of differential operators for a membrane prestress state in which the axial and circumferential stress are constant and the inplane shear stress is zero, become

$$L_{11} = \frac{\partial^2}{\partial\alpha^2} + \frac{(1-\nu)}{2B}\frac{\partial}{\partial\beta}\left(\frac{1}{B}\frac{\partial}{\partial\beta}\right) + N^o_\alpha \frac{\partial^2}{\partial\alpha^2} + \frac{N^o_\beta}{B}\frac{\partial}{\partial\beta}\left(\frac{1}{B}\frac{\partial}{\partial\beta}\right)$$

$$L_{12} = L_{21} = \frac{(1+\nu)}{2B}\frac{\partial^2}{\partial\alpha\partial\beta}$$

$$L_{31} = -L_{13} = \frac{\nu}{R_\beta}\frac{\partial}{\partial\alpha} \qquad (4)$$

$$L_{22} = \frac{1}{B}\frac{\partial}{\partial\beta}\left(\frac{1}{B}\frac{\partial}{\partial\beta}\right) + \frac{(1-\nu)}{2}\frac{\partial^2}{\partial\alpha^2} - \frac{N^o_\beta}{R^2_\beta} + \frac{N^o_\beta}{B}\frac{\partial}{\partial\beta}\left(\frac{1}{B}\frac{\partial}{\partial\beta}\right) + N^o_\alpha\frac{\partial^2}{\partial\alpha^2}$$

$$+ \frac{h^2}{12R^2_\beta}\left\{2(1-\nu)\frac{\partial^2}{\partial\alpha^2} + \frac{R_\beta}{B}\frac{\partial}{\partial\beta}\left(\frac{1}{B}\frac{\partial}{\partial\beta}\left(\frac{\cdot}{R_\beta}\right)\right)\right\}$$

$$L_{23} = -\frac{1}{B}\frac{\partial}{\partial\beta}\left(\frac{\cdot}{R_\beta}\right) - \frac{2N^o_\beta}{R_\beta B}\frac{\partial}{\partial\beta} + \frac{h^2}{12R_\beta}\left\{\frac{1}{B}\frac{\partial}{\partial\beta}\left(\frac{1}{B}\frac{\partial}{\partial\beta}\left(\frac{1}{B}\frac{\partial}{\partial\beta}\right)\right) + \frac{(2-\nu)}{B}\frac{\partial^3}{\partial\alpha^2\partial\beta}\right\}$$

$$L_{32} = \frac{1}{R_\beta B}\frac{\partial}{\partial\beta} + \frac{2N^o_\beta}{B}\frac{\partial}{\partial\beta}\left(\frac{\cdot}{R_\beta}\right) - \frac{h^2}{12B}\left\{\frac{\partial}{\partial\beta}\left(\frac{1}{B}\frac{\partial}{\partial\beta}\left(\frac{1}{B}\frac{\partial}{\partial\beta}\left(\frac{\cdot}{R_\beta}\right)\right)\right)\right. \tag{4}$$

$$\left. + (2-\nu)\frac{\partial}{\partial\beta}\left(\frac{1}{R_\beta}\frac{\partial^2}{\partial\alpha^2}\right)\right\}$$

$$L_{33} = -\frac{\cdot}{R_\beta^2} + N^o_\alpha\frac{\partial^2}{\partial\alpha^2} + \frac{N^o_\beta}{B}\frac{\partial}{\partial\beta}\left(\frac{1}{B}\frac{\partial}{\partial\beta}\right) - \frac{N^o_\beta}{R_\beta^2} - \frac{h^2}{12}\nabla^2\nabla^2$$

As we would expect, the prestress terms are the same as those in (3). The operators L_{23} and L_{32} differ by more than the sign, but recalling the definition of a self adjoint differential operator it can be shown that they are the adjoints of each other. For two dimensional systems, the adjoint operator of $\partial\{a(\alpha,\beta)\,u(\alpha,\beta)\}/\partial\alpha$, where $a(\alpha,\beta)$ is a coefficient of the independent variables only, is by definition $(-1)\,a(\alpha,\beta)\,\partial u(\alpha,\beta)/\partial\alpha$ and similarly for higher order derivatives. We note that since all cylinders are developable surfaces it is always possible to choose coordinates such that both Lamé parameters are unity, i.e., we can replace $Bd\beta$ by ds wherever convenient. This is particularly advantageous when demonstrating that the operators are self adjoint. For a circular cross section, the operators of (4) can be easily simplified by putting $\alpha = x$, $\beta = \phi$ and $R_\beta = B = R$.

The prestress terms in these operators are then precisely those obtained by Armenakas and Herrmann [17]. They can also be derived by a variational method when the nonlinear in-plane displacement terms are retained in the strain-displacement relations and the strains are considered

to be small. However, when the circumferential prestress is due to hydrostatic pressure, [17] shows that certain prestress terms are cancelled by force components that arise from the rotation of the applied pressure. This fact is particularly important as we shall demonstrate later, but is usually not mentioned in the literature.

It is of interest to note that Flügge's equations, as used by Anliker and Maxwell [18] are identical with those of Herrmann and Armenakas [13] and the succeeding papers based on this work; if the same assumption is made concerning the application of the prestresses. In [18] the authors consider that after the axial prestress is applied, axial expansion of the cylinder is prevented while the cylinder pressurized. This yields an axial prestress resultant of $N_x^o + \nu N_\phi^o$, rather than N_x^o if the shell is not restrained. We allow the vessel to be unrestrained. In our notation the corresponding self adjoint operators for the theories based on [4] and [13] are

$$
\begin{aligned}
L_{11} &= \frac{\partial^2}{\partial x^2} + \frac{(1-\nu)}{2R^2}(1+d^2)\frac{\partial^2}{\partial \phi^2} + N_x^o \frac{\partial^2}{\partial x^2} + \frac{N_\phi^o}{R^2}\frac{\partial^2}{\partial \phi^2} \\
L_{12} &= L_{21} = \frac{(1+\nu)}{2R}\frac{\partial^2}{\partial x \partial \phi} \\
L_{31} &= -L_{13} = \frac{\nu}{R}\frac{\partial}{\partial x} - \frac{d^2}{R}\left\{\frac{\partial^3}{\partial x^3} - \frac{(1-\nu)\partial^3}{2R^2\,\partial x \partial \phi^2}\right\} - \frac{N_\phi^o}{R}\frac{\partial}{\partial x} \\
L_{22} &= \frac{1}{R^2}\frac{\partial^2}{\partial \phi^2} + \frac{(1-\nu)}{2}(1+d^2)\frac{\partial^2}{\partial x^2} + N_x^o \frac{\partial^2}{\partial x^2} + \frac{N_\phi^o}{R^2}\frac{\partial^2}{\partial \phi^2}
\end{aligned}
\qquad (5)
$$

$$L_{32} = -L_{23} = +\frac{1}{R}\frac{\partial}{\partial\phi} - \frac{d^2(3-\nu)}{2}\frac{\partial^3}{\partial x^2\,\partial\phi} - \frac{N^o_\phi}{R^2}\frac{\partial}{\partial\phi}$$

$$L_{33} = -\frac{1}{R^2} - d^2\left(R^2\nabla^2\nabla^2 + \frac{2}{R^2}\frac{\partial^2}{\partial\phi^2} + \frac{1}{R^2}\right) - N^o_x\frac{\partial^2}{\partial x^2} + \frac{N^o_\phi}{R^2}\frac{\partial^2}{\partial\phi^2} \qquad (5)$$

The differences between (4) and (5) arise from two different causes. Firstly in (5) the equilibrium equations in terms of the stress resultants, the last terms in the operators L_{13} and L_{31} do not occur in Washizu's derivation. However they have $-N^o_\phi(v + \partial w/\partial\phi)/R^2$ in the second equation and $-N^o_\phi(w + \partial v/\partial\phi)/R^2$ in the third that do not appear in (5). These discrepancies will be shown later to be caused by neglect of the changes of the hydrostatic pressure force component that occurs when the shell undergoes perturbation rotations and midsurface strains. Secondly the other differences that do not involve the prestress terms are due to [4] and [13] using, for the definitions of the stress resultants expressions such as

$$N_x = \int_{-h/2}^{h/2} \sigma_x\left(1 + \frac{z}{R}\right) dz$$

while in many other works, z/R is neglected compared to unity. These terms are recognizable in (5) as those containing d^2 in all operators except L_{23}, L_{32}, and L_{33}.

In spite of the efforts of many investigators and as we have just partially demonstrated there does not appear to be a generally accepted "correct" set of equations based on the Kirchoff-Love hypothesis which describe the behavior of prestressed thin shells. For many investigations,

the "small strain and moderately small rotations" assumptions has frequently been invoked to remove the nonlinear terms in u and v from the strain displacement relations. While controversy over the linear formulation has been very pronounced until recently, we are even further from complete agreement on the equations that should be used in the nonlinear problem. There is no intent here to devise a new approach to the general problem but rather to review existing knowledge to explain certain facets of the behavior of prestressed cylindrical shells of general cross section while retaining the assumption of small strains, but admitting rotations about the normal to the midsurface

Koiter [5], Naghdi [6], Kempner [8], Dill [9], Sanders [10], and Budiansky [11] are among those who have devoted considerable effort to geometrically nonlinear shell problems. As an example let us consider the equations on [10], which allow for the rotation of the shell element about the normal to the middle surface. With this degree of complexity we have, for the strain-displacement relations

$$\epsilon_\alpha = \frac{\partial u}{\partial \alpha} + \frac{1}{2}\left(\frac{\partial w}{\partial \alpha}\right)^2 + \frac{1}{2}\left(\frac{\partial v}{\partial \alpha} - \frac{1}{B}\frac{\partial u}{\partial \beta}\right)^2$$

$$\epsilon_\beta = \frac{1}{B}\frac{\partial v}{\partial \beta} + \frac{w}{R_\beta} + \frac{1}{2}\left(\frac{1}{B}\frac{\partial w}{\partial \beta} - \frac{v}{R_\beta}\right)^2 + \frac{1}{2}\left(\frac{\partial v}{\partial \alpha} - \frac{1}{B}\frac{\partial u}{\partial \beta}\right)^2$$

$$\epsilon_{\alpha\beta} = \frac{1}{2}\left\{\frac{\partial v}{\partial \alpha} + \frac{1}{B}\frac{\partial u}{\partial \beta} + \frac{\partial w}{\partial \alpha}\left(\frac{1}{B}\frac{\partial w}{\partial \beta} - \frac{v}{R_\beta}\right)\right\} \qquad (6)$$

$$K_\alpha = -\frac{\partial^2 w}{\partial \alpha^2} \qquad K_\beta = -\frac{1}{B}\frac{\partial}{\partial \beta}\left(\frac{1}{B}\frac{\partial w}{\partial \beta}\right) + \frac{1}{B}\frac{\partial}{\partial \beta}\left(\frac{v}{R_\beta}\right)$$

$$K_{\alpha\beta} = \frac{1}{2}\left\{-\frac{2}{B}\frac{\partial^2 w}{\partial \alpha \partial \beta} + \frac{1}{R_\beta}\frac{\partial v}{\partial \alpha} + \frac{1}{2R_\beta}\left(\frac{\partial v}{\partial \alpha} - \frac{1}{B}\frac{\partial u}{\partial \beta}\right)\right\}$$

The terms underlined by dashes represent the influence of rotation about the normal to the middle surface. In many types of problems it is justifiable to state that the rotation normal to the middle surface is markedly smaller than the two rotations about axes in the plane of the middle surface. When this assumption is justified and the underlined terms are removed from (6) we have the strain displacement relations which are frequently used in investigations of shell stability. It is worth pointing out that nonlinear terms have been retained only in the direct strains, leaving the curvatures as linear in the displacements. Sanders [10] shows that retaining all terms in (6) yields the following differential operators in the displacement equations of equilibrium for a circular cross section when $N^{o}_{x\phi} = 0$ and the other two prestress resultants are constants:

$$
\begin{aligned}
L_{11} &= \frac{\partial^2}{\partial x^2} + \frac{(1-\nu)}{2R^2}\left(1 + \frac{d^2}{4}\right)\frac{\partial^2}{\partial \phi^2} + \underline{\frac{(N^{o}_{x} + N^{o}_{\phi})}{2R^2}\frac{\partial^2}{\partial \phi^2}} \\
L_{12} &= L_{21} = \frac{(1+\nu)}{2R}\frac{\partial^2}{\partial x \partial \phi} - \frac{3(1-\nu)d^2}{8R}\frac{\partial^2}{\partial x \partial \phi} - \underline{\frac{(N^{o}_{x} + N^{o}_{\phi})}{2R}\frac{\partial^2}{\partial x \partial \phi}} \\
L_{31} &= -L_{13} = \frac{\nu}{R}\frac{\partial}{\partial x} + \frac{(1-\nu)\,d^2}{2R^2}\frac{\partial^3}{\partial x \partial \phi^2} \\
L_{22} &= \frac{(1+d^2)}{R^2}\frac{\partial^2}{\partial \phi^2} + \frac{(1-\nu)}{2}\left(1 + \frac{9d^2}{4}\right)\frac{\partial^2}{\partial x^2} - \frac{N^{o}_{\phi}}{R^2} + \underline{\frac{(N^{o}_{x} + N^{o}_{\phi})}{2}\frac{\partial^2}{\partial x^2}} \\
L_{32} &= -L_{23} = \frac{1}{R^2}\frac{\partial}{\partial \phi} - \frac{d^2}{R^2}\frac{\partial^3}{\partial \phi^3} - \frac{(3-\nu)d^2}{2}\frac{\partial^3}{\partial x^2 \partial \phi} + \frac{N^{o}_{\phi}}{R^2}\frac{\partial}{\partial \phi} \\
L_{33} &= -d^2R^2\nabla^2\nabla^2 - \frac{1}{R^2} + N^{o}_{x}\frac{\partial^2}{\partial x^2} + \frac{N^{o}_{\phi}}{R^2}\frac{\partial^2}{\partial \phi^2} \quad .
\end{aligned}
\tag{7}
$$

These operators are self adjoint and differ quite considerably from (3) as we would expect since certain large inplane displacements are neglected in (7).

4.4. Geometrically Non-Linear Thin Circular Cylindrical Shell Analyses Allowing for Large Strains.

In studying most of the contributions mentioned that are based on the small strain assumption, it is soon demonstrated that the displacement equilibrium equations are self adjoint and thus, for the thin circular cylinder can be written in symmetric form. Since self adjointness reduces to symmetry in cartesian coordinates we have reason to be curious about this conflict with Biot's and Pflüger's demonstrations that the equations of elasticity for incremental deformations are non-symmetric in cartesian coordinates. The clue to this paradox comes from the fact that the majority of authors on shell theory, neglect, in the strain displacement relations, all non-linear terms involving the tangential displacements u and v. This means that they assume small strains and rotations, from the start. Self adjointness of differential operators, at least as usually defined (see e.g. [19]) has meaning only for linear equations. Hence when the potential energy contains displacement terms to powers higher than the second, the self adjointness of the final equations from which the eigenmatrix is formed, depends on the assumptions made to linearize the Euler equations of the variational method. Two contributions which retain the nonlinear terms in u and v are Washizu [12] and Herrmann-Armenakas [13] whose strain displacement relations for a circular cylinder are

$$\epsilon_x = \frac{\partial u}{\partial x} + \frac{1}{2}\left\{\left(\frac{\partial u}{\partial x}\right)^2 + \left(\frac{\partial v}{\partial x}\right)^2 + \left(\frac{\partial w}{\partial x}\right)^2\right\}$$

$$\epsilon_\phi = \frac{1}{R}\left(\frac{\partial v}{\partial \phi} - w\right) + \frac{1}{2R^2}\left\{\left(\frac{\partial u}{\partial \phi}\right)^2 + \left(\frac{\partial v}{\partial \phi} - w\right)^2 + \left(v + \frac{\partial w}{\partial \phi}\right)^2\right\} \tag{8}$$

$$\epsilon_{x\phi} = \frac{1}{R}\frac{\partial u}{\partial \phi} + \frac{\partial v}{\partial x} + \frac{1}{R}\left\{\frac{\partial u}{\partial x}\frac{\partial u}{\partial \phi} + \frac{\partial v}{\partial x}\left(\frac{\partial v}{\partial \phi} - w\right) + \frac{\partial w}{\partial x}\left(v + \frac{\partial w}{\partial \phi}\right)\right\}$$

$$K_x = \frac{\partial^2 w}{\partial x^2}; \quad K_\phi = \frac{1}{R^2}\left(\frac{\partial^2 w}{\partial \phi^2} + \frac{\partial v}{\partial \phi}\right); \quad K_{x\phi} = \frac{1}{R}\left(\frac{\partial^2 w}{\partial x \partial \phi} + \frac{\partial v}{\partial x}\right) .$$

Inserting (8) into the expression for the strain energy, neglecting z/R relative to unity and utilizing the calculus of variations in the time honored manner, we obtain the large displacement equilibrium equations which were derived by Washizu using the theorem of virtual displacements. They are

$$\frac{\partial}{\partial x}\left\{N_x(1 + \ell_x) + \frac{N_{x\phi}}{R}\frac{\partial u}{\partial \phi}\right\} + \frac{1}{R}\frac{\partial}{\partial \phi}\left\{\frac{N_\phi}{R}\frac{\partial u}{\partial \phi} + N_{x\phi}(1 + \ell_x)\right\} + X = 0$$

$$\frac{1}{R}\frac{\partial}{\partial \phi}\left\{N_\phi(1 + \ell_\phi) + N_{x\phi}\frac{\partial v}{\partial x}\right\} + \frac{\partial}{\partial x}\left\{N_x\frac{\partial v}{\partial x} + N_{x\phi}(1 + \ell_\phi)\right\}$$

$$- \frac{1}{R}\left\{N_\phi \omega_x + N_{x\phi}\omega_\phi + \frac{1}{R}\frac{\partial M_\phi}{\partial \phi} + \frac{\partial M_{x\phi}}{\partial x}\right\} + Y = 0 \tag{9}$$

$$\frac{\partial}{\partial x}\left\{N_x \omega_\phi + N_{x\phi}\omega_x\right\} + \frac{1}{R}\frac{\partial}{\partial \phi}\left\{N_\phi \omega_x + N_{x\phi}\omega_\phi\right\} + N_\phi(1+\ell_\phi) + \frac{1}{R}N_{x\phi}\frac{\partial v}{\partial x}$$

$$+ \frac{\partial^2 M_x}{\partial x^2} + \frac{2}{R}\frac{\partial^2 M_{x\phi}}{\partial x \partial \phi} + \frac{1}{R^2}\frac{\partial^2 M_\phi}{\partial \phi^2} + Z = 0$$

in which we have used the linearized strain displacement relations

$$\ell_x = \frac{\partial u}{\partial x}; \quad \ell_\phi = \frac{1}{R}\left(\frac{\partial v}{\partial \phi} - w\right); \quad \omega_x = \frac{1}{R}\left(\frac{\partial w}{\partial \phi} + v\right); \quad \omega_\phi = \frac{\partial w}{\partial x} \quad .$$

These equilibrium equations consist of terms of two types, namely stress resultants and their derivatives plus stress resultants times midsurface rotations, which constitute the equations usually found in shell analyses which invoke the "small strain" assumption. The second type of terms are those consisting of stress resultants times midsurface strains. These latter terms result from a variational formulation only when the non-linear terms in the in lane displacements are retained in the strain-displacement relations. When equation (4) are particularized for a circular cross section and we introduce into (9) the assumption that the strains are negligible compared to unity, the resulting equations are identical.

The complexity of the equations describing the motions relative to the prestressed state, depend, to a large measure on the prestressed state. A simple situation, of frequent interest, particularly in the field of biomechanics is when uniform axial stretch and internal pressure constitute the prestressed state. When solving the linear membrane equations for this loading, we obtain for a circular cross section N_x^o and N_ϕ^o as constants and $N_{x\phi}^o$ vanishes. For non-circular shells the prestress solution is much more involved. If we now assume an isotropic shell in which the Young's modulus is independent of the prestressed state the perturbation equations derived from (9) assume a relatively elegant form. To obtain them, we use the standard technique of inserting $N_x = N_x^o + N_x'$, $\partial u/\partial x = \partial u^o/\partial x + \partial u'/\partial x$ etc., extracting all terms involving only the

zeroth state and assuming that the primed quantities are all small enough for their products to be negligible.

Now we may write the equations for perturbations about a pre-stressed state defined by the constant strains in differential operator form as

$$[L_{ij}] \begin{vmatrix} u \\ v \\ w \end{vmatrix} + \begin{vmatrix} X \\ Y \\ Z \end{vmatrix} = 0 \qquad (10)$$

where

$$L_{11} = (1 + 2\ell_x^o + \nu\ell_\phi^o) \frac{\partial^2}{\partial x^2} + \frac{1}{R^2}\left\{\frac{(1-\nu)}{2}(1 + \ell_x^o) + \ell_\phi^o + \nu\,\ell_x^o\right\} \frac{\partial^2}{\partial \phi^2}$$

$$L_{12} = \frac{(1+\nu)}{2R}(1 + \ell_x^o) \frac{\partial^2}{\partial x \partial \phi}$$

$$L_{13} = -(1 + \ell_x^o) \frac{\nu}{R} \frac{\partial}{\partial x}$$

$$L_{21} = \frac{(1+\nu)}{2R}(1 + \ell_\phi^o) \frac{\partial^2}{\partial x \partial \phi}$$

$$L_{22} = \frac{(1 + 2\ell_\phi^o + \nu\ell_x^o)}{R^2} \frac{\partial^2}{\partial \phi^2} + \left\{\frac{(1-\nu)}{2}(1 + \ell_\phi^o) + \ell_x^o + \nu\ell_\phi^o\right\} \frac{\partial^2}{\partial x^2}$$

$$- \frac{(\ell_\phi^o + \nu\ell_x^o)}{R^3} + d^2\left\{\frac{1}{R^2}\frac{\partial^2}{\partial \phi^2} + \frac{2(1-\nu)}{R}\frac{\partial^2}{\partial x^2}\right\}$$

$$L_{23} = -\frac{1}{R^2}(1 + 3\ell_\phi^o + 2\nu\,\ell_x^o) \frac{\partial}{\partial \phi} + d^2\left\{\frac{1}{R^2}\frac{\partial^3}{\partial \phi^3} + (2-\nu)\frac{\partial^3}{\partial x^2 \partial \phi}\right\}$$

$$L_{31} = (1 + \ell^{o}_{\phi}) \frac{\nu}{R} \frac{\partial}{\partial x}$$

$$L_{32} = \frac{1}{R^2} (1 + 3\ell^{o}_{\phi} + 2\nu\, \ell^{o}_{x}) \frac{\partial}{\partial \phi} - d^2 \left\{ \frac{1}{R^2} \frac{\partial^3}{\partial \phi^3} + (2-\nu) \frac{\partial^3}{\partial x^2 \partial \phi} \right\}$$

$$L_{33} = (\ell^{o}_{x} + \nu \ell^{o}_{\phi}) \frac{\partial^2}{\partial x^2} + \frac{(\ell^{o}_{\phi} + \nu \ell^{o}_{x})}{R^2} \frac{\partial^2}{\partial \phi^2} - \frac{(1 + 2\ell^{o}_{\phi} + \nu \ell^{o}_{x})}{R^2}$$

$$- d^2 \left(R^2 \frac{\partial^4}{\partial x^4} + \frac{2\partial^4}{\partial x^2 \partial \phi^2} + \frac{1}{R^2} \frac{\partial^4}{\partial \phi^4} \right) .$$

It is clear that these operators are self adjoint for large strains only when $\ell^{o}_{\phi} = \ell^{o}_{x}$, i.e., when the prestress state is hydrostatic, substantiating completely Biot's and Pflüger's conclusion. The usual manner in which the influence of the prestressed state is illustrated (see for example [14], [15], [16]) is to show that the non-symmetry in Cartesian coordinates occurs in the stress strain relations and the degree of asymmetry is of the order of the initial stress as divided by the elastic modulus. In our derivation the classic symmetric stress strain law was assumed and the non-self adjointness was also shown to be of the order of the initial strain. In virtually all metallic structures the initial membrane strains are indeed negligible compared to unity and the operators in (10) can be simplified to those resulting from (4) and (9). However in blood flow problems they can be as high or higher than 0.6 and neglecting them is less justified. Throughout our discussion it must be borne in mind that while an elastic stress strain law is reasonable for the perturbation stresses in the blood vessel, but it is not valid for the prestressed

state. The determination of the actual prestressed state in blood vessels is extremely difficult compared with virtually all metal structures experiments.

The equations we have discussed are considered typical of the literature and to see how significant some of the differences are, let us turn to the numerical evaluation of the phase velocities.

To study the importance of the assumptions made in the shell theories that have been discussed in relation to certain biomechanics problems, it is of interest to compute the phase velocity as a function of frequency and prestress levels. The displacement relations for axially propagating waves in a cylinder of circular cross section were substituted into the equations of motion and the resulting eigenvalue problem solved for specified wave numbers. The form of the displacement relations was

$$u(x, \phi, t) = A \cos kx \cos s\phi \sin \sigma t$$

$$v(x, \phi, t) = B \sin kx \sin s\phi \sin \sigma t \qquad (11)$$

$$w(x, \phi, t) = C \sin kx \cos s\phi \sin \sigma t$$

These were inserted into (7) for Sander's [10] theory and (10) for Washizu's [12] theory and into (5) for the Anliker-Maxwell utilization of Flügge's [4] theory and Herrman-Armenakas [13] theory. The computations were also accomplished using Budiansky's theory [11]. The substitution of (11) into (5) and (7) leads to a symmetric matrix because of the self adjointness of the operators, but that derived from (10) naturally remains nonsymmetric.

4.5. Presentation of the Numerical Results and Discussion.

A digital program was written using a readily available non-self-adjoint eigenvalue routine to extract the modes and frequencies for prescribed shell-fluid parameters and wave number. After using the results presented by Anliker and Maxwell [18] to check the accuracy, the nondimensional wave speeds were found as functions of the nondimensional frequency for the theories mentioned previously. The results are shown in Figs. 1 and 2 and correspond to axi-symmetric waves. The former shows the influence of axial stretch, while the latter illustrates how the wave speeds vary as a function of transmural pressure. Data for the $s = 2$ waves did not show any differences from the Anliker-Maxwell results that could be considered significant for physiological applications and therefore have not been illustrated.

For axi-symmetric waves and $N_{\phi}^{o} = 0$, the predictions based on [10], [11], [20] and our equation (5) agree very closely with each other for the type I and type III waves. The lack of agreement with [18] is solely due to the different assumption concerning the prestress application. The behavior of Washizu's theory will be reviewed presently.

A somewhat surprising result is that unlike other shell equations, those of Sanders and Washizu predict a cut-off frequency for the type II or torsion waves whenever the shell is subjected to transmural pressures (see Fig. 2). The cause for this can be seen by noting that the equation for axi-symmetric torsion waves is

$$L_{22}\, v - \frac{\partial^2 v}{\partial t^2} = 0$$

since for $s = 0$, $L_{12} = L_{21} = L_{32} = L_{23} = 0$ and the equilibrium equation for the circumferential torsional direction becomes uncoupled from the other two. For the Anliker-Maxwell [18] utilization of Flügge's theory we have the characteristic equation

$$c^2 = \left(\frac{\sigma}{k}\right)^2 = \left[\frac{(1-\nu)\ \frac{(1+3d^2)}{2} + N_x^o + \nu\ N_\phi^o}{\rho}\right]$$

in which the term νN_ϕ^o vanishes when we use (5). According to this equation the torsion waves are nondispersive and have no cut-off frequency below which they do not propagate. This is in contradiction with the other two theories mentioned. For example, from (10) we have according to Washizu's [12] theory

$$c^2 = \left(\frac{\sigma}{k}\right)^2 = \left[\frac{(1-\nu)\ \frac{(1+\epsilon_\phi^o)}{2} + 2d^2(1-\nu) + N_x^o}{\rho}\right] + \frac{N_\phi^o}{\rho k^2}$$

while Sanders' [10] theory yields

$$c^2 = \left(\frac{\sigma}{k}\right)^2 = \left[\frac{(1-\nu)\ \frac{(1+9d^2/4)}{2} + \frac{(N_x^o + N_\phi^o)}{2}}{\rho}\right] + \frac{N_\phi^o}{\rho k^2} \quad .$$

In both of these cases it is the last term $(N_\phi^o/\rho k^2)$ that introduces both the dispersion and the cut-off frequency from non-zero transmural pressure. As the wave number approaches zero, so does the frequency and the wave speed becomes very large as the frequency approaches zero, and we obtain the cut-off frequency. The existence of the cut-off frequencies

is demonstrated by noting that for finite values of σ, k can be zero. In fact, the above equations show that $\sigma^2 = N^o_\phi/\rho$ for zero wave number. Therefore $\sigma = (N^o_\phi/\rho)^{1/2}$ is the cut-off frequency below which waves do not propagate.

This behavior for the rotationally symmetric torsion waves is so completely contrary to all experimental evidence that it cannot be glossed over. An explanation for the case of shells subjected to hydrostatic pressures is given in the paper by Herrmann and Shaw [20] (which uses the equations derived in [13]). It is shown that the erroneous cut-off frequency arises when certain terms are omitted in the derivation of the equations by neglecting the change in the direction of the hydrostatic pressure force induced by the perturbation rotations. If we retain these terms and use equation (16) of [20], the equilibrium condition for the rotationally symmetric torsion mode and for pressures acting on the shell midsurface is

$$\left\{(1-\nu)\ \frac{(1+3d^2)}{2}\ + N^o_x\right\}\frac{\partial^2 v}{\partial x^2} - \frac{N^o_\phi v}{R^2} - \frac{\partial^2 v}{\partial t^2} + \Delta F_\phi = 0 \qquad (12)$$

where $\Delta F_\phi = N^o_\phi v/R^2$, is the change of the circumferential force component arising from the displacement. By taking the pressure to act on the shell midsurface the moment components Δm_ϕ and m_z, discussed in [13], [17] and [20], are identically zero. If we substitute the above expression for ΔF_ϕ in (12) it becomes

$$\left\{\frac{(1-\nu)}{2}\ (1+3d^2)\ + N^o_x\right\}\frac{\partial^2 v}{\partial x^2} - \frac{\partial^2 v}{\partial t^2} = 0\ . \qquad (13)$$

The questionable terms in Washizu's and Sanders' theories has been cancelled out by ΔF_ϕ and the torsion waves are now also nondispersive. This demonstrates the difficulties that can arise when the displacements and rotations of a prestressed system are being neglected while the stress resultants are retained. For many metal shell analyses this approximation may well be entirely satisfactory. In the case of blood vessels however, the displacements and rotations are generally much larger than in metal structures and must be properly accounted for. For a circular cylindrical shell, this is accomplished by using either the equations of [11] or those of [13] and [20], which reduce to those of Flügge [4]. Hence the results given by [18] are indeed correct.

However, if we accept the reasoning of Armenakas and Herrmann in [17] which is also employed in their subsequent papers, e.g., [20], the torsion waves retain their cut-off frequency in the case of constant directional pressure since ΔF_ϕ is zero in this situation. This produces a cut-off frequency and therefore results which we also find to be at variance with our intuition.

Consider an infinitely long shell whose internal pressure does not change direction and which is undergoing rotationally symmetric torsional oscillations. The rotation about the tangential base vector, namely $\partial w/\partial x$ does indeed vanish. Therefore, ΔF_x is zero. However, the other component of rotation of the normal to midsurface is v/R, and therefore not zero and ΔF_ϕ is again equal to $N^o_\phi v/R$. Thus the extraneous term causing the cut-off frequency is always cancelled out. This small

modification is of little physical significance since the fluid pressure is hydrostatic in virtually all cases of practical interest.

The contributions to the equilibrium equations of the terms involving the applied pressure times the perturbation rotations and strains are accounted for by Budiansky [11]. The two inplane equilibrium equations contain the rotations times the hydrostatic pressure while in the normal equation the pressure is multiplied by the sum of the inplane strains. A situation entirely analagous to the one involving the behavior of the torsion waves, occurs in the third equilibrium equation. The variation of the strain energy yields a term which is cancelled by the pw/R element in the expression accounting for the hydrostatic pressure. The neglect of this pressure term is the cause of the behavior of Washizu's equations and all others which make the same approximation. Thus Sanders' theory [10] predicts phase velocities that are independent of internal pressurization for types I and III waves by properly accounting for the change in direction of the pressure. This is also true in the theories of [11] and [20] in addition to our form of Flügge's theory in (5). The only reason for the dependence on internal pressure of phase velocities for the rotationally symmetric modes in [18] is due to the method in which the prestresses are applied.

Another item of interest in connection with the torsion modes is that the results of [18] do not exhibit the same dependence on axial prestress as does Fig. 2. This discrepancy has been explained by noting the different methods in which the prestress is applied. In our applications, we did not restrict the axial motion and hence applying the pressure

does not contribute to the axial prestress. It should be mentioned that this latter assumption affects the torsional phase velocities. However, it is not necessarily representative of blood vessels under "in vivo" conditions since they are anchored by branches and connective tissue and therefore do not change their length with pressure.

A third item of interest illustrated in Fig. 1 is the consistent nondispersive character of the type III waves. Only Sanders' theory predicts axial phase velocities independent of axial stretch while the other theories applied, in particular Washizu's, show a strong influence of axial stretch. The reason for this is to be found in the absence of the $(\partial u/\partial x)^2$ term in the expression for the axial strain and its influence on the operator L_{11}. For rotationally symmetric waves, the L_{11} coefficient in the frequency determinant for Sanders' theory is simply k^2 while in the other two theories it is k^2 times a function of the axial stretch which accounts for the noted dependence.

Another interesting result of the method of application of the prestress comes to light when we note that in (5), all the phase velocities are independent of internal pressurization. This disagrees with [18] only because of the previously mentioned application of the prestress, which results in terms involving Poisson's ratio times the circumferential prestress resultants. In our application of Flügge's theory, all three types of waves are independent of pressurization within drawing accuracy of the curves shown in Fig. 2.

Attention has been drawn to the fact that the "large strain" form of Washizu's equations are non-self-adjoint and thus we know from

well established theory (e.g. [19]) that the eigenvalues of the basic system and its adjoint are identical, but that the eigenvectors of the two systems are different and form a biorthogonal set. The adjoints of the operators in (12) are easily found by replacing ℓ_x^o by ℓ_ϕ^o and vice versa in the off-diagonal terms. The modal amplitude coefficients were indeed slightly different and we provide the following table as typical results.

TABLE I

TYPICAL MODAL COEFFICIENTS FOR THE ANLIKER-MAXWELL AND WASHIZU THEORY FOR $N_x^o = 0.4$, $N_\phi^o = 0$ AND $k = 5.0$

Wave Type	Shell Theory Modal Displacement								
	Anliker-Maxwell [18]			Washizu [12] Basic System			Washizu [12] Adjoint System		
	Axial	Torsion	Radial	Axial	Torsion	Radial	Axial	Torsion	Radial
I	-0.044	0	1.0	-0.0469	0	1.0	- .0335	0	1.0
II	0	1.0	0	0	1.0	0	0	1.0	0
III	1.0	0	0.044	1.0	0	0.0335	1.0	0	.0469

For this demonstration all coefficients less than 10^{-5} in absolute value have been replaced by zeroes in Table I.

These results illustrate the theory by showing that for the self adjoint operators of [18], the modes are orthogonal, while those of [12] for both the basic and adjoint equations are not orthogonal, but they are biorthogonal. However, the fact that the modes predicted by [12] are not quite orthogonal is of negligible importance in the study of pulse waves.

4.6. Conclusions.

The phase velocities predicted by the small strain theories of Herrmann and Shaw [20], Budiansky [11] and our application of Flügge's theory [4] are considered to be correct. Our results are nothing more than those of Anliker and Maxwell [18] with a different assumption concerning the application of the prestresses. All three wave speeds are essentially independent of internal hydrostatic pressure if the cylinder walls are not axially constrained.

Both Sanders [10] and Washizu [12], in addition to many other authors predict a cut-off frequency below which no torsion waves are propagated for non zero transmural pressure. This is demonstrated to be caused by neglecting the force component induced by the perturbation rotation of the applied pressure. The importance of including these contributions to the equilibrium accounts for the correctness of the theories mentioned. For future studies on shells of general geometry, those of Budiansky [11] are recommended.

The nonself adjointness of the large strain theory of Washizu is shown to be of negligible importance for the physiological problems of wave propagation in the arterial systems.

NOTATION

A, B	Lamé parameters
$c = \bar{c}/\bar{c}_0$	Nondimensional phase velocity
$\bar{c}_0^2 = \bar{E}/\bar{\rho}(1-\nu^2)$	Normalizing phase velocity
$d^2 =$	$h^2/12$
$\bar{E}$	Normalizing Young's modulus
e_α, e_β, $e_{\alpha\beta}$	Linear midsurface strains
$h = \bar{h}/\bar{R}_0$	Nondimensional shell wall thickness
$k = 2\pi\ \bar{R}_0/\bar{\lambda}$	Nondimensional wave number
L_{ij}	Differential operators
ℓ_{ij}	Midsurface strains and rotations
$M_\alpha, M_\beta, M_{\alpha\beta} = \bar{M}_\alpha(1-\nu^2)/\bar{E}$, etc.	Nondimensional moment resultants
$N_\alpha, N_\beta, N_{\alpha\beta} = \bar{N}_\alpha(1-\nu^2)\bar{E}\bar{h}$, etc.	Nondimensional force resultants
$R_\alpha, R_\beta = \bar{R}_\alpha/\bar{R}_0$, etc.	Nondimensional radii of curvature
$\bar{R}_0$	Normalizing geometric dimension
u, v, $w = \bar{u}/\bar{R}_0$, etc.	Nondimensional midsurface displacements in the axial, tangential and normal directions

x, ϕ	Axial and circumferential coordinates of a circular cylinder
$X,Y,Z = \bar{X}(1-\nu^2)/\bar{E}\,\bar{h}$, etc.	Nondimensional applied force resultants
α, β	Axial and circumferential coordinates of a general cylinder
$\epsilon_\alpha, \epsilon_\beta, \epsilon_{\alpha\beta}$	Nonlinear midsurface strains
$K_\alpha, K_\beta, K_{\alpha\beta}$	Curvatures
$\lambda = \bar{\lambda}/\bar{R}_0$	Nondimensional wave length
$\rho = \bar{\rho}\,\bar{R}_0^2(1-\nu^2)\bar{\sigma}_0^2/\bar{E}$	Nondimensional density
$\sigma = \bar{\sigma}/\bar{\sigma}_0$	
$\bar{\sigma}_0^2 = \bar{E}/\bar{\rho}\,\bar{R}_0^2(1-\nu^2)$	Normalizing frequency
$\omega_\alpha, \omega_\beta$	Rotations
$\nabla^2\nabla^2(\cdot) =$	$\partial^4(\cdot)/\partial\alpha^4 + 2\partial^4(\cdot)/B^2\partial\alpha^2\partial\beta^2 + \partial^4(\cdot)/B^4\partial\beta^4$

Superscripts

$\bar{\cdot}$	Denotes a dimensional quantity
$\overset{o}{\cdot}$	Denotes a prestress quantity

REFERENCES

[1] Fung, Y. C., "Biomechanics--Its Scope, History and Some Problems of Continuum Mechanics in Physiology", App. Mech. Review 21, No. 1, January 1968 and the Bibliography of this paper.

[2] Lee, J. S., V. G. Frasher and Y. C. Fung, "Two Dimensional Finite Deformation Experiments on Dog's Arteries and Veins", AFOSR 67-1980, July 1967.

[3] Prager, W., "On the Formulation of Constitutive Equations for Living Soft Tissues", AFOSR 67-2599, November 1967.

[4] Flügge, W. Stresses in Shells, Springer-Verlag, 1960, pp. 208 et seq.

[5] Koiter, W. T. "On the Nonlinear Theory of Thin Elastic Shells", Proc. Royal Netherlands Academy 69, No. 1 pp. 1-54 (1966).

[6] Naghdi, P., "Foundations of Elastic Shell Theory", Progress in Solid Mechanics, North Holland, 1963.

[7] Bolotin, V. V., The Dynamic Stability of Elastic Systems, Holden-Day, San Francisco, 1966, p. 417 et seq.

[8] Kempner, J., "Unified Thin Shell Theory", PIBAL Report No. 566, March 1960.

[9] Dill, E. H., "General Theory of Large Deflections of Thin Shells", NASATND826, September 1959.

[10] Sanders, J. R., "Non-Linear Theories of Thin Shells", Q. App. Mech. XXI, No. 1, pp. 21-36 (1963).

[11] Budiansky, B.,"Notes on Nonlinear Shell Theory", J. App. Mech. pp. 393-401 (1968).

[12] Washizu, K., "Some Considerations on Shell Theory", A.S.R.L. Rept. 1001, M.I.T., October 1960.

[13] Herrmann, G., and A. E. Armenakas, "Dynamic Behavior of Cylindrical Shells Under Initial Stress", Proc. U.S. Nat. Congress of App. Mech. pp. 203-213 (1962).

[14] Biot, M., "Non-Linear Theory of Elasticity and the Linearized Case of a Body under Initial Stress", Philo. Mag. Series 7, 27, No. 183, April 1939.

[15] Biot, M., Mechanics of Incremental Deformations, John Wiley and Sons, New York, 1965.

[16] Pflüger, A., Stabilitats Probleme Der Elastostatik, Springer, Berlin

[17] Armenakas, A. E. and G. Herrmann,"Buckling of Thin Shells under External Pressure", J. Eng. Mech. Div. A.S.C.E. 89, No. EM 2, pp. 131-146 (June 1963).

[18] Anliker, M. and J. E. Maxwell, "Dispersion of Waves in Blood Vessels", Biomechanics Symposium, ASME, New York, pp. 47-67 (1967).

[19] Morse, P. M. and Feshbach, H., Methods of Theorectical Physics, McGraw-Hill Co., New York, 1953.

[20] Herrmann, G. and J. Shaw, "Vibrations of Shells under Initial Stress", J. Eng. Mech. Div. A.S.C.E. EM5, October 1965, pp. 37-59.

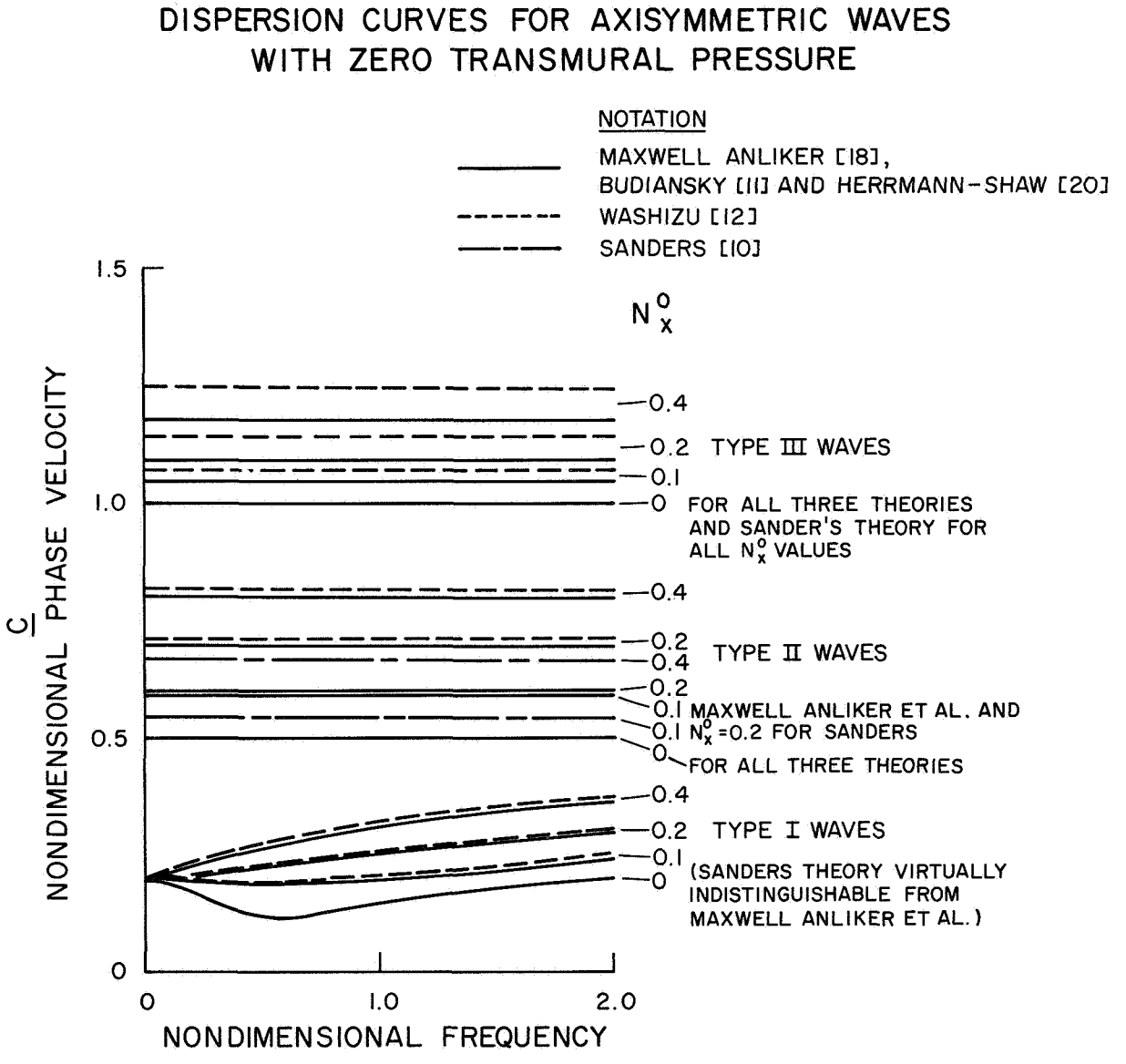

Fig. 1. Dispersion Curves of Axisymmetric Waves for Zero Transmural Pressure Predicted by Different Shell Theories

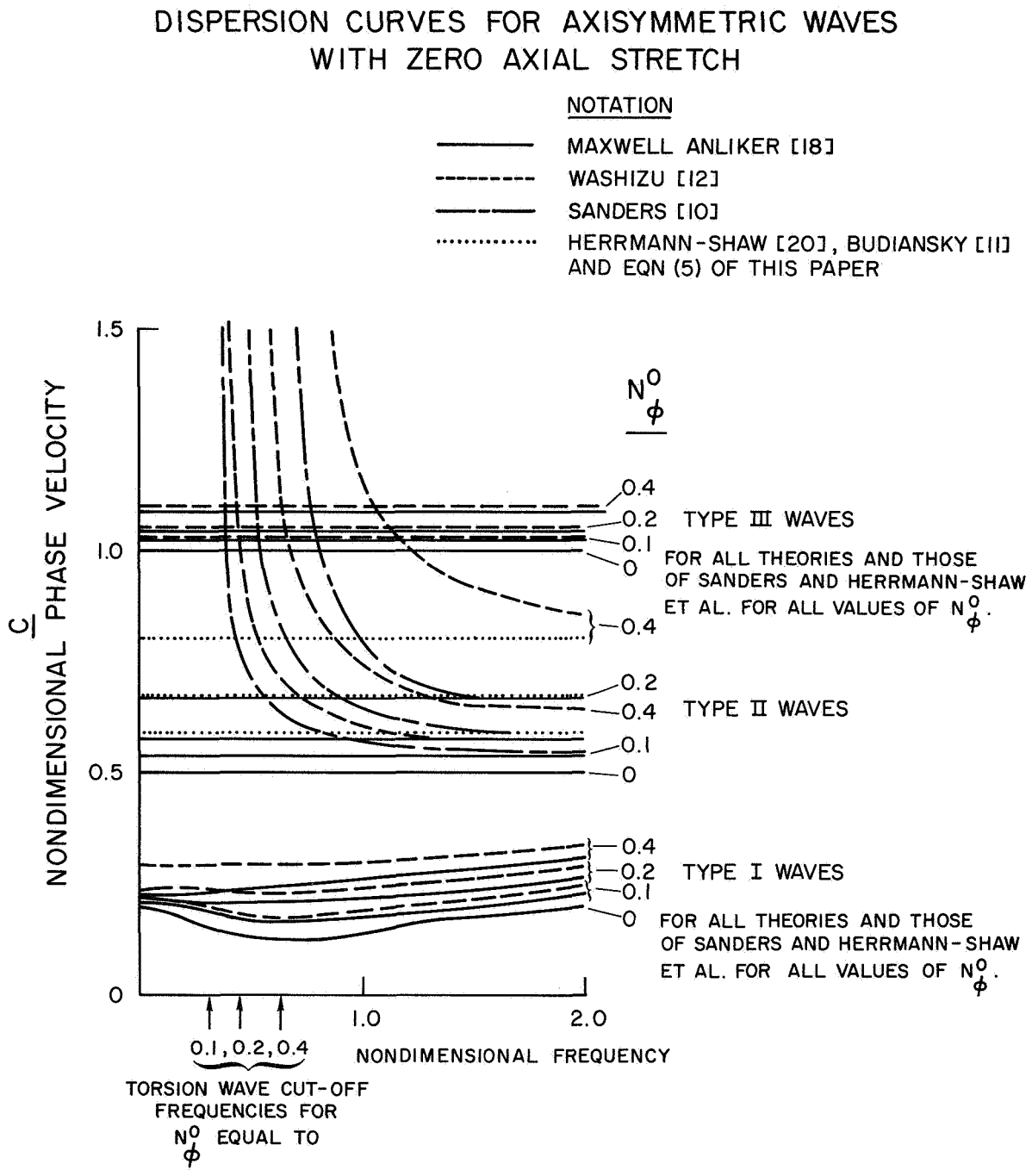

Fig. 2. Dispersion Curves of Axisymmetric Waves for Zero Axial Sketch Predicted by Different Shell Theories